Title	Photoinduced Copper-Catalyzed Asymmetric Acylation Reactions
Author(s)	上田, 悠介
Citation	北海道大学. 博士(理学) 甲第15390号
Issue Date	2023-03-23
DOI	10.14943/doctoral.k15390
Doc URL	http://hdl.handle.net/2115/91525
Type	theses (doctoral)
File Information	UEDA_Yusuke.pdf

Photoinduced Copper-Catalyzed Asymmetric Acylation Reactions

(光銅触媒不斉アシル化反応)

Yusuke Ueda

2023

Contents

General Introduction

Transition metal catalysis has promoted the development of valuable molecular transformations in organic synthesis. In recent years, transition metal catalysis under photoirradiation has further developed more challenging transformation reactions for organic synthesis which is complementary to thermal catalysis. The broadly investigated reactions employ synergistic catalytic systems that combine visible-light-excited photocatalysts and transition metal catalysts. On the other hand, photoinduced transition-metal-catalyzed reactions in which the single metal plays a dual role as a photoabsorbent and a center for chemical bond cleavage/formation offer advantages of simplicity of the reaction system and cost-effectiveness by avoiding the use of expensive external substances. In addition, better reaction control with metal-bound ligands is an attractive feature of this methodology, and the use of chiral ligands allows the development of highly enantioselective reactions. Generally, the proposed mechanism for these reactions involves intermolecular single-electron transfer between the excited metal complex and the substrate to generate highly active radical species. In contrast to this intermolecular strategy, intramolecular electron transfer from metal centers to ligands (MLCT) is rarely reported. On the other hand, since carbonyl compounds are contained in various natural products, pharmaceuticals, pesticides, and functional materials, it is important to develop efficient synthetic methods for these compounds. In particular, umpolung acylation is a straightforward method to synthesize carbonyl compounds. However, stereoselective umpolung acylation has not yet been explored because it is difficult to generate a chiral acyl anion equivalent in a catalytic manner. Thus, the author aimed at development of new umpolung asymmetric acylation reaction by direct excitation of chiral transition metal complex.

1. The Merger of Photoredox and Transition Metal Catalysis in Organic Synthesis

Over the past century, transition metal-catalyzed cross-coupling reactions have evolved into one of the most commonly used C–C and C–heteroatom bond-forming reactions in chemical synthesis.[1] The broad functional group tolerance of these reactions enabled highly modular molecular construction with various building blocks. On the other hand, visible light photoredox catalysts have recently been a powerful method for organic synthesis.[2] This catalyst is excited with visible light, and the organic molecule is activated by the excited catalyst through single-electron transfer (SET). This approach is attractive for its ability to generate active species distinct from conventional thermal activation, which facilitates the use of abundant and inexpensive starting materials. By combining these two powerful bond-forming methods, the metallaphotoredox catalyst method was born and has become the mainstay of synthetic methodologies in recent years.[3] Photoredox catalyzed generation of radical species and transition-metal-catalyzed bond activation and formation have made it possible to form previously difficult bonds from simple starting materials.

1.1. Nickel Metallaphotocatalysis

In 2014, Macmillan, Doyle, and co-workers reported photoredox and nickel transition metal catalyzed C(sp^2)-C(sp^3) decarboxylative cross-coupling of carboxylic acids and aryl halide electrophiles (Scheme 1).[4]

Scheme 1. Photoredox and nickel catalyzed C(sp^2)-C(sp^3) decarboxylative cross-coupling.

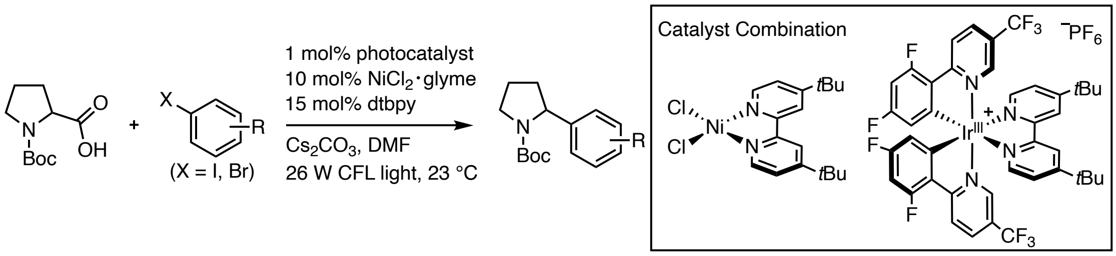

Excitation and intersystem crossing of the photocatalyst produce a strongly oxidative and long-lived triplet excited state, which reacts with a carboxylic acid nucleophile in SET. A subsequent decarboxylation reaction produces an alkyl-centered radical. Concurrently, nickel(0) species, which is probably generated via two sequential electron-transfer events from a nickel(II) precatalyst, can undergo oxidative addition with the aryl halide electrophile to afford nickel-aryl species. Oxidative radical capture by this intermediate produces Ni(III)-aryl-alkyl complex, which can undergo rapid reductive elimination to give the desired C(sp^2)−C(sp^3) coupled product. Finally, the generated nickel(I) species and the reduced photocatalyst undergo SET, regenerating both active catalysts simultaneously (Figure 1).

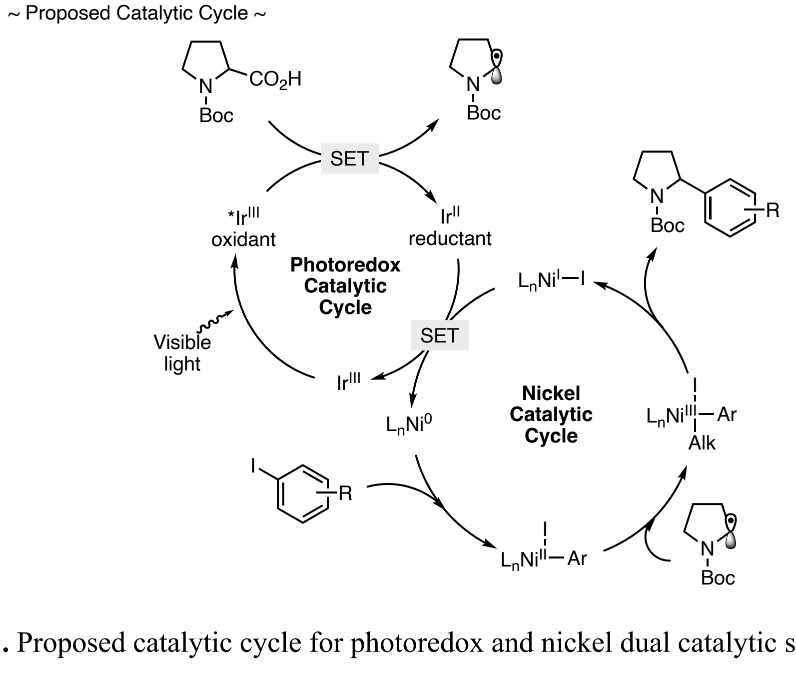

Figure 1. Proposed catalytic cycle for photoredox and nickel dual catalytic system.

In 2014, at the same time as the previous reaction, a photoredox and nickel-catalyzed cross-coupling using alkylboron nucleophiles was described by Molander and co-workers (Scheme 2).[5] They found that alkyltrifluoroborates are converted to carbon-centered radicals by SET using an excited photocatalyst, leading to a C(sp^2)-C(sp^3) cross-coupling reaction with an aryl bromide. The reaction pathway forming the alkyl−nickel species avoids a traditional transmetallation with alkylboron reagents. These methods have since been expanded to a number of mechanistically related transformations not only for carbon-carbon bond formation but also for carbon-heteroatom bond formation.[6]

Scheme 2. Photoredox and nickel catalyzed cross-coupling using alkylboron nucleophiles.

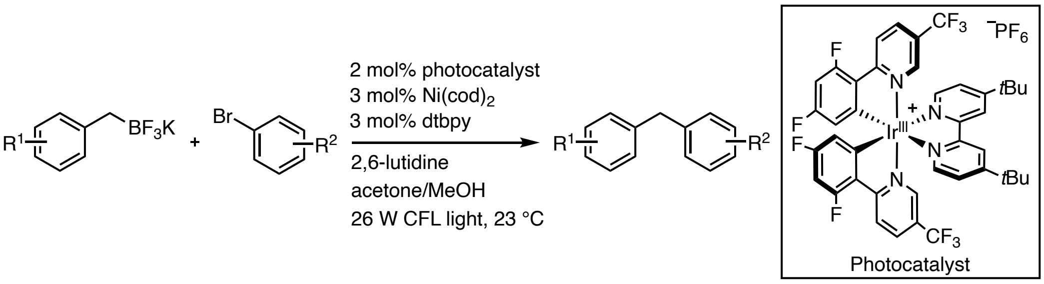

1.2 Copper Metallaphotocatalysis

In 2012, Sanford and co-workers reported the photoredox and copper-catalyzed trifluoromethylation of arylboronic acids to synthesize valuable trifluoromethylarenes (Scheme 3).[7] The reaction involves the addition of reductively generated trifluoromethyl radical to an appropriate Cu(II) species, followed by transmetallation with an arylboronic acid nucleophile to generate a key Cu(III)-aryl-CF_3 species. Reductive elimination from this high-valent copper complex produces the desired product, and SET between the excited photocatalyst and reduced Cu(I) complex regenerates both active catalysts.

Scheme 3. Photoredox and copper-catalyzed trifluoromethylation of arylboronic acids.

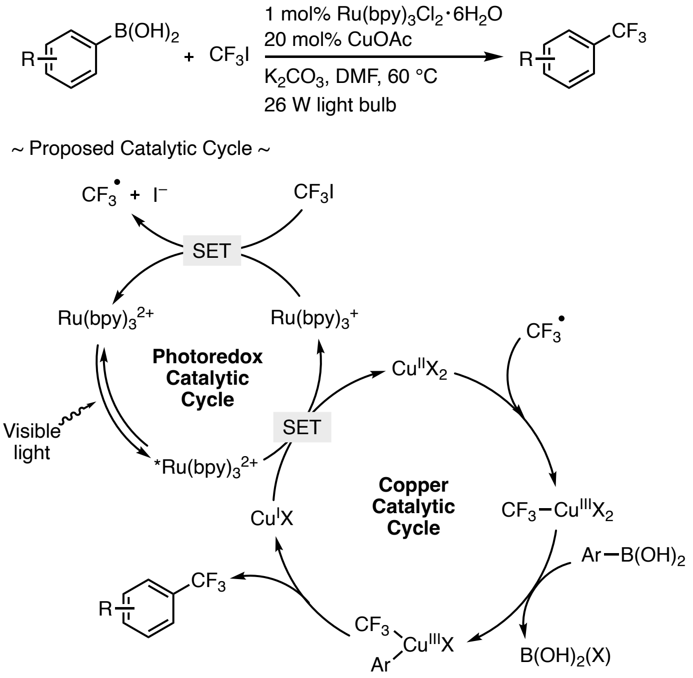

This protocol has been applied not only to the trifluoromethylation of various (hetero)arylboronic acids, but also to the decarboxylative trifluoromethylation of carboxylic acids and the trifluoromethylation of aryl and alkyl bromides (Scheme 4).[8] Additionally, the protocol was extended to other related electrophiles with similar efficiency.[9]

Scheme 4. Photoredox- and copper-catalyzed trifluoromethylation

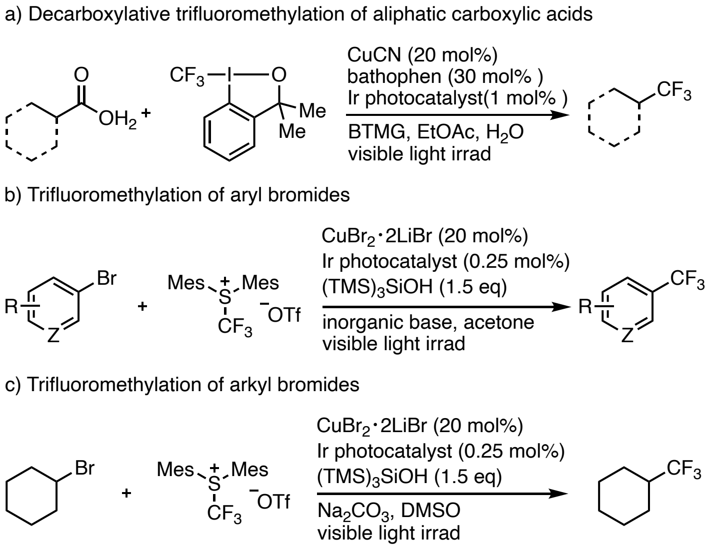
a) Decarboxylative trifluoromethylation of aliphatic carboxylic acids

b) Trifluoromethylation of aryl bromides

c) Trifluoromethylation of arkyl bromides

2. Visible Light-Induced Excited-State Transition-Metal Catalysis

The development of transition metal catalysis under visible light that dose not rely on typical photoredox catalysts is a rapidly developing research area and has been actively investigated in recent years.[10] Distinct from the metallaphotoredox reaction, a transition metal complex performs two roles as an absorbent of light energy and a center of bond forming/breaking mostly via a single catalytic cycle, thus contrasting the established dual photocatalysis in which an exogenous photosensitizer is employed. This protocol offers the advantages of simplicity and cost effectiveness of the reaction system by avoiding the use of expensive external substances. In addition, the better reaction control by metal-bound ligands is an attractive feature of this methodology as evidenced by the growing number of reports in this regard, some of which detail highly enantioselective reactions by the use of chiral ligands.

2.1 Direct Excitation of Palladium Catalysts

The first visible light-induced palladium-catalyzed transformation was reported by Gevorgyan's group in 2016 by disclosing the generation of an unprecedented hybrid aryl palladium-radical species from aryl iodides (Scheme 5).[11] In this case, visible light excitation led to the formation of a high-energy Pd(0) species, that can transfer a single electron to aryl iodide, thereby engaging it in hybrid palladium-radical chemistry. To date, the majority of palladium visible light photocatalytic reactions take place via this oxidative quenching pathway, resulting in SET from photoexcited palladium to an organic halide or its equivalent.[12]

Scheme 5. Palladium-catalyzed desaturation via direct excitation of palladium catalyst

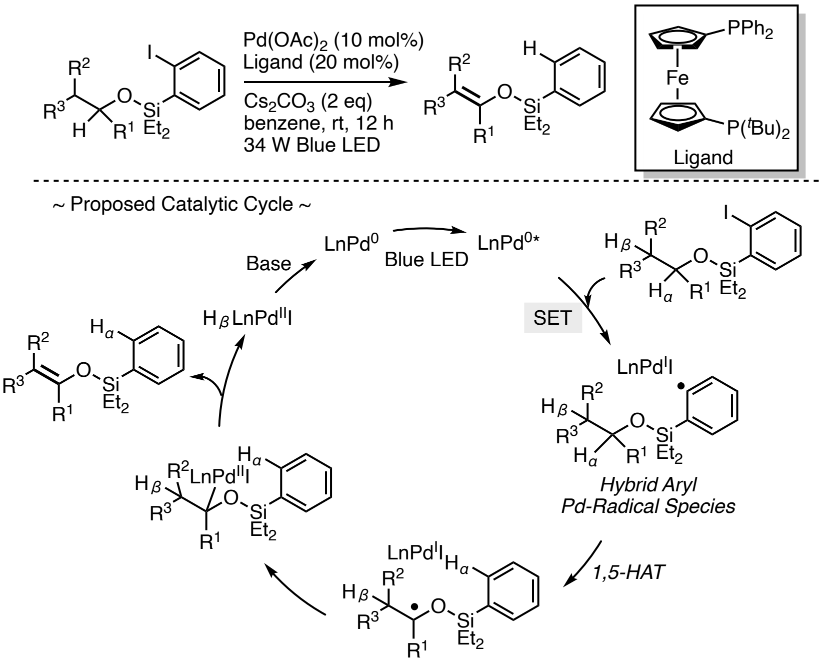

2.1 Direct Excitation of Copper Catalysts

In 2012, Fu, Peters, and co-workers reported the photoinduced Ullmann C−N coupling reaction via an unprecedented radical pathway (Scheme 6a).[13] This is the first report on the reactivity of copper catalysts under visible light irradiation. In the same year, Hwang's group demonstrated that Sonogashira coupling, which typically requires a copper/palladium dual catalyst, could be achieved using a single copper catalyst under visible light irradiation (Scheme 6b).[14] In both cases, a Cu(I)−nucleophile complex (amide and acetylide, respectively) is involved, which upon photoexcitation acts as a single electron reductant and engages the aryl halide coupling partner in a SET pathway (Scheme 6c). Since then, various visible light induced copper-catalyzed reactions based on these mechanisms have been achieved.[15]

Scheme 6. Pioneering works for photoinduced copper-catalyzed reactions

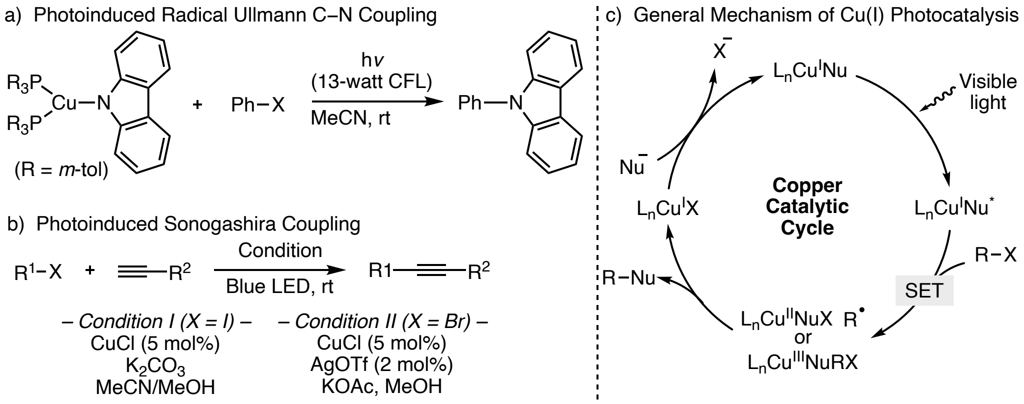

2.3 Direct Excitation of Chiral Copper Catalyst

In 2016, Fu, Peters, and co-workers expanded their visible-light-induced copper-catalyzed asymmetric C–N couplings to an enantio-convergent reaction of racemic tertiary alkyl chlorides by using a chiral photo-copper catalyst (Scheme 7).[16] This is the first report of asymmetric synthesis in a photoinduced copper-catalyzed reaction with a single catalyst. The catalytic cycle begins with the in situ formation of Cu(I)–nucleophile complex, which upon photoexcitation involves the electrophilic substrate in the SET process. The resulting intermediate may have a radical character, or exist as a conventional Cu(III) oxidative addition complex. A subsequent formation of carbon–heteroatom bond furnishes product with enantioselectivity controlled by the chiral catalyst and releases Cu(I) species. The photoactive complex is then regenerated by ligand exchange with another nucleophile molecule. The authors reported various asymmetric C–N coupling reactions using this approach.[17]

Scheme 7. Visible-light-induced copper-catalyzed asymmetric C–N couplings

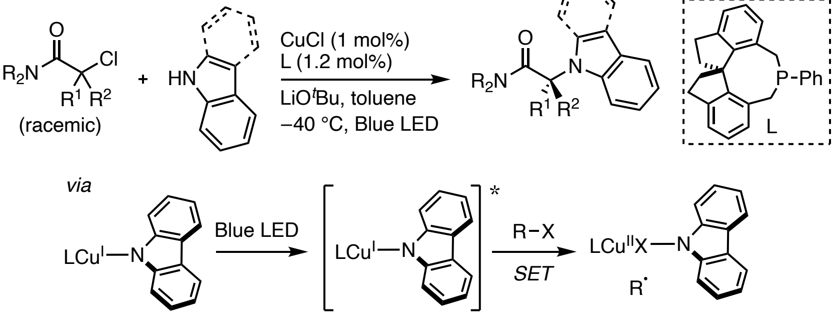

In 2020, Liu and co-workers reported the photo-induced asymmetric alkyl Sonogashira coupling with a copper catalyst having a quinine-derived chiral ligand (Scheme 8).[18] Following their previous report on asymmetric alkyl Sonogashira coupling using secondary alkyl halides in 2018[19], the redox-active esters were used as secondary alkyl radical precursors to perform similar transformation under photoirradiation. In addition to these reports, various asymmetric reactions based on photoexcitation of organocopper species have been developed for C–C and C–O bond formations.[20]

Scheme 8. Visible-light-induced asymmetric alkyl Sonogashira coupling

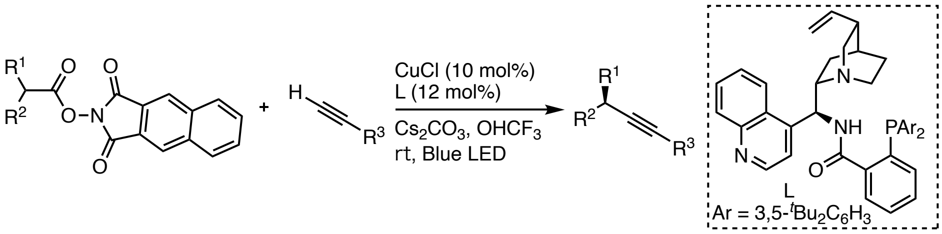

3. Acylation Reaction

Carbonyl compounds are found in a wide variety of natural products, pharmaceuticals, agricultural chemicals, and functional materials.[21] A carbonyl group is also a useful functional group which can be converted to other functionalities in organic synthesis. Therefore, development of methodology for introducing a carbonyl group into organic molecules has attracted much interest in synthetic chemistry for a long time.[22]

An acylation reaction of a carbon nucleophile with a carboxylic acid derivative is known as the well-studied method.[23] In recent years, transition metal catalysts have been used to achieve acylation reactions under mild reaction conditions with excellent functional group tolerance. The key to these reactions is the formation of acyl metal species through oxidative addition of transition metal catalysts to acylating agents, and carbonyl compounds can be synthesized using various organometallic reagents as nucleophiles (Scheme 9a). The use of transition metal catalysts to catalytically generate nucleophilic species in the reaction system is attractive in that it does not require prior preparation of organometallic reagents.[24] In this context, several reductive coupling reactions have been reported using vinyl arenes as nucleophile precursors and carboxylic acid derivatives as acylating electrophiles in the presence of hydrosilanes or H_2 as hydrogen sources (Scheme 9b). Acylboration reactions have also been achieved using diborane as a nucleophile.

Scheme 9. Transition-metal-catalyzed acylation reactions

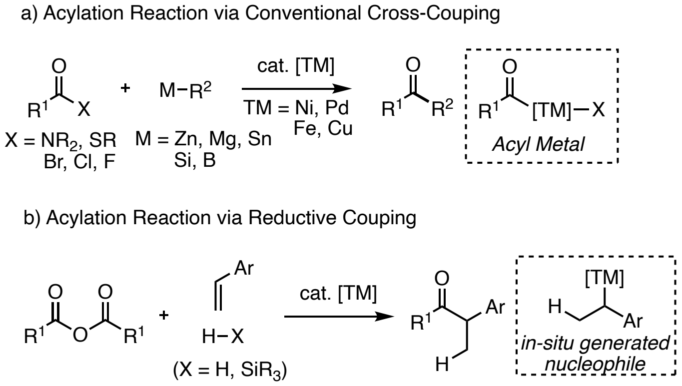

In 2020, the author, Iwai, and Sawamura reported a synergistic dual metal-catalyzed acylation reaction that combines nickel-catalyzed activation of acyl electrophiles and copper-catalyzed in-situ formation of nucleophiles (Scheme 10).[25] The reaction tolerates broad functional groups because mildly reactive acyl fluorides can be used as acylation reagents.

Scheme 10. Nickel-copper-catalyzed hydroacylation of vinylarenes

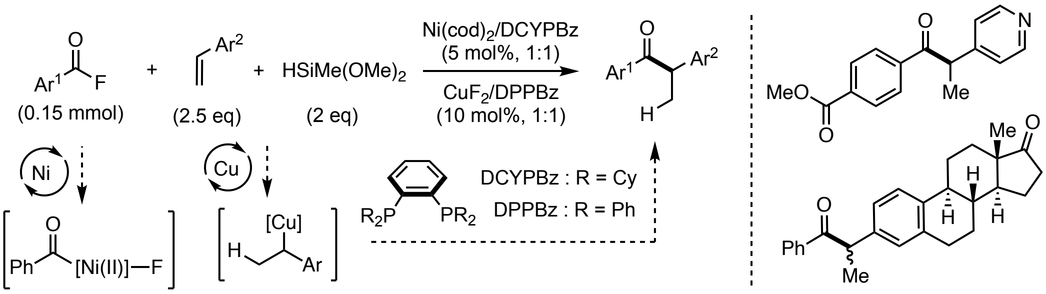

3.2 Umpolung Acylation

The umpolung reaction that reverses the original reactivity of the functional group has attracted attention because it can improve the efficiency of the synthetic route in organic synthesis. In the case of an acylation reaction, while the carbon of a common carbonyl group has an electrophilic property, it can work as a nucleophile by converting the polarity, allowing access to carbonyl compounds that were otherwise difficult to synthesize.

3.2.1 Dithiane as an acyl anion equivalent

The concept of umpolung was first proposed by Corey and Seebach in 1975 (Scheme 11).[26] They succeeded in employing an aldehyde, which was originally an "electrophile", as a "nucleophile" through protection of carbonyl group with dithiane. Recently, the method has been applied to an asymmetric synthesis by combining with a chiral Pd catalyst (Scheme 12).[27]

Scheme 11. Concept of carbonyl umpolug via dithiane

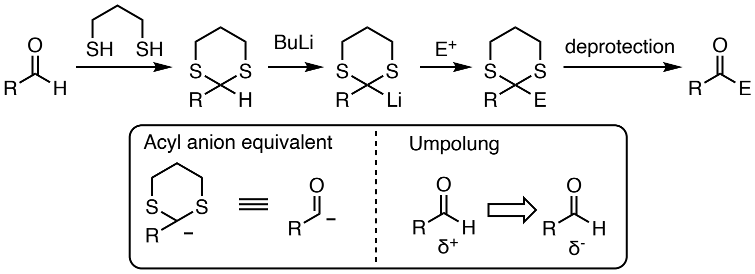

Scheme 12. Pd-catalyzed asymmetric allylic substitution with 1,3-dithianes

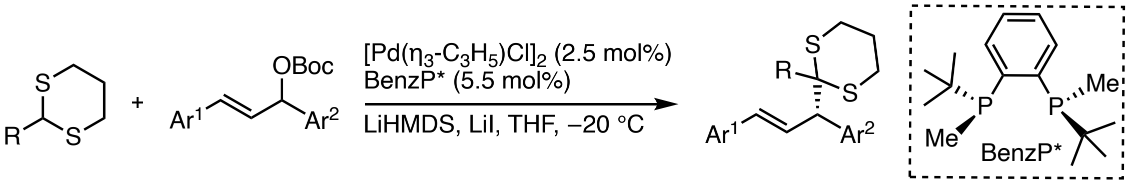

3.2.2 Breslow intermediate as an acyl anion equivalent

Another method for umpolung of a carbonyl group is given by a formation of Breslow intermediates from aldehydes and *N*-heterocyclic carbenes (NHC), which works as an acyl anion equivalent.[28] Various bond-forming reactions including acylation of aryl iodide, allylic alcohol, allylic esters, and unsaturated carbonyl compounds have been developed by combining them with organometallic catalysts.[29]

Scheme 13. Umpolung acylation through hybrid NHC/Pd catalysis

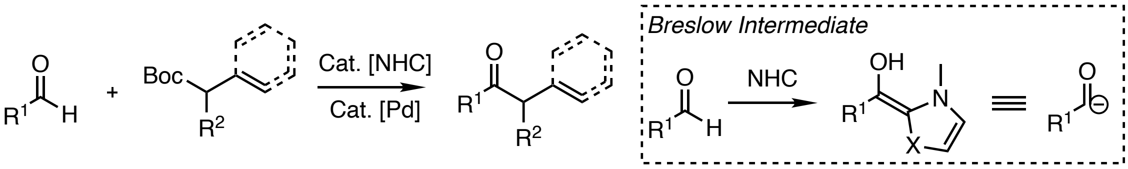

3.2.3 Acyl radical

Nucleophilic acyl radicals serve as versatile synthetic intermediates in Giese-type additions to activated alkenes, Minisci-type acylations of heteroarenes, and in the preparation of a wide range of natural and bioactive molecules.[30] The conventional methods for generating acyl radicals, however, generally require harsh reaction conditions such as UV irradiation or high temperatures.[31] Recently, various methods to generate acyl radicals have been reported using visible light photoredox catalysts.[32]

In 2017, MacMillan and co-workers reported arylation, vinylation, and alkylation of aldehydes via an acyl radical intermediate using aryl, vinyl, and alkyl bromides as coupling partners through a triple catalytic protocol with quinuclidine, Ni^{II}, and a photocatalyst (Scheme 14).[33] The mechanistic hypothesis for this protocol is shown in Scheme 14. SET from quinuclidine to the excited iridium photocatalyst generates an electrophilic quinuclidinium cation radical, which selectively abstracts the hydrogen atom of aldehyde to form the acyl radical. Oxidative addition of the aryl bromide to Ni^0 on the other hand produces an aryl-Ni^{II} species, which is intercepted by the acyl radical to form acyl-Ni^{III} complex. Reductive elimination then forms the desired ketone product and a Ni^I species. A single-electron transfer between Ir^{II} and Ni^I regenerates the Ir^{III} and Ni^0 catalysts and closes the catalytic cycle.

Scheme 14. Direct C–H arylation via the combination of triple catalysis

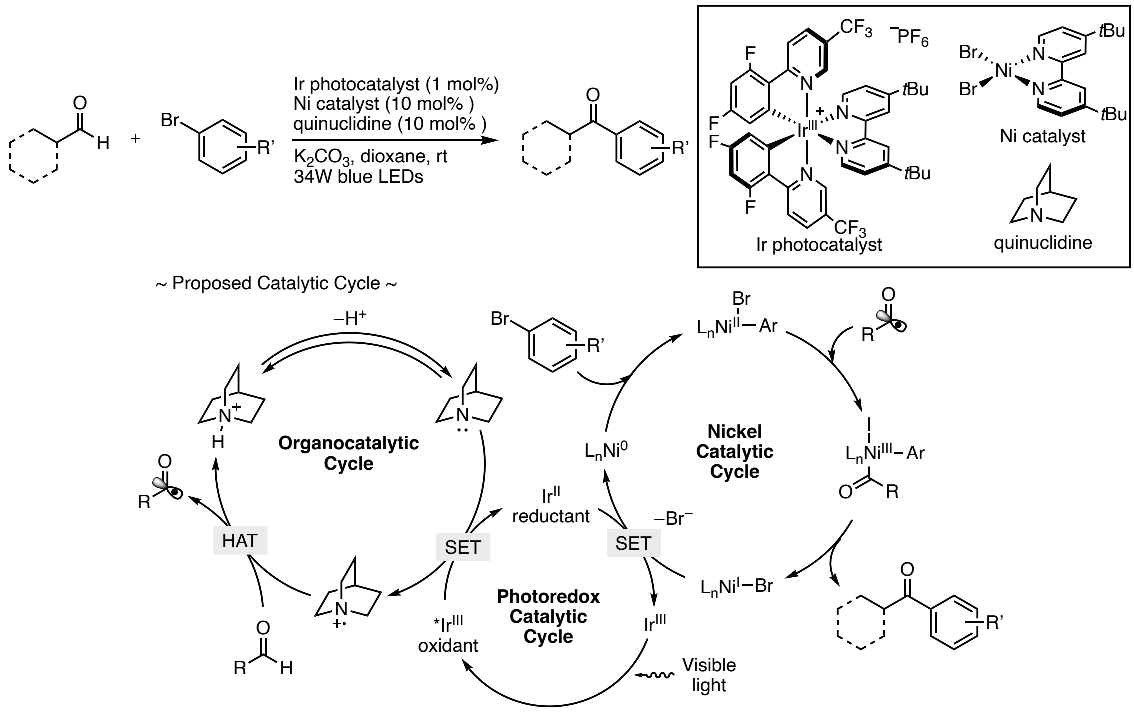

This protocol was extended to other related electrophiles.[34] Additionally, various visible-light-driven acyl radical generation methods have been reported using not only aldehydes but also α-ketocarboxylic acids, carboxylic acids, carboxylic acid anhydrides, acylthioesters, acid chlorides, or acylsilanes as acyl radical precursors.[35]

4. Overview of This Thesis

The author developed the photoinduced copper-catalyzed asymmetric umpolung acylation reactions. These reactions proceeded with high regioselectivities and stereoselectivities. Generally, the proposed reaction mechanism of photoinduced transition metal catalysts consists of intermolecular single-electron transfer (SET) between the catalytic metal complex and the substrate, followed by homolytic bond dissociation in the resulting open-shell state of the substrate to liberate a highly reactive free radical, which may then recombine with the metal (Figure 2a). In a clear departure from this reaction design, we envisaged that metal-to-ligand charge transfer (MLCT) photoexcitation of organometallic intermediates may lead to mechanistically different photoinduced metal catalysis centered at a charge-separated species (Figure 2b).[36]

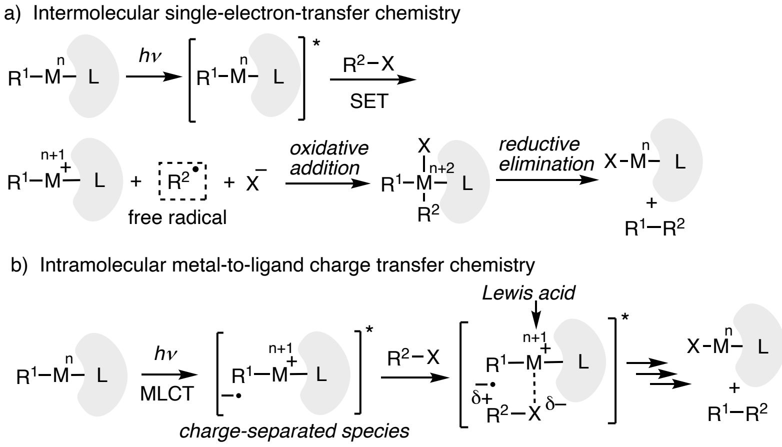

Figure 2. SET vs MLCT

In Chapter 1, development of photoinduced copper-catalyzed asymmetric acylation of allylic phosphates with acylsilanes is described. In Chapter 2, the author discusses the reaction mechanism of photoinduced copper-catalyzed asymmetric acylation of allylic phosphates, which is based on copper-to-acyl metal-to-ligand charge transfer (MLCT) photoexcitation that generates a charge-separated triplet state as a highly reactive intermediate. In Chapter 3, the strategy for the synthesis of chiral 1.4-dicarbonyl compounds via photoinduced copper-catalyzed asymmetric conjugate addition reaction of acylsilanes to α,β-unsaturated ketones and aldehydes is described.

4.1 Photoinduced Copper-Catalyzed Asymmetric Acylation of Allylic Phosphates with Acylsilanes

In Chapter 1, the author describes that visible-light irradiation with a blue LED lamp induced copper-catalyzed highly enantioselective umpolung acylation of γ-monosubstituted or γ,γ-disubstituted primary allylic phosphates with acylsilanes as acyl anion equivalents (Scheme 15). This reaction offers straightforward access to enantioenriched α-branched β,γ-unsaturated ketones, which serve as versatile chiral building blocks in organic synthesis. For the reaction design, we envisioned the formation of an acylcopper(I)−alkene complex coordinated with a chiral NHC ligand via photoisomerization of an acylsilane to a siloxycarbene and subsequent Cu-to-acyl MLCT photoexcitation. Formalistically, this MLCT produces a charge-separated triplet species with an α-oxy-anion-substituted carbon radical and a positively charged Lewis-acidic Cu(II) center covalently bound together through a Cu−C σ-bond.

Scheme 15. Photoinduced Cu-catalyzed enantioselective umpolung allylic acylation

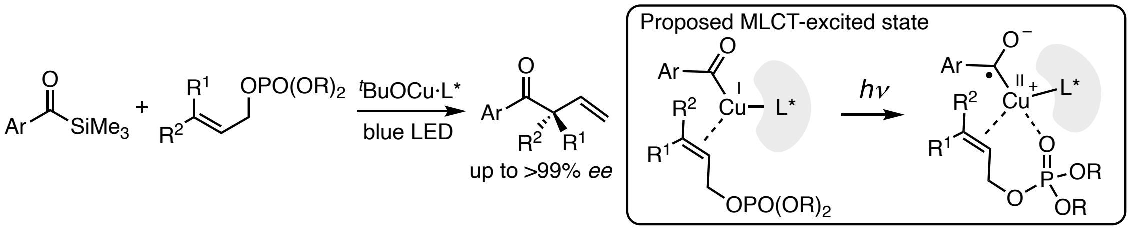

4.2 Mechanistic Investigation of Photoinduced Copper-Catalyzed Asymmetric Acylation of Allylic Phosphates with Acylsilanes

The author developed the photoinduced copper-catalyzed asymmetric acylation of allylic phosphates with acylsilanes (Chapter 1). In this work, the author assumes that the reaction proceeds by MLCT from the copper center to the acyl group due to photoexcitation. In Chapter 2, the author performed mechanistic investigation combined experiments and calculations to elucidate the proposed mechanism. These results suggest a novel photochemical reaction pathway featuring molecular activation by the charge-separated MLCT species. In this process, the author obtained an interesting finding that the photoexcited acyl copper activates the leaving group of the allylic phosphate to generate allyl radicals, which weakly bound to the copper complex (Scheme 16).

Scheme 16. A novel photochemical reaction pathway supported by mechanistic investigation

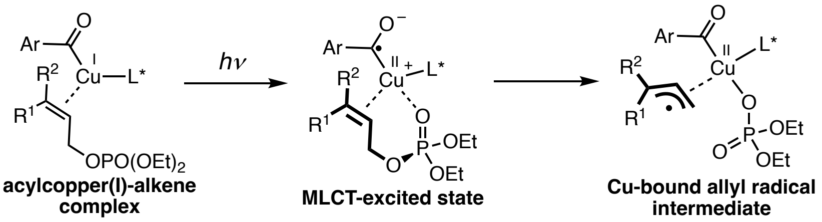

4.3 Photoinduced Copper-Catalyzed Asymmetric Conjugate Addition Reaction of Acylsilanes to α,β-unsaturated Ketones and Aldehydes

Chiral 1,4-dicarbonyl compounds are important synthetic intermediates for a variety of natural products and pharmaceuticals. In Chapter 3, the author describes an asymmetric conjugate addition reaction of acylsilanes to synthesize chiral 1,4-dicarbonyl compounds by using α,β-unsaturated ketones or aldehydes as substrates in place of the allylic phosphates (Scheme 17). The desired asymmetric conjugate addition reaction occurred with high enantioselectivity with copper/chiral N-heterocyclic carbene catalysts under the modified reaction conditions.

Scheme 17. Photoinduced Cu-catalyzed asymmetric conjugate addition reaction of acylsilanes

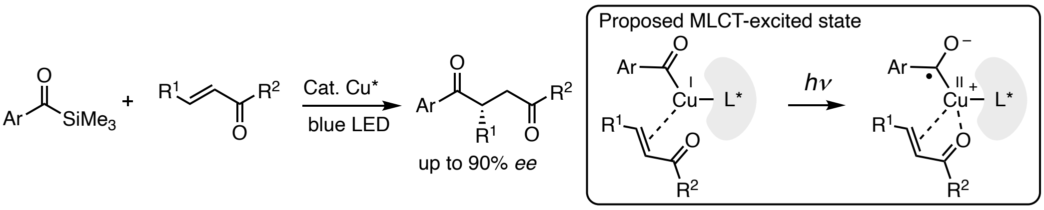

References

(1) (a) Nicolaou, K. C.; Bulger, P. G.; Sarlah, D. *Angew. Chem., Int. Ed.* **2005**, *44*, 4442−4489. (b) Ruiz-Castillo, P.; Buchwald, S. L. *Chem. Rev.* **2016**, *116*, 12564−12649. (c) Jana, R.; Pathak, T. P.; Sigman, M. S. *Chem. Rev.* **2011**, *111*, 1417–1492. (d) Leonori, D.; Aggarwal, V. K. *Angew. Chem., Int. Ed*. **2015**, *54*, 1082–1096. (e) Cherney, A. H.; Kadunce, N. T.; Reisman, S. E. *Chem. Rev*. **2015**, *115*, 9587–9652,

(2) (a) Shaw, M. H.; Twilton, J.; MacMillan, D. W. C. *J. Org. Chem*. **2016**, *81*, 6898−6926. (b) Marzo, L.; Pagire, S. K.; Reiser, O.; König, B. *Angew. Chem., Int. Ed*. **2018**, *57*, 10034−10072. (c) Narayanam, J. M. R.; Stephenson, C. R. J. *Chem. Soc. Rev.* **2011**, *40*, 102−113. (d) Huang, X.; Meggers, E. *Acc. Chem. Res*. **2019**, *52*, 833−847. (e) Schultz, D. M.; Yoon, T. P. *Science* **2014**, *343*, 1239176. (f) Romero, N. A.; Nicewicz, D. A. *Chem. Rev*. **2016**, *116*, 10075−10166.

(3) Chan, A. Y.; Perry, I. B.; Bissonnette, N. B.; Buksh, B. F.; Edwards, G. A.; Frye, L. I.; Garry, O. L.; Lavagnino, M. N.; Li, B. X.; Liang, Y.; Mao, E.; Millet, A.; Oakley, J. V.; Reed, N. L.; Sakai, H. A.; Seath, C. P.; MacMillan, D. W. C. *Chem. Rev*. **2022**, *122*, 1485−1542.

(4) Zuo, Z.; Ahneman, D. T.; Chu, L.; Terrett, J. A.; Doyle, A. G.; MacMillan, D. W. C. *Science* **2014**, *345*, 437−440.

(5) Tellis, J. C.; Primer, D. N.; Molander, G. A. *Science* **2014**, *345*, 433−436.

(6) (a) Terrett, J. A.; Cuthbertson, J. D.; Shurtleff, V. W.; MacMillan, D. W. C. *Nature* **2015**, *524*, 330−334. (b) Corcoran, E. B.; Pirnot, M. T.; Lin, S.; Dreher, S. D.; Dirocco, D. A.; Davies, I. W.; Buchwald, S. L.; MacMillan, D. W. C. *Science* **2016**, *353*, 279−283.

(7) Ye, Y.; Sanford, M. S. *J. Am. Chem. Soc*. **2012**, *134*, 9034−9037.

(8) (a) Kautzky, J. A.; Wang, T.; Evans, R. W.; MacMillan, D. W. C. *J. Am. Chem. Soc*. **2018**, *140*, 6522−6526. (b) Le, C.; Chen, T. Q.; Liang, T.; Zhang, P.; MacMillan, D. W. C. *Science* **2018**, *360*, 1010−1014. (c) Kornfilt, D. J. P.; MacMillan, D. W. C. *J. Am. Chem. Soc*. **2019**, *141*, 6853−6858.

(9) (a) Perepichka, I.; Kundu, S.; Hearne, Z.; Li, C. J. E. *Org. Biomol. Chem.* **2015**, *13*, 447−451. (b) Zhang, H.; Zhang, P.; Jiang, M.; Yang, H.; Fu, H. *Org. Lett*. **2017**, *19*, 1016-1019.

(10) (a) Parasram, M.; Gevorgyan, V. *Chem. Soc. Rev.* **2017**, *46*, 6227−6240. (b) Kancherla, R.; Muralirajan, K.; Sagadevan, A.; Rueping, M. *Trends Chem.* **2019**, *1*, 510−523. (c) Cheng, W. M.; Shang, R. *ACS Catal.* **2020**, *10*, 9170−9196. (d) Shing Cheung, K. P.; Sarkar, S.; Gevorgyan, V. Chem. Rev. **2022**, *122*, 1543−1625.

(11) Parasram, M.; Chuentragool, P.; Sarkar, D.; Gevorgyan, V. *J. Am. Chem. Soc*. **2016**, *138*, 6340−6343.

(12) (a) Sumino, S.; Fusano, A.; Fukuyama, T.; Ryu, I. *Acc. Chem. Res.* **2014**, *47*, 1563−1574. (b) Chuentragool, P.; Kurandina, D.; Gevorgyan, V. *Angew. Chem., Int. Ed.* **2019**, *58*, 11586−11598.

(13) Creutz, S. E.; Lotito, K. J.; Fu, G. C.; Peters, J. C. *Science* **2012**, *338*, 647−651.

(14) Sagadevan, A.; Hwang, K. C. *Adv. Synth. Catal.* **2012**, *354*, 3421−3427.

(15) (a) Hossain, A.; Bhattacharyya, A.; Reiser, O. *Science* **2019**, *364*, eaav9713. (b) Matier, C. D.; Schwaben, J.; Peters, J. C.; Fu, G. C. *J. Am. Chem. Soc*. **2017**, *139*, 17707−17710. (c) Hazra, A.; Lee, M. T.; Chiu, J. F.; Lalic, G. *Angew. Chem., Int. Ed.* **2018**, *57*, 5492−5496.

(16) Kainz, Q. M.; Matier, C. D.; Bartoszewicz, A.; Zultanski, S. L.; Peters, J. C.; Fu, G. C. *Science* **2016**, *351*, 681─684.

(17) (a) Bartoszewicz, A.; Matier, C. D.; Fu, G. C. *J. Am. Chem. Soc*. **2019**, *141*, 14864–14869. (b) Chen, C.; Peters, J. C.; Fu, G. C. *Nature* **2021**, *596*, 250–256. (c) Lee, H.; Ahn, J. M.; Oyala, P. H.; Citek, C.; Yin, H.; Fu, G. C.; Peters, J. C. *J. Am. Chem. Soc*. **2022**, *144*, 4114–4123. (d) Cho, H.; Suematsu, H.; Oyala, P. H.; Peters, J. C.; Fu, G. C. *J. Am. Chem. Soc*. **2022**, *144*, 4550–4558.

(18) Xia, H. D.; Li, Z. L.; Gu, Q. S.; Dong, X. Y.; Fang, J. H.; Du, X. Y.; Wang, L. L.; Liu, X. Y. *Angew. Chem., Int. Ed.* **2020**, *59*, 16926−16932.

(19) Dong, X. Y.; Zhang, Y. F.; Ma, C. L.; Gu, Q. S.; Wang, F. L.; Li, Z. L.; Jiang, S. P.; Liu, X. Y. *Nat. Chem*. **2019**, *11*, 1158−1166.

(20) (a) Qi, R.; Wang, C.; Huo, Y.; Chai, H.; Wang, H.; Ma, Z.; Liu, L.; Wang, R.; Xu, Z. *J. Am. Chem. Soc*. **2021**, *143,* 12777−12783. (b) Chen, J.; Liang, Y.-J.; Wang, P.-Z.; Li, G.-Q.; Zhang, B.; Qian, H.; Huan, X.-D.; Guan, W.; Xiao, W.-J.; Chen, J.-R. *J. Am. Chem. Soc.* **2021**, *143*, 13382−13392. (c) Li, C.; Chen, B.; Ma, X.; Mo, X.; Zhang, G. *Angew. Chem., Int. Ed*. **2021**, *60*, 2130−2134.

(21) (a) Romines, K. R.; Freeman, G. A.; Schaller, L. T.; Cowan, J. R.; Gonzales, S. S.; Tidwell, J. H.; Andrews, C. W.; Stammers, D. K.; Hazen, R. J.; Ferris, R. G. S.; Short, A.; Chan, J. H.; Boone, L. R. *J. Med. Chem.* **2006**, *49*, 727-739. (b) Vooturi, S. K.; Cheung, C. M.; Rybak, M. J.; Firestine, S. M. *J. Med. Chem.* **2009**, *52*, 5020-5031. (c) Cuquerella, M. C.; Lhiaubet-Vallet, V.; Cadet, J.; Miranda, M. A. *Acc. Chem. Res.* **2012**, *45*, 1558-1570. (d) Toh, Q. Y.; McNally, A.; Vera, S.; Erdmann, N.; Gaunt, M. J. *J. Am. Chem. Soc.* **2013**, *135*, 3772-3775.

(22) (a) Gore, P. H. *Chem. Rev.* **1955**, *55*, 229-281. (b) Pearson, D. E.; Buehlr, C. A. *Synthesis*, **1972**, 533-542. (c) Ianni, A.; Waldvogel, S. R. *Synthesis*, **2006**, 2103-2112. (d) Kim, H. Y.; Song, E.; Oh, K. *Org. Lett.* **2017**, *19*, 312-315. (e) Effenberger, F.; Epple, G. *Angew. Chem. Int. Ed. Engl.* **1972**, *77*, 300-301. (f) Yato, M.; Ohwada, T.; Shudo, K. *J. Am. Chem. Soc.* **1991**, *113*, 691-692. (g) Izumi, J.; Mukaiyama, T. *Chem. Lett.* **1996**, 739-740. (h) Brink, G. J. T.; Arends, I. W. C. E.; Sheldon, R. A. *Science* **2000**, *287*, 1636-1639. (i) Miyaura, N.; Suzuki, A. *Chem. Rev.* **1995**, *95*, 2457-2483. (j) Takemiya, A.; Hartwig, J. F. *J. Am. Chem. Soc.* **2006**, *128*, 14800-14801. (k) Willis, M. C. *Chem. Rev.* **2010**, 110, 725-748.

(23) (a) Dieter, R. K. *Tetrahedron* **1999**, *55*, 4177-4236. (b) Fukuyama, T.; Tokuyama, H. *Aldrichimica Acta* **2004**, *37*, 87-96. (c) Gooßen, L. J.; Rodríguez, N.; Gooßen, K. *Angew. Chem., Int. Ed.* **2008**, *47*, 3100–3120.

(24) (a) Nguyen, K. D.; Park, B. Y.; Luong, T.; Sato, H.; Garza, V. J.; Krische, M. J. *Science* **2016**, *354*, aah 5133. (b) Holmes, M.; Schwartz, L. A.; Krische, M. J. *Chem. Rev.* **2018**, *118*, 6026–6052.

(25) Ueda, Y.; Iwai, T.; Sawamura, M. *Chem. Eur. J.* **2019,** *25*, 9410–9414.

(26) (a) Corey, E. J.; Seebach, D. *Angew. Chem. Int. Ed.* **1965**, *4*, 1077-1078. (b) Page, P. C. B.; Vanniel, M. B.; Prodger, J. C. *Tetrahedron* **1989**, *45*, 7643-7677. (c) Smith, A. B.; Adams, C. M. *Acc. Chem. Res.* **2004**, *37*, 365–377.

(27) Yao, K.; Liu, D.; Yuan, Q.; Imamoto, T.; Liu, Y.; Zhang, W. *Org. Lett.* **2016**, *18*, 6296–6299.

(28) (a) Flanigan, D. M.; Romanov-Michailidis, F.; White, N. A.; Rovis, T. *Chem. Rev.* **2015**, *115*, 9307−9387. (b) Hopkinson, M. N.; Richter, C.; Schedler, M.; Glorius, F. *Nature* **2014**, *510*, 485−496. (c) Zhang, C.; Hooper, J. F.; Lupton, D. W. *ACS Catal.* **2017**, *7*, 2583−2596. (d) Bugaut, X.; Glorius, F. *Chem. Soc. Rev.* **2012**, *41*, 3511−3522.

(29) (a) Liu, K.; Hovey, M. T.; Scheidt, K. A. *Chem. Sci.* **2014**, *5*, 4026−4031. (b) Guo, C.; Fleige, M.; Janssen-Müller, D.; Daniliuc, C. G.; Glorius, F. *J. Am. Chem. Soc.* **2016**, *138*, 7840−7843. (c) Guo, C.; Janssen-Müller, D.; Fleige, M.; Lerchen, A.; Daniliuc, C. G.; Glorius, F. *J. Am. Chem. Soc.* **2017**, *139*, 4443−4451. (d) Yasuda, S.; Ishii, T.; Takemoto, S.; Haruki, H.; Ohmiya, H. *Angew. Chem., Int. Ed.* **2018**, *57*, 2938−2942. (e) Takemoto, S.; Ishii, T.; Yasuda, S.; Ohmiya, H. *Bull. Chem. Soc. Jpn.* **2019**, *92*, 937−940. (f) Haruki, H.; Yasuda, S.; Nagao, K.; Ohmiya, H. *Chem. Eur. J.* **2019**, *25*, 724−727. (g) Ohnishi, N.; Yasuda, S.; Nagao, K.; Ohmiya, H. *Asian J. Org. Chem.* **2019**, *8*, 1133−1135. (h) Yang, W.; Ling, B.; Hu, B.; Yin, H.; Mao, J.; Walsh, P. J. *Angew. Chem., Int. Ed.* **2020**, *59*, 161−166. (i) Zhang, Z.-J.; Zhang, L.; Geng, R.-L.; Song, J.; Chen, X.-H.; Gong, L.-Z. *Angew. Chem., Int. Ed.* **2019**, *58*, 12190−12194. (j) Ohmiya, H. *ACS Catal.* **2020**, *10*, 6862−6869.

(30) (a) Caronna, T.; Fronza, G.; Minisci, F.; Porta, O.; Gardini, G. P. *J. Chem. Soc., Perkin Trans. 2* **1972**, 1477-1481. (b) Enders, D.; Niemeier, O.; Henseler, A. *Chem. Rev.* **2007**, *107*, 5606-5655. (c) Duncton, M. A. J. *Med. Chem. Commun.* **2011**, *2*, 1135-1161. (d) Boger, D. L.; Mathvink, R. J. *J. Org. Chem.* **1992**, 57, 1429-1443. (e) Chatgilialoglu, C.; Crich, D.; Komatsu, M.; Ryu, I. *Chem. Rev.* **1999**, *99*, 1991-2070.

(31) (a) Liu, W.; Li, Y.; Liu, K.; Li, Z. *J. Am. Chem. Soc.* **2011**, *133*, 10756-10759. (b) Benati, L.; Calestani, G.; Leardini, R.; Minozzi, M.; Nanni, D.; Spagnolo, P.; Strazzari, S. *Org. Lett.* **2003**, *5*, 1313-1316. (c) Bath, S.; Laso, N. M.; Lopez-Ruiz, H.; Quiclet-Sire, B.; Zard, S. Z. *Chem. Commun.* **2003**, 204-205.

(32) (a) Prier, C. K.; Rankic, D. A.; MacMillan, D. W. C. *Chem. Rev.* **2013**, *113*, 5322-5363. (b) Skubi, K. L.; Blum, T. R.; Yoon, T. P. *Chem. Rev.* **2016**, *116*, 10035-10074. (c) Karkas, M. D.; Porco, J. A.; Stephenson, C. R. J. *Chem. Rev.* **2016**, *116*, 9683-9747. (d) Douglas, J. J.; Sevrin, M. J.; Stephenson, C. R. J. *Org. Process Res. Dev.* **2016**, *20*, 1134-1147.

(33) Zhang, X.; MacMillan, D. W. C. *J. Am. Chem. Soc.* **2017**, *139*, 11353-11356.

(34) (a) Mukherjee, S.; Garza-Sanchez, R. A.; Tlahuext-Aca, A.; Glorius, F. *Angew. Chem. Int. Ed.* **2017**, *56*, 14723. (b) Vu, M. D.; Das, M.; Liu, X. W. *Chem. Eur. J.* **2017**, *23*, 15899-15902. (c) Kawaai, K.; Yamaguchi, T.; Yamaguchi, E.; Endo, S.; Tada, N.; Ikari, A.; Itoh, A. *J. Org. Chem.* **2018**, *83*, 1988-1996.

(35) Ngai, M.-Y.; Banerjee, A.; Lei, Z. *Synthesis* **2019**, *51*, 303–333.

(36) Vogler, A.; Kunkely, H. *Coord. Chem. Rev.* **2000**, *208*, 321− 329.

Chapter 1

Photoinduced Copper-Catalyzed Asymmetric Acylation of Allylic Phosphates with Acylsilanes

Introduction

Transition-metal-catalyzed enantioselective allylic substitutions are important methods for a C–C bond formation with constructing a stereogenic carbon center.[1] The palladium-catalyzed Tsuji–Trost reaction is a pioneering and representative example of catalytic asymmetric allylic couplings, which has been applied to total syntheses of various complex molecules.[2] In addition to palladium catalyst, other metals such as copper, rhodium, iridium, molybdenum, etc. have also been used in recent years for catalytic allylic coupling.[3] In particular, copper is the most studied metal for the catalytic reactions compared to other rare metals, because "copper" is attractive in terms of its low-cost, low-toxic, and abundant presence on earth.[4]

Previously the author's laboratory reported several copper-catalyzed asymmetric allylic substitution reactions using a new chiral *N*-heterocyclic carbene (NHC) ligand bearing a phenolic hydroxyl group.[5] Among them, copper-catalyzed three-component coupling of isocyanides, hydrosilanes, and γ,γ-disubstituted allylic phosphates has been developed for an asymmetric synthesis of α-quaternary formimides.[5d] Since there is the only example of using a special acyl anion equivalent, formimidoyl anion, in copper-catalyzed asymmetric allylic acylation,[6] the author conceived the use of acylsilanes as a more general acylating reagent. The photoisomerization of acylsilanes to siloxycarbene has been known for a long time, and Kusama and co-workers recently reported a series of interesting synthetic reactions utilizing acylsilanes.[7] The author hypothesized that the siloxycarbene formed under photoirradiation could coordinate onto an appropriate copper(I) complex, and the basic ligand on the copper would nucleophilically attack the silicon group to form acylcopper(I) (Scheme 1).

Scheme 1. The strategy for generating acylcopper(I) species

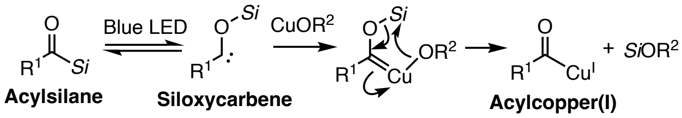

In chapter 1, the author describes the development of a photoinduced copper-catalyzed asymmetric allylic acylation reaction based on this hypothesis. Unlike copper-catalyzed allylic substitution reactions previously reported in the laboratory, the phenolic hydroxyl group was unexpectedly not required for the asymmetric ligand, and the acylcopper(I) complex showed high reactivity and stereoselectivity, while in the neutral reaction conditions. The author assumed that this unusual reactivity was attributed to MLCT photoexcitation of the acyl copper complex.

Working Hypothesis

Prior to the development of this reaction, the author envisioned a reaction pathway that involves the generation of acylcopper(I) species and its photoexcitation as shown in the Scheme 2. The author conceived this study by considering the possibility that acylcopper would be produced by the reaction of CuOtBu and siloxycarbene (Scheme 1). This generated acyl copper (I) complex does not have sufficient nucleophilicity to react with the allylic phosphate. However, irradiation of this species with blue LED results to a MLCT from the copper(I) center to the acyl ligand leading to the formation of copper(II) complex consisting of a cationic copper(II) and a ketyl radical-type ligand. The cationic copper(II) center then captures and activates the leaving group of the allylic phosphate substrate as a Lewis acid, and at the same time, a nucleophilic carbon radical at the ketyl radical site is added to the allylic substrate to form β,γ-unsaturated ketone and copper(I) phosphate. Similar to CuOtBu, this complex also reacts with siloxycarbene to regenerate acyl copper(I) complex and establishes a complete catalytic cycle.

Scheme 2. Plausible reaction pathway for photoinduced Cu-catalyzed asymmetric allylic acylation

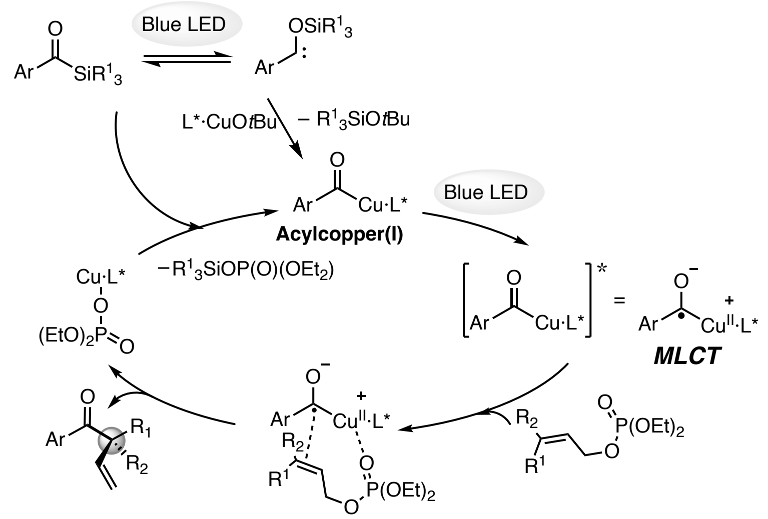

Result and Discussion

Based on the working hypothesis, the author commenced the initial reaction development by investigating the coupling between benzoyltrimethylsilane (**1a**, 0.15 mmol) and (Z)-allylicphosphate **2a** (0.15 mmol) with a combination of CuCl (10 mol %), achiral ligands (12 mol %), and NaOtBu (10 mol %) in THF at 25 °C under blue LED photoirradiation (465 nm) over 12 h (Table 1, entries 1-7). The employment of Cu(I) as a metal center was inspired by the ubiquitous MLCT activities of d^{10} Cu(I) complexes involving π-acceptor ligands[8] and by successful utilizations of chiral copper(I) complexes for enantioselective γ-selective allylic substitution reactions.[9] While phosphine- and pyridine-based ligands did not induce any reactivity (entries 1−3), N-heterocyclic carbene (NHC) ligand IMes (1,3-dimesitylimidazol-2-ylidene, as 1:1 IMes· HCl/NaOtBu) caused complete consumption of the acylsilane (**1a**), producing the γ-acylation product (**3aa**) in 33% yield based on ^{1}H NMR analysis (entry 4). The low yield of **3aa** was due to side reactions of the photochemically produced siloxycarbene intermediate generating diacyl **4** and acyloin **5**. Other NHC ligands (SIMes·HCl, IPr·HCl) were also examined, but the yield did not improve (entry 5,6). The allylic acylation product **3aa** (20%) was produced even at −40 °C with complete consumption of **1a**, suggesting the generation of a highly reactive organocopper species (entry 7).

Table 1. Achiral ligand screening of photoinduced copper-catalyzed asymmetric allylic acylation.

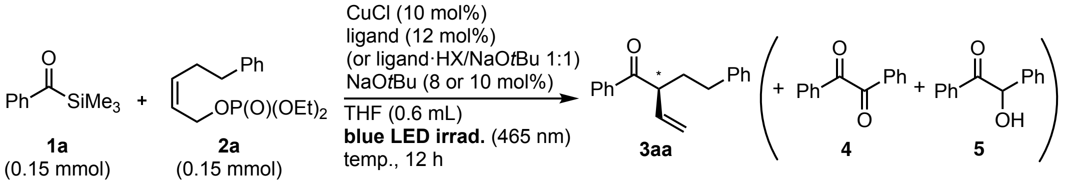

entry	ligand	temp. ºC	Yield of **3aa** %[a]
1[b]	PPh_3	25	0
2[b]	DPPBz	25	0
3[b]	dtbpy	25	0
4[c]	IMes·HCl/NaO*t*Bu	25	33
5[c]	SIMes·HCl/NaO*t*Bu	25	33
6[c]	IPr·HCl/NaO*t*Bu	25	33
7[c]	IMes·HCl/NaO*t*Bu	–40	20

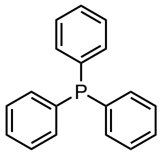

PPh_3

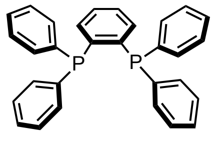

DPPBz

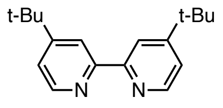

dtbpy

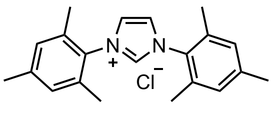

IMes·HCl

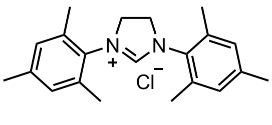

SIMes·HCl

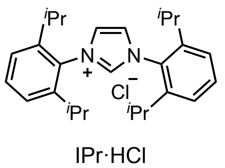

IPr·HCl

[a] Yield determined by ^{1}H NMR analysis. [b] Conditions: **1a** (0.15 mmol), **2a** (0.15 mmol), CuCl (10 mol%), ligand (12 mol%), NaO*t*Bu (10 mol%), THF (0.60 mL), blue LED irradiation, 12 h. [c] Conditions: **1a** (0.15 mmol), **2a** (0.15 mmol), CuCl (10 mol%), NHC·HX (12 mol%), NaO*t*Bu (20 mol%), THF (0.60 mL), blue LED irradiation, 12 h.

Next, various chiral NHC ligands with a (*S,S*)-1,2-diphenylethylenediamine backbone were employed toward developing an enantioselective reaction (Table 2). Surprisingly, the simple C_2-symmetric *N,N′*-diphenyl NHC ligand (**L1**) gave enantioenriched **3aa** with an enantiomeric excess (ee) as high as 85% in favor of the *S* configuration in 51% yield (entry 1). *N,N′*- Dimesityl ligand **L2** gave an even better chemical yield (60%) with slightly decreased enantioselection (81% ee) (entry 2). Ligand modification at one of the two N-aryl groups with the other remaining as the mesityl group (entry 3-7) identified the o-MeO-Ph- substituted ligand (**L4**) as the optimal ligand, providing excellent enantioselectivity (98% ee) with good chemical yield (61%) (entry 4). When the more compact ligand **L8** was used, in which the mesityl group of **L4** was replaced by a Ph group, the yield and enantioselectivity were decreased (entry 8). The author also examined a chiral NHC ligand with a phenolic hydroxyl group previously developed in the author's laboratory (entry 9-12). The ligand **L12**, which is structurally similar to **L4** and has 2-hydroxyphenyl and mesityl groups on the nitrogen atom of the imidazolium salt, also showed good yields and high stereoselectivity (entry 9). Contrary to the results of previous studies, the phenolic hydroxyl group of the ligand was not required in this reaction, and the acylcopper(I) complex showed high reactivity even in the neutral conditions. This result supports the hypothesis, that photoexcitation of the copper center acquires the unusual reactivity. The author also studied several structures of NHC ligands with phenolic hydroxyl groups, referring to previous reports, but failed to improve yield and stereoselectivity (entry 10-12). Finally, a quantitative yield of **3aa** based on the allylic phosphate (**2a**) was achieved by using 2 equiv of the acylsilane (**1a**) without affecting the enantioselectivity (98% ee). Diacyl **4** (0.014 mmol) and acyloin **5** (0.006 mmol) were also obtained as byproducts (entry 13). No reaction occurred without blue LED irradiation under the same conditions leaving both substrates intact (entry 14).

Table 2. Chiral NHC ligand screening of photoinduced copper-catalyzed asymmetric allylic acylation.

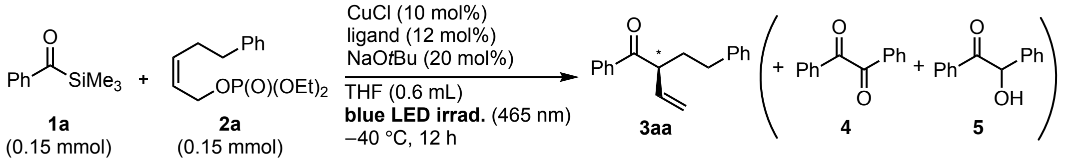

entry	ligand	3aa yield, %[a]	 ee, %[b]
1[c]	**L1**·HBF_4/NaO*t*Bu	51	85
2[c]	**L2**·HBF_4/NaO*t*Bu	60	81
3[c]	**L3**·HBF_4/NaO*t*Bu	60	97
4[c]	**L4**·HBF_4/NaO*t*Bu	61	98
5[c]	**L5**·HBF_4/NaO*t*Bu	43	96

6^c	**L6**·HBF$_4$/NaO*t*Bu	62	97
7^c	**L7**·HBF$_4$/NaO*t*Bu	62	97
8^c	**L8**·HBF$_4$/NaO*t*Bu	46	92
9^c	**L9**·HBF$_4$/NaO*t*Bu	71	96
10^c	**L10**·HBF$_4$/NaO*t*Bu	64	96
11^c	**L11**·HBF$_4$/NaO*t*Bu	37	86
12^c	**L12**·HBF$_4$/NaO*t*Bu	24	46
13^{c,d}	**L4**·HBF$_4$/NaO*t*Bu	quant (93)^e	98
14^f	**L4**·HBF$_4$/NaO*t*Bu	N.R.	-

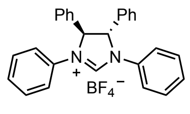

L1·HBF$_4$

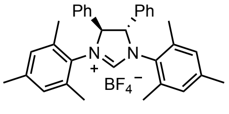

L2·HBF$_4$

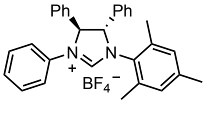

L3·HBF$_4$

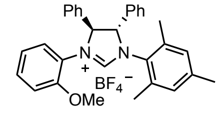

L4·HBF$_4$

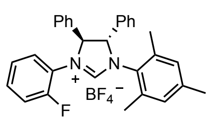

L5·HBF$_4$

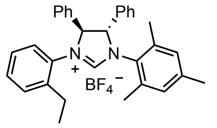

L6·HBF$_4$

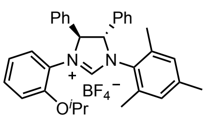

L7·HBF$_4$

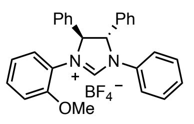

L8·HBF$_4$

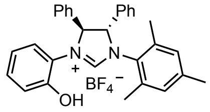

L9·HBF$_4$

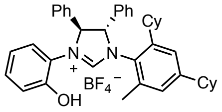

L10·HBF$_4$

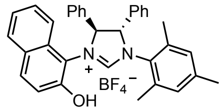

L11·HBF$_4$

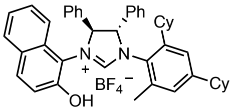

L12·HBF$_4$

[a] Yield determined by ^{1}H NMR analysis. [b] Enantiomeric excess determined by chiral HPLC analysis. [c] Conditions: **1a** (0.15 mmol), **2a** (0.15 mmol), CuCl (10 mol%), NHC·HX (12 mol%), NaOtBu (20 mol%), THF (0.60 mL), blue LED irradiation, 12 h. [d] 2.0 equiv of **1a** (0.30 mmol) were used. [e] Yield of isolated product. [f] Conditions: **1a** (0.15 mmol), **2a** (0.15 mmol), CuCl (10 mol%), NHC·HX (12 mol%), NaOtBu (20 mol%), THF (0.60 mL), No blue LED irradiation, 12 h, 25 °C

Next, the effect of silyl group on acylsilane was investigated (Table 3). When the trimethylsilyl (TMS) group was replaced with triethylsilyl (TES) group, no significant change was observed in yield and enantioselectivity (entry 1,2). When bulkier *t*-butyldimethylsilyl (TBS) and triisopropylsilyl (TIPS) groups were used instead of TMS groups, yield of **3aa** was significantly reduced, while enantioselectivity remined high (entry 3, 4). This result suggests that the silyl group is not involved in the enantioselectivity determination step.

The effect of solvent is also shown in Table 3. Reaction in toluene gave better yield of **3aa** than in THF (entry 5). Dichloromethane (DCM) and acetonitrile (MeCN) were ineffective in the reaction (entry 6,7). Although the reaction proceeded with high stereoselectivity in any solvents, it was not as good as in THF.

Table 3. Effect of silyl group and solvents [a]

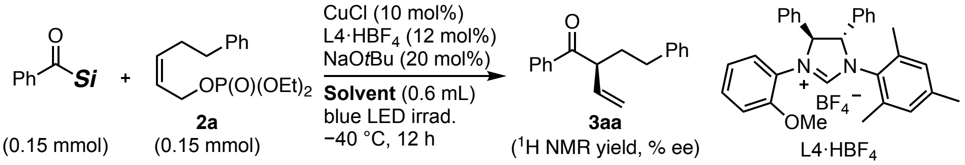

entry	*Si*	solvent	yield, %[b]	ee, %[c]
1	**TMS**	**THF**	**61**	**98**
2	TES	THF	60	97
3	TBS	THF	32	97
4	TIPS	THF	0	-
5	TMS	Toluene	70	97
6	TMS	DCM	39	97
7	TMS	MeCN	53	96

[a] Conditions: acylsilane (0.15 mmol), **2a** (0.15 mmol), CuCl (10 mol%), L4·HBF$_4$ (12 mol%), NaOtBu (20 mol%), Solvent (0.60 mL), blue LED irradiation, 12 h. [b] Yield determined by ^{1}H NMR analysis. [c] Enantiomeric excess determined by chiral HPLC analysis.

The effect of leaving group of allylic substrate was summarized in Table 4. The use of allyl ester, acetate or chloride as an allylic electrophile under the conditions described for entry 1, decreased both yield and enantioselectivity (entries 2-4). The alkene configuration affected the enantioselectivity, e.g., (E)-2a afforded (S)-3aa in 53% yield with diminished enantiomeric excess (62% ee) as was the case for the previous report.

Table 4. Effect of leaving group [a]

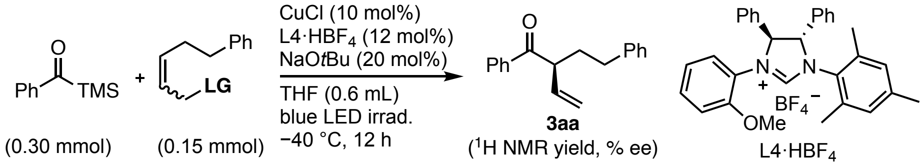

entry	allylic substrate	yield, %[b]	ee, %[c]
1	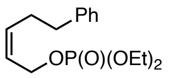	**quant**	**98**

2	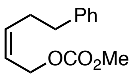	0	-
3	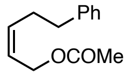	0	-
4	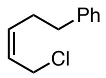	19	91
5	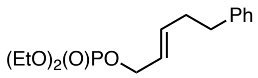	53	62

[a] Conditions: **1a** (0.30 mmol), allylic substrate (0.15 mmol), CuCl (10 mol%), L4·HBF$_4$ (12 mol%), NaOtBu (20 mol%), THF (0.60 mL), blue LED irradiation, −40 °C, 12 h. [b] Yield determined by ^{1}H NMR analysis. [c] Enantiomeric excess determined by chiral HPLC analysis.

With the optimal conditions in hand, the author explored the generality of the reaction with different acylsilanes (**1**) and allylic phosphates (**2**) (Table 5). Benzoyltrimethylsilanes (**1b**–**1e**) with electron-withdrawing or -donating substituents at the para position reacted with **2a** to give the products **3ba**–**3ea** in high yields with excellent enantioselectivities. In particular, the p-fluorobenzoylsilane **2b** reacted with virtually perfect enantioselectivity (>99.9% ee). Various disubstituted benzoylsilanes (**1f**–**1h**) served as suitable substrates to give the corresponding products (**3fa**—**3ha**). The protocol was also applicable to acylsilanes with a more ex-tended π system or a heterocycle (**3ia**, **3ja**). An acylsilane derived from Probenecid, a uricosuric drug, participated in this reaction to afford **3ka** with 90% ee. Alkanoylsilanes are known to isomerize to siloxycarbenes by energy transfer from a suitable photocatalyst under visible light irradiation conditions.[10] The author investigated the reaction of alkanoylsilanes under the conditions with an Ir photocatalyst, but the reaction did not proceed (**3la, 3ma**).

The scope of allylic phosphates [(*Z*)-**2**] with a *Z* configuration was investigated employing **1a** as a coupling partner (Table 5A). The allylic phosphate with a *γ*-Me substituent (**2b**) reacted cleanly with **1a** to afford *α*-methyl-branched ketone **3ab** with 97% ee (*S*) in 71% yield. The *S* configuration of **3ab** was determined by comparing the specific rotation with the literature data[11] and was used as the basis of configuration assignment for the other α-tertiary β,γ-unsaturated ketones (**3**). The protocol showed a broad functional group compatibility as demonstratedby the preparation of **3ac**–**3ak**. For instance, allylic phosphates bearing pivalate (**2c**), *p*-toluenesulfonate (**2d**), 1,3-benzodioxole (**2e**), and silyl ether (**2f**) groups in the aliphatic *γ*-substituent reacted with **1a** to afford the corresponding ketones (**3ac**–**3af**) in good to high yields with excellent enantioselectivities (87–98% ee). Bromo (-Br), trifluoromethyl (-CF_3), cyano (-CN), and dimethylamino (-NMe_2) substitutions were tolerated on the aromatic ring of benzoate-substituted phosphate substrates (**2g**–**2j**). The compatibility of a cyclic carbamate was indicated by the efficient formation of **3ak** (92% yield, 93% ee). The significant tolerance of the protocol toward steric demand was demonstrated by the synthesis of *α*-phenyl- or *α*-cyclohexyl-branched ketones (**3al**, 70% yield, 95% ee; **3am**, 90% yield, 99% ee).

The protocol was also applicable to the construction of quaternary asymmetric carbon centers (Table 5B). The reactions of **1a** with allylic phosphate (*Z*)-**2n** having *γ*-methyl and *γ*-2-phenylethyl groups occurred with exclusive *γ*-selectivity and high enantioselectivity (85% ee), affording the corresponding *α*-quaternary *β,γ*-unsaturated ketone (**3an**) in 52% yield. The *γ*-methyl-*γ*-prenylmethyl-substituted allylic phosphate [(*Z*)-**2o**] also reacted for generating a quaternary asymmetric center (**3ao**, 47% yield, 78% ee).

Table 5. Scope of the photoinduced copper-catalyzed asymmetric allylic acylation constructing tertiary (a) and quaternary (b) stereogenic centers [a]

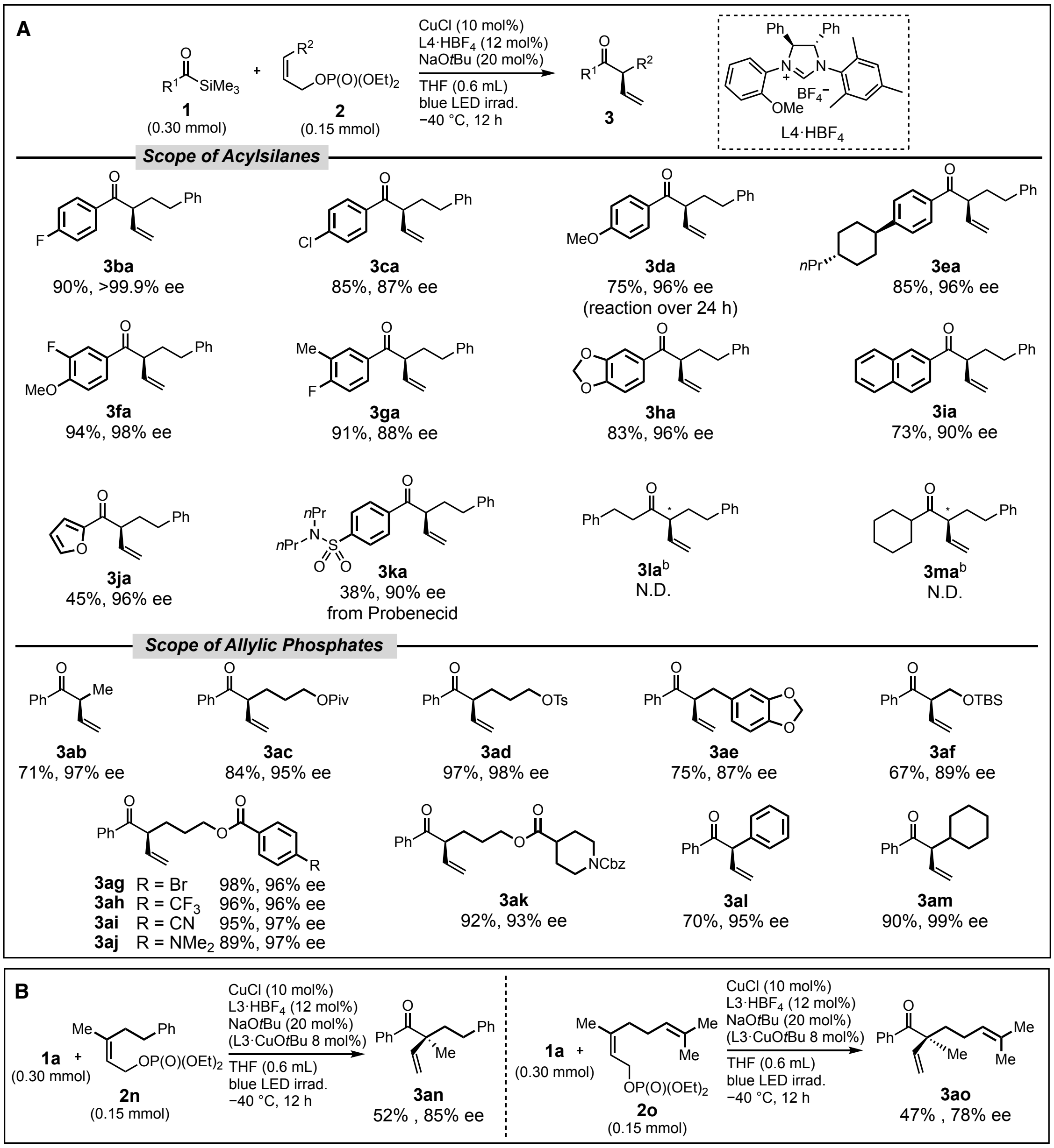

[a] Conditions: **1a**–**1m** (0.30 mmol), **2a**–**2o** (0.15 mmol), CuCl (10 mol%), **L3**·HBF_4 (12 mol%), NaO*t*Bu (20 mol%), THF (0.60 mL), blue LED irradiation (465 nm), 12 h. Yields of isolated products (**3**) are reported. [b] 2 mol% of $[Ir\{dFCF_3ppy\}_2(bpy)]PF_6$ was added.

Conclusion

In summary, the author developed a photoinduced copper-catalyzed asymmetric acylation of allylic phosphates with acyl silanes. The reaction was promoted by a copper(I)/chiral NHC catalyst under visible light irradiation, affording *α*-stereogenic *β,γ*-unsaturated ketones with excellent enantioselectivity. Unlike copper-catalyzed asymmetric allylic substitution reactions previously reported, this reaction does not require a phenolic hydroxyl group on the chiral NHC ligand. Based on these results, the author assumes that the acylcopper(I) intermediate formed *in situ* is converted into a highly active species by MLCT photoexcitation, and further mechanistic investigations are discussed in Chapter 2.

Experimental Section

Instrumentation and Chemicals

NMR spectra were recorded on a JEOL ECX-400, operating at 400 MHz for ^{1}H NMR, 101 MHz for ^{13}C NMR. Chemical shift values for ^{1}H NMR and ^{13}C NMR are referenced to Me_4Si (0.00 ppm for ^{1}H NMR) and $CDCl_3$ (77.0 ppm for ^{13}C NMR). Chemical shifts are reported in δ ppm. High-resolution mass spectra were recorded at the Instrumental Analysis Division, Global Facility Center, Creative Research Institution, Hokkaido University (Thermo Fisher Scientific Exactive or JEOL JMS-T100LP for ESI-MS) and the GC–MS & NMR Laboratory, Research Faculty of Agriculture, Hokkaido University (JEOL JMS-T100GCv for FD-MS). HPLC analyses were conducted on a HITACHI ELITE LaChrom system with a HITACHI L-2455 diode array detector. Optical rotations were measured on a JASCO P-2200. TLC analyses were performed on commercial glass plates bearing 0.25-mm layer of Merck Silica gel $60F_{254}$. Silica gel (Kanto Chemical Co., Silica gel 60 N, spherical, neutral) was used for column chromatography. IR spectra were measured with a PerkinElmer Frontier instrument.

All reactions were carried out under nitrogen or argon atmosphere. Materials were obtained from commercial suppliers or prepared according to standard procedures unless otherwise noted. CuCl was purchased from Aldrich Chemical Co., stored under nitrogen, and used as received. THF was purchased from Kanto Chemical Co., and purified by passing through activated alumina under positive argon pressure as described by Grubbs *et al.*[12] NaO*t*Bu was purchased from TCI Chemical Co., stored under nitrogen, and used as received.

Preparation of Substrates and Ligands

Substrates

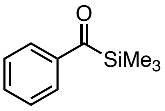
1a

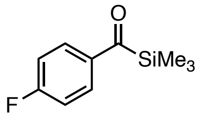
1b

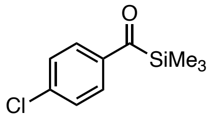
1c

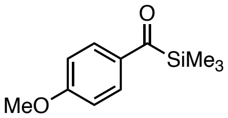
1d

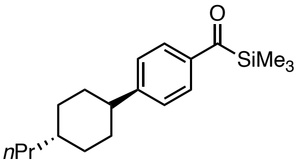
1e

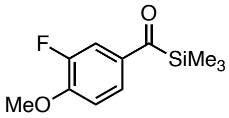
1f

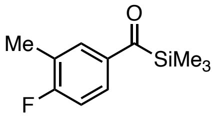
1g

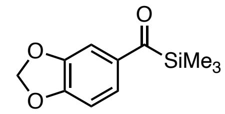
1h

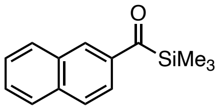
1i

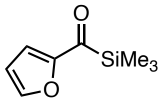
1j

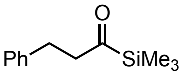
1l

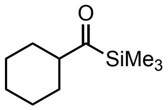
1m

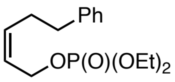
2a

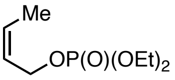
2b

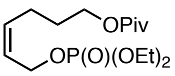
2c

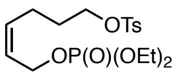
2d

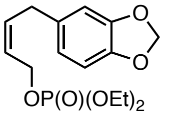
2e

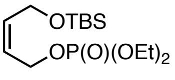
2f

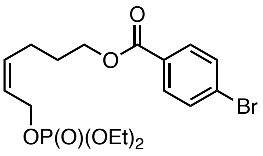
2g

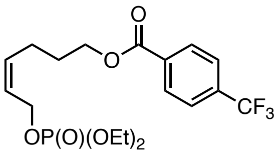
2h

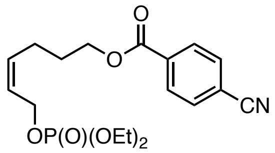
2i

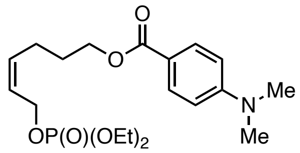
2j

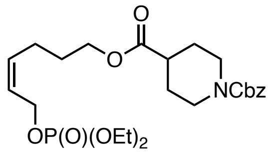
2k

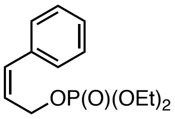
2l

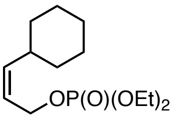
2m

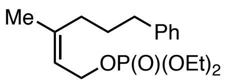
2n

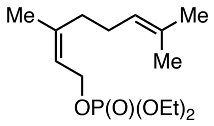
2o

Figure 1. Substrates utilized in this work.

Acylsilanes **1a**-**1l**[7d,7e,10,13] and allylic phosphates **2a**-**2o**[5,14] were synthesized according to the literature methods.

Ligands

The preparation of the chiral NHC ligands was previously reported.[5,14] See the section for reaction optimization for the variants of this ligand system.

Synthesis of Acylsilane 1k

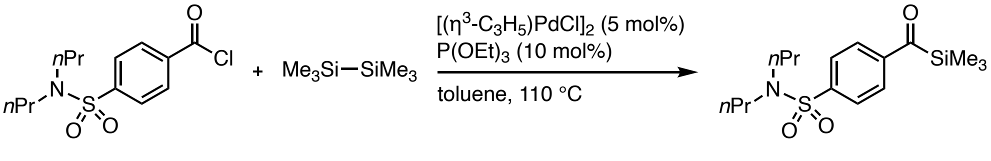

Acylsilane **1k** were prepared according to reported literature.[13b] Acid chloride (304 mg, 10.0 mmol) was added in dropwise to a stirred solution of allylpalladium chloride dimer (183 mg, 0.50 mmol, 5 mol%), triethyl phosphite (166 mg, 1.0 mmol, 10 mol%), and hexamethyldisilane (2.4 g, 16.5 mmol, 1.65 equiv) in toluene (6 mL) at 0 °C. This mixture was stirred overnight at 110 °C in an oil bath. After cooling to room temperature, the reaction was transferred to eggplant flask and concentrated under reduced pressure. The product was isolated by silica gel column chromatography with hexane/CH_2Cl_2 (50:50) as yellow oil (511 mg, 1.5 mmol, 15% yield).

N,*N*-dipropyl-4-((trimethylsilyl)carbonyl)benzenesulfonamide (1k)

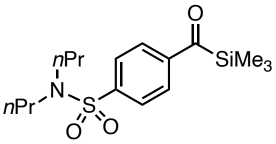

^{1}H NMR (400 MHz, $CDCl_3$): δ 7.92 (s, 4H), 3.11 (t, J = 7.8 Hz, 4H), 1.62–1.51 (m, 4H), 0.88 (t, J = 7.4 Hz, 6H), 0.39 (s, 9H); **^{13}C NMR** (101 MHz, $CDCl_3$): δ 235.4, 143.4, 143.2, 127.7 (2C), 127.4 (2C), 49.9 (2C), 21.9 (2C), 11.1 (2C), −1.6 (3C); **IR** (ATR): 2966, 2877, 1617, 1589, 1561, 1467, 1394, 1341, 1291, 1251, 1198, 1173, 1155, 1088, 1041, 991, 937, 838, 797, 776, 743, 701, 677 cm^{-1}; **HRMS** (ESI) *m/z* : $[M+Na]^+$ Calcd for $C_{16}H_{27}NNaO_3SSi$ 364.13786, found 364.13673.

Reaction Setup

Reaction vials were irradiated with a photo-reactor Kessil A 160 WE Tuna Blue 40W (λmax = 465 nm) in the constant temperature bath filled with 2-propanol. Blue LED lamp was placed **at a distance of 5 cm** diagonally above the reaction vials to allow all vials to be evenly exposed to light. The entire reaction apparatus was covered with aluminum foil (Figure 2). (*Note*: Longer distances between the LED lamp and the reaction vials, for example 15 cm, resulted in the lower product yield.)

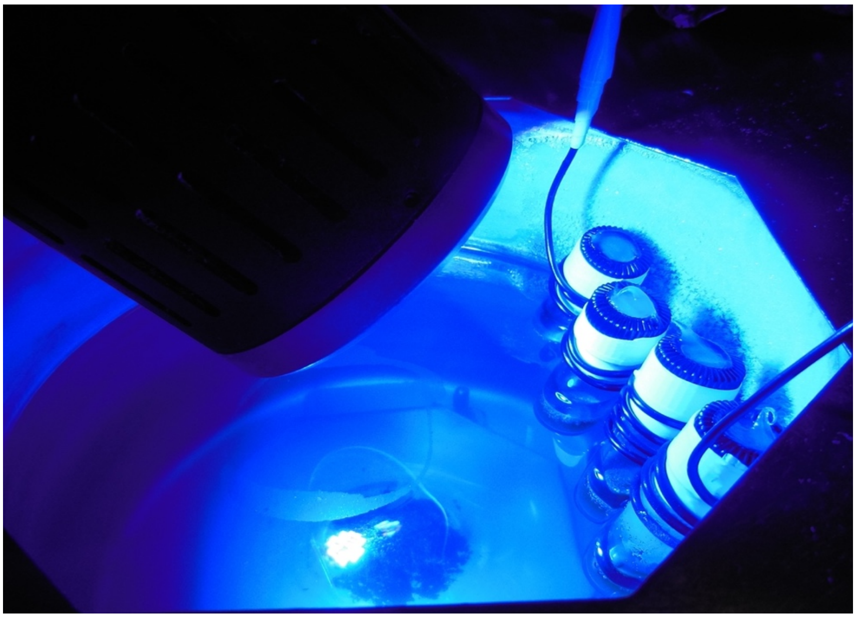

Figure 2. Photoreaction Setup.

Substrate Scope

General Procedure for the Cu-Catalyzed Asymmetric Allylic Acylation Reaction.

In a N_2-filled glove box, CuCl (1.5 mg, 0.015 mmol), **L3**·HBF_4 (9.6 mg, 0.018 mmol), and NaO^{t}Bu (2.9 mg, 0.030 mmol) were placed in a vial containing a magnetic stirring bar. THF (0.6 mL) was added to the vial, which was sealed with a cap and was removed from the glove box. The mixture was stirred at room temperature for 10 min. Next, allylic phosphate **2** (0.15 mmol) and acylsilane **1** (0.30 mmol) were added *via* a syringe. After 12 h stirring at –40 °C under blue LED irradiation, the reaction mixture was diluted with Et_2O and filtered through a pad of silica gel (eluting with Et_2O). The volatiles were removed under vacuum, and then an internal standard (dibenzyl) was added to determine the ^{1}H NMR yield. The crude product was purified by silica gel column chromatography. Enantiomeric excess of the products was determined by HPLC analysis with a chiral stationary phase column.

(*S*)-2-Phenethyl-1-phenylbut-3-en-1-one (3aa)

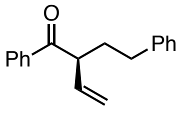

The product was isolated by silica gel column chromatography with hexane/EtOAc (99:1 to 90:10) as a colorless oil (34.9 mg, 0.14 mmol, 93% yield). The ee value (98% ee) was determined by HPLC analysis [CHIRALCEL® IA-3 column, 4.6 mm × 250 mm, Daicel Chemical Industries, hexane/2-propanol 99.0:1.0, 1.0 mL/min, 40 °C, 254 nm UV detector, retention time = 7.4 min for the *S* isomer and 8.3 min for the *R* isomer]. **^{1}H NMR** (400 MHz, $CDCl_3$): δ 7.88 (d, *J* = 6.8 Hz, 2H), 7.55 (t, *J* = 7.2 Hz, 1H), 7.43 (t, *J* = 7.6 Hz, 2H), 7.30–7.23 (m, 2H), 7.22–7.15 (m, 3H), 5.98–5.88 (m, 1H), 5.22–5.16 (m, 2H), 4.04 (q, *J* = 7.2 Hz, 1H), 2.72–2.59 (m, 2H), 2.28–2.18 (m, 1H), 1.98–1.89 (m, 1H); **^{13}C NMR** (101 MHz, $CDCl_3$): δ 200.7, 141.5, 136.8, 136.5, 133.0, 128.6 (4C), 128.44 (2C), 128.39 (2C), 126.0, 118.1, 50.7, 33.4, 33.2; **IR** (ATR): 3062, 3027, 2929, 2859, 1679, 1634, 1597, 1497, 1448, 1337, 1221, 1179, 1075, 1029, 993, 971, 920, 847, 749, 697 cm^{-1}; **HRMS** (ESI) *m/z* : $[M+Na]^+$ Calcd for $C_{18}H_{18}NaO$ 273.12553, found 273.12499; $[\alpha]_D^{25}$ = +60.9 (*c* = 1.0, $CHCl_3$).

(*S*)-1-(4-Fluorophenyl)-2-phenethylbut-3-en-1-one (3ba)

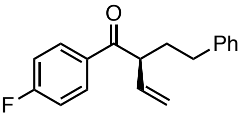

The product was isolated by silica gel column chromatography with hexane/EtOAc (99:1 to 90:10) as a colorless oil (36.2 mg, 0.14 mmol, 90% yield). The ee value (>99.9% ee) was determined by HPLC analysis [CHIRALCEL® OD-3 column, 4.6 mm × 250 mm, Daicel Chemical Industries, hexane/2-propanol 99.0:1.0, 1.0 mL/min, 40 °C, 254 nm UV detector, retention time = 8.5 min for the *S* isomer and 9.6 min for the *R* isomer]. **^{1}H NMR** (400 MHz, $CDCl_3$): δ 7.92–7.87 (m, 2H), 7.31–7.25 (m, 2H), 7.22–7.14 (m, 3H), 7.09 (t, *J* = 8.4 Hz, 2H), 5.96–5.86 (m, 1H), 5.23–5.16 (m, 2H), 3.97 (q, *J* = 7.6 Hz, 1H), 2.72–2.59 (m, 2H), 2.27–2.18 (m, 1H), 1.98–1.89 (m, 1H); **^{13}C NMR** (101 MHz, $CDCl_3$): δ 199.0, 165.7 (d, *J* = 255 Hz), 141.4, 136.6, 132.8, 131.1 (d, *J* = 10 Hz, 2C), 128.6 (2C), 128.4 (2C), 126.0, 118.2, 115.6 (d, *J* = 22 Hz, 2C), 50.6, 33.4, 33.1; **IR** (ATR): 3064, 3027, 2929, 2850, 1681, 1634, 1597, 1506, 1458, 1408, 1335, 1297, 1224, 1155, 1100, 1030, 994, 971, 921, 845, 747, 699, 641 cm^{-1}; **HRMS** (ESI) *m/z* : $[M+Na]^+$ Calcd for $C_{18}H_{17}FNaO$ 201.11611, found 291.11556. $[\alpha]_D^{25}$ = +52.9 (*c* = 1.0, $CHCl_3$).

(*S*)-1-(4-Chlorophenyl)-2-phenethylbut-3-en-1-one (3ca) [15]

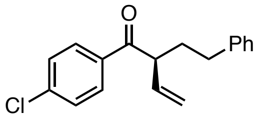

The product was isolated by silica gel column chromatography with hexane/EtOAc (99:1 to 90:10) as yellow solids (36.3 mg, 0.13 mmol, 85% yield). The ee value (87% ee) was determined by chiral HPLC analysis [CHIRALCEL® OD-3 column, 4.6 mm × 250 mm, Daicel Chemical Industries, hexane/2-propanol 99.0:1.0, 1.0 mL/min, 40 °C, 254 nm UV detector, retention time = 9.2 min for the *R* isomer and 10.3 min for the *S* isomer]. **^{1}H NMR** (400 MHz, $CDCl_3$): δ 7.79 (d, J = 8.8 Hz, 2H), 7.39 (d, J = 8.0 Hz, 2H), 7.31–7.28 (m, 2H), 7.22–7.19 (m, 1H), 7.15 (d, J = 7.2 Hz, 2H), 5.95–5.85 (m, 1H), 5.23–5.16 (m, 2H), 3.96 (q, J = 7.6 Hz, 1H), 2.72–2.59 (m, 2H), 2.26–2.16 (m, 1H), 1.96–1.88 (m, 1H); **^{13}C NMR** (101 MHz, $CDCl_3$): δ 199.4, 141.3, 139.5, 136.4, 134.7, 129.9 (2C), 128.8 (2C), 128.6 (2C), 128.4 (2C), 126.0, 118.4, 50.6, 33.3, 33.0; $[\alpha]_D^{25}$ = +36.8 (c = 1.0, $CHCl_3$). Spectral data match those reported in the literature.[15]

(*S*)-1-(4-Methoxyphenyl)-2-phenethylbut-3-en-1-one (3da)

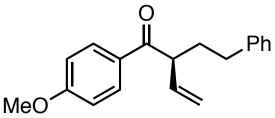

The product was isolated by silica gel column chromatography with hexane/EtOAc (99:1 to 90:10) as white solids (29.4 mg, 0.11 mmol, 75% yield). The ee value (96% ee) was determined by HPLC analysis [CHIRALCEL® IA-3 column, 4.6 mm × 250 mm, Daicel Chemical Industries, hexane/2-propanol 99.0:1.0, 1.0 mL/min, 40 °C, 254 nm UV detector, retention time = 14.4 min for the *R* isomer and 19.1 min for the *S* isomer]. **^{1}H NMR** (400 MHz, $CDCl_3$): δ 7.87 (d, J = 8.8 Hz, 2H), 7.30–7.26 (m, 2H), 7.22–7.14 (m, 3H), 6.90 (d, J = 7.2 Hz, 2H), 5.97–5.88 (m, 1H), 5.20–5.15 (m, 2H), 3.99 (q, J = 7.6 Hz, 1H), 3.87 (s, 3H), 2.67–2.58 (m, 2H), 2.24–2.18 (m, 1H), 1.97–1.87 (m, 1H); **^{13}C NMR** (101 MHz, $CDCl_3$): δ 199.2, 163.4, 141.6, 137.1, 130.7 (2C), 129.5, 128.6 (2C), 128.4 (2C), 125.9, 117.7, 113.7 (2C), 55.4, 50.3, 33.5, 33.2; **IR** (ATR): 3065, 3020, 2951, 2926, 2863, 2837, 2047, 1663, 1632, 1600, 1573, 1509, 1494, 1459, 1436, 1423, 1346, 1317, 1263, 1209, 1176, 1027, 988, 923, 859, 843, 820, 766, 741, 697, 640 cm^{-1}; **HRMS** (ESI) *m/z* : $[M+Na]^+$ Calcd for $C_{19}H_{20}NaO_2$ 303.13610, found 303.13555; $[\alpha]_D^{25}$ = +31.3 (c = 1.0, $CHCl_3$).

(*S*)-2-Phenethyl-1-(4-(*trans*-4-propylcyclohexyl)phenyl)but-3-en-1-one (3ea)

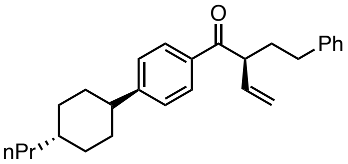

The product was isolated by silica gel column chromatography with hexane/EtOAc (99:1 to 90:10) as white solids (47.8 mg, 0.13 mmol, 85% yield). The ee value (96% ee) was determined by HPLC analysis [CHIRALCEL® IG-3 column, 4.6 mm × 250 mm, Daicel Chemical Industries, hexane/2-propanol 99.0:1.0, 1.0 mL/min, 40 °C, 254 nm UV detector, retention time = 16.0 min for the *S* isomer and 24.2 min for the *R* isomer]. **^{1}H NMR** (400 MHz, $CDCl_3$): *δ* 7.81 (d, *J* = 8.4 Hz, 2H), 7.30–7.22 (m, 4H), 7.21–7.13 (m, 3H), 5.99–5.87 (m, 1H), 5.20–5.15 (m, 2H), 4.03 (q, *J* = 7.6 Hz, 1H), 2.71–2.48 (m, 3H), 2.27–2.16 (m, 1H), 1.97–1.83 (m, 4H), 1.50–1.18 (m, 8H), 1.12–0.99 (m, 2H), 0.90 (t, *J* = 7.2 Hz, 3H); **^{13}C NMR** (101 MHz, $CDCl_3$): *δ* 200.2, 153.6, 141.6, 137.0, 134.3, 128.6 (2C), 128.5 (2C), 128.3 (2C), 127.0 (2C), 125.9, 117.8, 50.6, 44.7, 39.6, 33.9 (2C), 33.5, 33.3 (3C), 33.2, 20.0, 14.4; **IR** (ATR): 3031, 2953, 2923, 2850, 1670, 1629, 1603, 1569, 1497, 1449, 1417, 1361, 1295, 1256, 1209, 1183, 994, 921, 849, 834, 744, 700, 673 cm^{-1}; **HRMS** (ESI) *m/z* : $[M+Na]^+$ Calcd for $C_{27}H_{34}NaO$ 397.25074, found 397.25019; $[\boldsymbol{\alpha}]_{\boldsymbol{D}}^{\mathbf{25}}$ = +25.9 (*c* = 1.0, $CHCl_3$).

(*S*)-1-(3-Fluoro-4-methoxyphenyl)-2-phenethylbut-3-en-1-one (3fa)

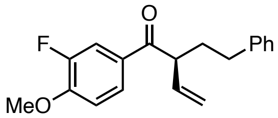

The product was isolated by silica gel column chromatography with hexane/EtOAc (98:2 to 80:20) as white solids (44.1 mg, 0.14 mmol, 94% yield). The ee value (98% ee) was determined by HPLC analysis [CHIRALCEL® IG-3 column, 4.6 mm × 250 mm, Daicel Chemical Industries, hexane/2-propanol 97.0:3.0, 1.0 mL/min, 40 °C, 254 nm UV detector, retention time = 14.0 min for the *S* isomer and 19.1 min for the *R* isomer]. **^{1}H NMR** (400 MHz, $CDCl_3$): *δ* 7.68–7.60 (m, 2H), 7.31–7.27 (m, 2H), 7.24–7.14 (m, 3H), 6.95 (t, *J* = 8.6 Hz, 1H), 5.96–5.82 (m, 1H), 5.22–5.13 (m, 2H), 3.97–3.89 (m, 4H), 2.69–2.57 (m, 2H), 2.27–2.16 (m, 1H), 1.97–1.87 (m, 1H); **^{13}C NMR** (101 MHz, $CDCl_3$): *δ* 198.3, 151.9 (d, *J* = 248 Hz), 151.8 (d, *J* = 12 Hz), 141.4, 136.8, 129.7, 128.5 (2C), 128.4 (2C), 126.0, 125.7 (d, *J* = 3 Hz), 118.1, 116.1 (d, *J* = 19 Hz), 112.2, 56.2, 50.3, 33.4, 33.1; **IR** (ATR): 2954, 1672, 1610, 1578, 1519, 1434, 1329, 1285, 1223, 1136, 1025, 991, 925, 817, 791, 764, 738, 698, 645 cm^{-1}; **HRMS** (ESI) *m/z* : $[M+Na]^+$ Calcd for $C_{19}H_{19}FNaO_2$ 321.12668, found 321.12613; $[\boldsymbol{\alpha}]_{\boldsymbol{D}}^{\mathbf{25}}$ = +37.7 (*c* = 1.0, $CHCl_3$).

(*S*)-1-(4-Fluoro-3-methylphenyl)-2-phenethylbut-3-en-1-one (3ga)

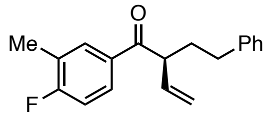

The product was isolated by silica gel column chromatography with hexane/EtOAc (99:1 to 90:10) as colorless oil (38.5 mg, 0.14 mmol, 91% yield). The ee value (88% ee) was determined by HPLC analysis [CHIRALCEL® OJ-H column, 4.6 mm × 250 mm, Daicel Chemical Industries, hexane/2-propanol 99.0:1.0, 1.0 mL/min, 40 °C, 254 nm UV detector, retention time = 12.9 min for the *S* isomer and 14.9 min for the *R* isomer]. **^{1}H NMR** (400 MHz, CDCl$_3$): δ 7.72–7.68 (m, 2H), 7.31–7.26 (m, 2H), 7.22–7.17 (m, 1H), 7.16 (d, J = 6.8 Hz, 2H), 7.02 (t, J = 8.6 Hz, 1H), 5.97–5.87 (m, 1H), 5.22–5.15 (m, 2H), 3.97 (q, J = 7.6 Hz, 1H), 2.72–2.58 (m, 2H), 2.28 (s, 3H), 2.26–2.15 (m, 1H), 1.97–1.87 (m, 1H); **^{13}C NMR** (101 MHz, CDCl$_3$): δ 199.4, 164.3 (d, J = 254 Hz), 141.4, 136.7, 132.5 (d, J = 3 Hz), 132.3 (d, J = 7 Hz), 128.6 (2C), 128.4 (2C), 128.3, 126.0, 125.3 (d, J = 17 Hz), 118.1, 115.2 (d, J = 23 Hz), 50.4, 33.5, 33.1, 14.6 (d, J = 3 Hz); **IR** (ATR): 3063, 3027, 2928, 2850, 1680, 1634, 1609, 1587, 1497, 1455, 1337, 1281, 1247, 1146, 1113, 993, 918, 826, 754, 699, 646, 622 cm^{-1}; **HRMS** (ESI) *m/z* : [M+Na]$^+$ Calcd for $C_{19}H_{19}FNaO$ 305.13176, found 305.13121; $[\boldsymbol{\alpha}]_{\boldsymbol{D}}^{\mathbf{25}} = +36.4$ (c = 1.0, CHCl$_3$).

(*S*)-1-(Benzo[d][1,3]dioxol-5-yl)-2-phenethylbut-3-en-1-one (3ha)

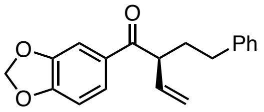

The product was isolated by silica gel column chromatography with hexane/EtOAc (98:2 to 80:20) as pale yellow solids (36.6 mg, 0.12 mmol, 83% yield). The ee value (96% ee) was determined by HPLC analysis [CHIRALCEL® IG-3 column, 4.6 mm × 250 mm, Daicel Chemical Industries, hexane/2-propanol 97.0:3.0, 1.0 mL/min, 40 °C, 254 nm UV detector, retention time = 15.2 min for the *S* isomer and 20.2 min for the *R* isomer]. **^{1}H NMR** (400 MHz, CDCl$_3$): δ 7.46 (dd, J = 8.0, 1.6 Hz, 1H), 7.38 (d, J = 2.0 Hz, 1H), 7.31–7.25 (m, 2H), 7.20 (d, J = 7.6 Hz, 1H), 7.15 (d, J = 6.8 Hz, 2H), 6.81 (d, J = 8.0 Hz, 1H), 6.03 (s, 2H), 5.96–5.86 (m, 1H), 5.21–5.14 (m, 2H), 3.94 (q, J = 7.6 Hz, 1H), 2.70–2.56 (m, 2H), 2.26–2.14 (m, 1H), 1.97–1.86 (m, 1H); **^{13}C NMR** (101 MHz, CDCl$_3$): δ 198.7, 151.7, 148.2, 141.5, 137.0, 131.3, 128.6 (2C), 128.4 (2C), 126.0, 124.7, 117.8, 108.3, 107.8, 101.8, 50.4, 33.6, 33.1; **IR** (ATR): 3084, 3028, 2912, 1714, 1672, 1657, 1634, 1603, 1502, 1487, 1440, 1355, 1329, 1248, 1158, 1106, 1037, 991, 936, 923, 892, 835, 806, 796, 757, 740, 720, 697, 666. cm^{-1}; **HRMS** (ESI) *m/z* : [M+Na]$^+$ Calcd for $C_{19}H_{18}NaO_3$ 317.11536, found 317.11482; $[\boldsymbol{\alpha}]_{\boldsymbol{D}}^{\mathbf{25}}$ = +35.7 (c = 1.0, CHCl$_3$).

(*S*)-1-(Naphthalen-2-yl)-2-phenethylbut-3-en-1-one (3ia)

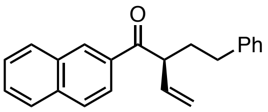

The product was isolated by silica gel column chromatography with hexane/EtOAc (99:1 to 90:10) as pale yellow solids (32.9 mg, 0.11 mmol, 73% yield). The ee value (90% ee) was determined by HPLC analysis [CHIRALCEL® OD-3 column, 4.6 mm × 250 mm, Daicel Chemical Industries, hexane/2-propanol 99.0:1.0, 1.0 mL/min, 40 °C, 254 nm UV detector, retention time = 12.7 min for the *R* isomer and 14.2 min for the *S* isomer]. **^{1}H NMR** (400 MHz, $CDCl_3$): δ 8.31 (s, 1H), 7.97 (dd, J = 8.4, 1.4 Hz, 1H), 7.91–7.85 (m, 3H), 7.62–7.51 (m, 2H), 7.31 (t, J = 7.0 Hz, 2H), 7.26–7.17 (m, 3H), 6.06–5.94 (m, 1H), 5.30–5.21 (m, 2H), 4.20 (q, J = 7.5 Hz, 1H), 2.79–2.62 (m, 2H), 2.47–2.24 (m, 1H), 2.06–1.93 (m, 1H); **^{13}C NMR** (101 MHz, $CDCl_3$): δ 200.7, 141.5, 136.8, 135.5, 133.7, 132.4, 130.1, 129.6, 128.6 (2C), 128.4 (4C), 127.7, 126.6, 126.0, 124.2, 118.1, 50.5, 33.6, 33.1; **IR** (ATR): 3059, 3027, 2920, 2862, 2162, 1958, 1716, 1674, 1624, 1593, 1494, 1460, 1438, 1413, 1385, 1366, 1297, 1273, 1257, 1169, 1129, 1155, 1026, 992, 966, 923, 864, 822, 784, 758, 698, 650 cm^{-1}; **HRMS** (ESI) *m/z* : $[M+Na]^+$ Calcd for $C_{22}H_{20}NaO$ 323.14118, found 323.14064; $[\alpha]_D^{25}$ = +7.1 (c = 1.0, $CHCl_3$).

(*S*)-1-(Furan-2-yl)-2-phenethylbut-3-en-1-one (3ja)

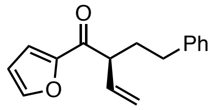

The product was isolated by silica gel column chromatography with hexane/EtOAc (90:10 to 80:20) as a red brown oil (16.2 mg, 0.07 mmol, 45% yield). The ee value (96% ee) was determined by HPLC analysis [CHIRALCEL® IG-3 column, 4.6 mm × 250 mm, Daicel Chemical Industries, hexane/2-propanol 99.0:1.0, 1.0 mL/min, 40 °C, 254 nm UV detector, retention time = 22.8 min for the *S* isomer and 25.7 min for the *R* isomer]. **^{1}H NMR** (400 MHz, $CDCl_3$): δ 7.57 (s, 1H), 7.29–7.26 (m, 2H), 7.21–7.11 (m, 4H), 6.52–6.50 (m, 1H), 5.94–5.85 (m, 1H), 5.23–5.18 (m, 2H), 3.81 (q, J = 7.6 Hz, 1H), 2.71–2.58 (m, 2H), 2.27–2.16 (m, 1H), 1.99–1.87 (m, 1H); **^{13}C NMR** (101 MHz, $CDCl_3$): δ 189.5, 152.2, 146.6, 141.5, 136.2, 128.5 (2C), 128.4 (2C), 125.9, 118.2, 117.8, 112.2, 51.7, 33.1, 33.0; **IR** (ATR): 3133, 3085, 3027, 2929, 2860, 1671, 1634, 1603, 1565, 1413, 1393, 1336, 1276, 1250, 1227, 1085, 1014, 994, 977, 920, 883, 829, 812, 759, 698, 650, 607 cm^{-1}; **HRMS** (ESI) *m/z* : $[M+Na]^+$ Calcd for $C_{16}H_{16}NaO_2$ 263.10480, found 263.10425; $[\alpha]_D^{25}$ = +54.4 (c = 0.7, $CHCl_3$).

(*S*)-4-(2-phenethylbut-3-enoyl)-*N*,*N*-dipropylbenzenesulfonamide (3ka)

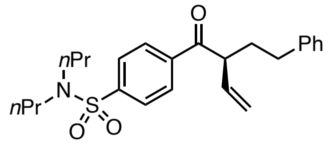

The product was isolated by silica gel column chromatography with hexane/EtOAc (98:2 to 80:20) as colorless oil (23.8 mg, 0.06 mmol, 38% yield). The ee value (90% ee) was determined by HPLC analysis [CHIRALCEL® IE-3 column, 4.6 mm × 291 mm, Daicel Chemical Industries, hexane/2-propanol 90.0:10.0, 1.0 mL/min, 40 °C, 254 nm UV detector, retention time = 16.5 min for the *S* isomer and 19.4 min for the *R* isomer]. **^{1}H NMR** (400 MHz, $CDCl_3$): δ 7.94 (d, *J* = 8.0 Hz, 2H), 7.84 (d, *J* = 8.4 Hz, 2H), 7.29 (t, *J* = 7.4 Hz, 2H), 7.23–7.14 (m, 3H), 5.96–5.86 (m, 1H), 5.26–5.18 (m, 2H), 4.00 (q, *J* = 7.6 Hz, 1H), 3.09 (t, *J* = 7.8 Hz, 4H), 2.74–2.59 (m, 2H), 2.27–2.16 (m, 1H), 2.01–1.90 (m, 1H), 1.62–1.49 (m, 4H), 0.87 (t, *J* = 7.4 Hz, 6H); **^{13}C NMR** (101 MHz, $CDCl_3$): δ 199.6, 144.0, 141.1, 139.2, 136.0, 128.9 (2C), 128.5 (2C), 128.4 (2C), 127.2 (2C), 126.1, 115.8, 51.0, 49.9 (2C), 33.2, 33.0, 22.0 (2C), 11.1 (2C); **IR** (ATR): 3027, 2935, 2876, 1723, 1686, 1634, 1596, 1570, 1497, 1456, 1398, 1341, 1272, 1216, 1156, 1108, 1089, 991, 924, 855, 797, 748, 700, 667 cm^{-1}; **HRMS** (ESI) *m/z* : $[M+Na]^+$ Calcd for $C_{24}H_{31}NNaO_3S$ 436.19223, found 436.19057; $[\boldsymbol{\alpha}]_{\boldsymbol{D}}^{\mathbf{25}}$ = +15.4 (*c* = 1.0, $CHCl_3$).

(*S*)-2-Methyl-1-phenylbut-3-en-1-one (3ab) [11]

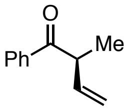

The product was isolated by silica gel column chromatography with hexane/EtOAc (99:1 to 90:10) as a colorless oil (17.1 mg, 0.11 mmol, 71% yield). The ee value (97% ee) was determined by HPLC analysis [CHIRALCEL® OJ-H column, 4.6 mm × 250 mm, Daicel Chemical Industries, hexane/2-propanol 99.0:1.0, 1.0 mL/min, 40 °C, 254 nm UV detector, retention time = 7.4 min for the *R* isomer and 7.8 min for the *S* isomer]. **^{1}H NMR** (400 MHz, $CDCl_3$): δ 7.98 (d, *J* = 6.8 Hz, 2H), 7.56 (t, *J* = 7.4 Hz, 1H), 7.48 (t, *J* = 7.6 Hz, 2H), 6.04–5.95 (m, 1H), 5.18 (d, *J* = 17.2 Hz, 1H), 5.14 (dd, *J* = 10.8 Hz, 1H), 4.18 (quin, *J* = 6.8 Hz, 1H), 1.34 (d, *J* = 6.8 Hz, 3H); **^{13}C NMR** (101 MHz, $CDCl_3$): δ 201.2, 138.1, 136.3, 133.0, 128.6 (2C), 128.5 (2C), 116.5, 45.6, 17.0; $[\boldsymbol{\alpha}]_{\boldsymbol{D}}^{\mathbf{25}}$ = +50.2 (*c* = 1.0, $CHCl_3$). Spectral data match those reported in the literature.[11]

(*S*)-4-Benzoylhex-5-en-1-yl Pivalate (3ac)

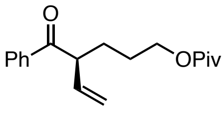

The product was isolated by silica gel column chromatography with hexane/EtOAc (99:1 to 90:10) as a colorless oil (36.3 mg, 0.13 mmol, 84% yield). The ee value (95% ee) was determined by chiral HPLC analysis [CHIRALCEL® IE-3 column, 4.6 mm × 250 mm, Daicel Chemical Industries, hexane/2-propanol 97.0:3.0, 1.0 mL/min, 40 °C, 254 nm UV detector, retention time = 9.3 min for the *R* isomer and 10.1 min for the *S* isomer]. **^{1}H NMR** (400 MHz, $CDCl_3$): *δ* 7.97 (d, *J* = 6.8 Hz, 2H), 7.57 (t, *J* = 7.4 Hz, 1H), 7.47 (t, *J* = 7.6 Hz, 2H), 5.94–5.84 (m, 1H), 5.23–5.17 (m, 2H), 4.09–4.03 (m, 3H), 1.99–1.90 (m, 1H), 1.74–1.64 (m, 3H), 1.18 (s, 9H); **^{13}C NMR** (101 MHz, $CDCl_3$): *δ* 200.5, 178.6, 136.6, 136.5, 133.1, 128.6 (2C), 128.4 (2C), 118.2, 63.8, 51.1, 38.7, 28.1, 27.2 (3C), 26.3; **IR** (ATR): 3053, 2959, 2873, 1724, 1683, 1635, 1597, 1542, 1480, 1448, 1398, 1365, 1343, 1283, 1209, 1152, 1075, 1036, 992, 917, 843, 771, 701, 687, 646 cm^{-1}; **HRMS** (ESI) *m/z* : $[M+Na]^+$ Calcd for $C_{18}H_{24}NaO_3$ 311.16231, found 311.16152; $[\alpha]_D^{25}$ = +60.9 (*c* = 1.0, $CHCl_3$).

(*S*)-4-Benzoylhex-5-en-1-yl 4-methylbenzenesulfonate (3ad)

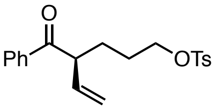

The product was isolated by silica gel column chromatography with hexane/EtOAc (85:15 to 70:30) as a dark brown oil (52.2 mg, 0.15 mmol, 97% yield). The ee value (98% ee) was determined by HPLC analysis [CHIRALCEL® OZ-H column, 4.6 mm × 250 mm, Daicel Chemical Industries, hexane/2-propanol 85.0:15.0, 1.0 mL/min, 40 °C, 254 nm UV detector, retention time = 14.8 min for the *R* isomer and 16.0 min for the *S* isomer]. **^{1}H NMR** (400 MHz, $CDCl_3$): *δ* 7.94 (d, *J* = 7.2 Hz, 2H), 7.77 (d, *J* = 8.0 Hz, 2H), 7.57 (t, *J* = 7.2 Hz, 1H), 7.46 (t, *J* = 7.8 Hz, 2H), 7.33 (d, *J* = 8.4 Hz, 2H), 5.86–5.76 (m, 1H), 5.18–5.14 (m, 2H), 4.06–3.99 (m, 3H), 2.44 (s, 3H), 1.92–1.84 (m, 1H), 1.73–1.62 (m, 3H); **^{13}C NMR** (101 MHz, $CDCl_3$): *δ* 200.1, 144.7, 136.2, 133.2, 132.9, 129.8 (2C), 129.1, 128.6 (2C), 128.4 (2C), 127.8 (2C), 118.4, 70.1, 50.7, 27.5, 26.4, 21.6; **IR** (ATR): 3065, 2958, 1682, 1635, 1597, 1579, 1495, 1448, 1355, 1307, 1291, 1275, 1218, 1189, 1173, 1120, 1097, 1019, 1000, 963, 926, 814, 792, 768, 730, 702, 687, 661 cm^{-1}; **HRMS** (ESI) *m/z* : $[M+Na]^+$ Calcd for $C_{20}H_{22}NaO_4S$ 381.11365, found 381.11271; $[\alpha]_D^{25}$ = +50.3 (*c* = 1.0, $CHCl_3$).

(*S*)-2-(Benzo[d][1,3]dioxol-5-ylmethyl)-1-phenylbut-3-en-1-one (3ae)

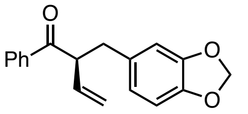

The product was isolated by silica gel column chromatography with hexane/EtOAc (99:1 to 90:10) as colorless oil (31.5 mg, 0.11 mmol, 75% yield). The ee value (87% ee) was determined by HPLC analysis [CHIRALCEL® IE-3 column, 4.6 mm × 250 mm, Daicel Chemical Industries, hexane/2-propanol 97.0:3.0, 1.0 mL/min, 40 °C, 254 nm UV detector, retention time = 13.6 min for the *R* isomer and 15.8 min for the *S* isomer]. ^{1}**H NMR** (400 MHz, $CDCl_3$): δ 7.92 (d, J = 6.8 Hz, 2H), 7.54 (t, J = 7.4 Hz, 1H), 7.44 (t, J = 7.8 Hz, 2H), 6.70–6.67 (m, 2H), 6.65–6.62 (m, 1H), 5.96–5.88 (m, 3H), 5.16–5.07 (m, 2H), 4.30 (q, J = 7.6 Hz, 1H), 3.19 (dd, J = 13.6, 6.8 Hz, 1H), 2.83 (dd, J = 13.6, 7.2 Hz, 1H); ^{13}**C NMR** (101 MHz, $CDCl_3$): δ 200.2, 147.4, 145.9, 136.6, 136.3, 133.1, 133.0, 128.6 (2C), 128.4 (2C), 122.1, 118.3, 109.6, 108.1, 100.8, 53.8, 37.8; **IR** (ATR): 3062, 2892, 2777, 1851, 1679, 1634, 1597, 1580, 1502, 1488, 1444, 1346, 1243, 1222, 1188, 1122, 1097, 1037, 1001, 991, 924, 854, 801, 775, 758, 701, 686, 667 cm^{-1}; **HRMS** (ESI) *m/z* : $[M+Na]^+$ Calcd for $C_{18}H_{16}NaO_3$ 303.09971, found 303.09895. $[\alpha]_D^{25}$ = +39.6 (c = 0.9, $CHCl_3$).

(*R*)-2-(((*tert*-Butyldimethylsilyl)oxy)methyl)-1-phenylbut-3-en-1-one (3af)

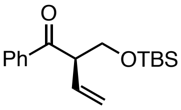

The product was isolated by silica gel column chromatography with hexane/EtOAc (99:1 to 90:10) as a colorless oil (29.2 mg, 0.10 mmol, 67% yield). The ee value (89% ee) was determined by HPLC analysis [CHIRALCEL® OD-3 column, 4.6 mm × 250 mm, Daicel Chemical Industries, hexane/2-propanol 99.0:1.0, 1.0 mL/min, 40 °C, 254 nm UV detector, retention time = 7.8 min for the *S* isomer and 8.3 min for the *R* isomer]. ^{1}**H NMR** (400 MHz, $CDCl_3$): δ 7.98 (d, J = 7.2 Hz, 2H), 7.55 (t, J = 7.4 Hz, 1H), 7.46 (t, J = 7.4 Hz, 2H), 5.94–5.85 (m, 1H), 5.24–5.18 (m, 2H), 4.36 (q, J = 7.6 Hz, 1H), 4.08 (t, J = 9.6 Hz, 1H), 3.77 (dd, J = 9.6 Hz, 6.0 Hz, 1H), 0.80 (s, 9H), 0.02 (s, 3H), –0.03 (s, 3H); ^{13}**C NMR** (101 MHz, $CDCl_3$): δ 200.5, 137.4, 134.0, 132.9, 128.5 (2C), 128.4 (2C), 118.8, 64.9, 54.4, 25.7 (3C), 18.2, –5.52, –5.56; **IR** (ATR): 3066, 2954, 2929, 2885, 2857, 1683, 1636, 1598, 1581, 1472, 1464, 1448, 1413, 1377, 1361, 1345, 1252, 1211, 1180, 1097, 1029, 1002, 965, 923, 875, 834, 775, 702, 686, 670 cm^{-1}; **HRMS** (ESI) *m/z* : $[M+Na]^+$ Calcd for $C_{17}H_{26}NaO_2Si$ 313.15998, found 313.15931; $[\alpha]_D^{25}$ = +40.5 (c = 1.0, $CHCl_3$).

(*S*)-4-Benzoylhex-5-en-1-yl 4-bromobenzoate (3ag)

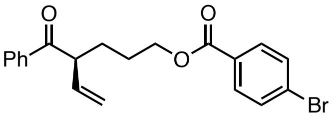

The product was isolated by silica gel column chromatography with hexane/EtOAc (98:2 to 80:20) as a colorless oil (56.7 mg, 0.15 mmol, 98% yield). The ee value (96% ee) was determined by HPLC analysis [CHIRALCEL® IE-3 column, 4.6 mm × 250 mm, Daicel Chemical Industries, hexane/2-propanol 97.0:3.0, 1.0 mL/min, 40 °C, 254 nm UV detector, retention time = 18.9 min for the *R* isomer and 20.2 min for the *S* isomer]. **^{1}H NMR** (400 MHz, $CDCl_3$): δ 7.95 (d, *J* = 7.6 Hz, 2H), 7.84 (d, *J* = 8.8 Hz, 2H), 7.54–7.52 (m, 3H), 7.42 (t, *J* = 7.4 Hz, 2H), 5.93–5.83 (m, 1H), 5.22–5.16 (m, 2H), 4.31 (t, *J* = 6.2 Hz, 2H), 4.09 (q, *J* = 6.4 Hz, 1H), 2.09–1.92 (m, 1H), 1.89–1.71 (m, 3H); **^{13}C NMR** (101 MHz, $CDCl_3$): δ 200.3, 165.8, 136.5, 136.4, 133.1, 131.6 (2C), 131.0 (2C), 129.1, 128.6 (2C), 128.4 (2C), 127.9, 118.3, 64.8, 51.1, 28.2, 26.3; **IR** (ATR): 2975, 2864, 1720, 1684, 1635, 1591, 1484, 1448, 1398, 1382, 1350, 1174, 1151, 1114, 1103, 1012, 1001, 920, 846, 757, 702, 685 cm^{-1}; **HRMS** (ESI) *m/z* : [M+Na]$^+$ Calcd for $C_{20}H_{19}BrNaO_3$ 409.04153, found 409.04109; $[\alpha]_D^{25}$ = +49.5 (*c* = 1.0, $CHCl_3$).

(*S*)-4-Benzoylhex-5-en-1-yl 4-(trifluoromethyl)benzoate (3ah)

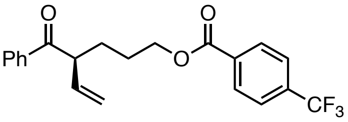

The product was isolated by silica gel column chromatography with hexane/EtOAc (99:1 to 90:10) as a colorless oil (54.2 mg, 0.14 mmol, 96% yield). The ee value (96% ee) was determined by HPLC analysis [CHIRALCEL® IE-3 column, 4.6 mm × 250 mm, Daicel Chemical Industries, hexane/2-propanol 97.0:3.0, 1.0 mL/min, 40 °C, 254 nm UV detector, retention time = 10.5 min for *R* isomer and 10.9 min for *S* isomer]. **^{1}H NMR** (400 MHz, $CDCl_3$): δ 8.13 (d, *J* = 8.0 Hz, 2H), 7.98 (d, *J* = 7.6 Hz, 2H), 7.69 (d, *J* = 8.4 Hz, 2H), 7.56 (t, *J* = 7.4 Hz, 1H), 7.45 (t, *J* = 7.6 Hz, 2H), 5.96–5.85 (m, 1H), 5.26–5.18 (m, 2H), 4.38 (t, *J* = 6.6 Hz, 2H), 4.12 (q, *J* = 6.6 Hz, 1H), 2.12–2.02 (m, 1H), 1.93–1.75 (m, 3H); **^{13}C NMR** (101 MHz, $CDCl_3$): δ 200.3, 165.3, 136.5, 136.4, 134.3 (q, *J* = 33 Hz), 133.4, 133.2, 129.9 (2C), 128.6 (2C), 128.4 (2C), 125.3 (q, *J* = 4 Hz, 2C), 124.7 (q, *J* = 273 Hz), 118.4, 65.2, 51.1, 28.2, 26.3; **IR** (ATR): 3063, 2959, 1720, 1683, 1635, 1597, 1581, 1514, 1449, 1412, 1324, 1272, 1167, 1123, 1100, 1017, 1001, 922, 862, 702, 687 cm^{-1}; **HRMS** (ESI) *m/z* : [M+Na]$^+$ Calcd for $C_{21}H_{19}F_3NaO_3$ 399.11840, found 399.11747; $[\alpha]_D^{25}$ = +60.5 (*c* = 1.0, $CHCl_3$).

(*S*)-4-Benzoylhex-5-en-1-yl 4-cyanobenzoate (3ai)

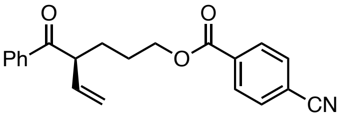

The product was isolated by silica gel column chromatography with hexane/EtOAc (98:2 to 80:20) as a colorless oil (47.5 mg, 0.14 mmol, 95% yield). The ee value (97% ee) was determined by HPLC analysis [CHIRALCEL® IF-3 column, 4.6 mm × 250 mm, Daicel Chemical Industries, hexane/2-propanol 95.0:5.0, 1.0 mL/min, 40 °C, 254 nm UV detector, retention time = 20.4 min for the *R* isomer and 22.0 min for the *S* isomer]. **^{1}H NMR** (400 MHz, $CDCl_3$): δ 8.11 (d, J = 8.8 Hz, 2H), 7.98 (d, J = 7.2 Hz, 2H), 7.73 (d, J = 8.4 Hz, 2H), 7.57 (t, J = 7.2 Hz, 1H), 7.46 (t, J = 7.6 Hz, 2H), 5.97–5.83 (m, 1H), 5.27–5.19 (m, 2H), 4.40–4.35 (m, 2H), 4.11 (q, J = 7.6 Hz, 1H), 2.12–2.01 (m, 1H), 1.92–1.74 (m, 3H); **^{13}C NMR** (101 MHz, $CDCl_3$): δ 200.2, 164.8, 136.4, 136.3, 133.9, 133.1, 132.1 (2C), 133.0 (2C), 128.6 (2C), 128.4 (2C), 118.3, 117.9, 116.2, 65.4, 51.1, 28.1, 26.2; **IR** (ATR): 3059, 2958, 2231, 1719, 1680, 1634, 1610, 1597, 1579, 1448, 1405, 1345, 1310, 1271, 1221, 1177, 1118, 1107, 1019, 1001, 992, 921, 861, 767, 702, 689, 643 cm^{-1}; **HRMS** (ESI) *m/z* : $[M+Na]^+$ Calcd for $C_{21}H_{19}NNaO_3$ 356.12626, found 356.12538; $[\alpha]_D^{25}$ = +56.1 (*c* = 1.0, $CHCl_3$).

(*S*)-4-Benzoylhex-5-en-1-yl 4-(dimethylamino)benzoate (3aj)

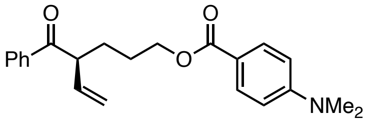

The product was isolated by silica gel column chromatography with hexane/EtOAc (98:2 to 80:20) as pale yellow solids (47.0 mg, 0.13 mmol, 89% yield). The ee value (97% ee) was determined by HPLC analysis [CHIRALCEL® IG-3 column, 4.6 mm × 250 mm, Daicel Chemical Industries, hexane/2-propanol 85.0:15.0, 1.0 mL/min, 40 °C, 254 nm UV detector, retention time = 36.0 min for the *R* isomer and 39.1 min for the *S* isomer]. **^{1}H NMR** (400 MHz, $CDCl_3$): δ 7.98 (d, J = 7.2 Hz, 2H), 7.89 (d, J = 8.8 Hz, 2H), 7.55 (t, J = 7.6 Hz, 1H), 7.45 (t, J = 7.4 Hz, 2H), 6.63 (dt, J = 9.2, 2.4 Hz, 2H), 5.96–5.85 (m, 1H), 5.24–5.16 (m, 2H), 4.29 (t, J = 6.2 Hz, 2H), 4.12 (q, J = 6.8 Hz, 1H), 3.04 (s, 6H), 2.10–1.99 (m, 1H), 1.90–1.72 (m, 3H); **^{13}C NMR** (101 MHz, $CDCl_3$): δ 200.6, 166.9, 153.2, 136.6, 136.4, 133.0, 131.2 (2C), 128.6 (2C), 128.4 (2C), 118.1, 116.9, 110.6 (2C), 63.7, 51.1, 40.0 (2C), 28.3, 26.4; **IR** (ATR): 3417, 3061, 2935, 2894, 2866, 2112, 1909, 1694, 1673, 1637, 1607, 1580, 1557, 1525, 1475, 1446, 1415, 1390, 1370, 1336, 1317, 1278, 1227, 1182, 1107, 1065, 1014, 1000, 958, 932, 851, 830, 792, 769, 757, 701, 685, 634 cm^{-1}; **HRMS** (ESI) *m/z* : $[M+Na]^+$ Calcd for $C_{22}H_{25}NNaO_3$ 374.17321, found 374.17235; $[\alpha]_D^{25}$ = +48.2 (*c* = 1.0, $CHCl_3$).

(*S*)-4-(4-Benzoylhex-5-en-1-yl) 1-benzyl piperidine-1,4-dicarboxylate (3ak)

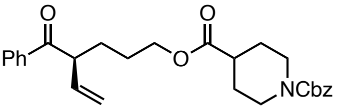

The product was isolated by silica gel column chromatography with hexane/EtOAc (90:10 to 50:50) as colorless oil (62.0 mg, 0.14 mmol, 92% yield). The ee value (93% ee) was determined by HPLC analysis [CHIRALCEL® OJ-H column, 4.6 mm × 250 mm/OD-H column, 4.6 mm × 250 mm, Daicel Chemical Industries, hexane/2-propanol 85.0:15.0, 1.0 mL/min, 40 °C, 254 nm UV detector, retention time = 33.0 min for the *S* isomer and 37.6 min for the *R* isomer]. **^{1}H NMR** (400 MHz, $CDCl_3$): *δ* 7.97 (d, *J* = 7.2 Hz, 2H), 7.56 (t, *J* = 7.6 Hz, 1H), 7.44 (t, *J* = 7.6 Hz, 2H), 7.36–7.35 (m, 4H), 7.34–7.29 (m, 1H), 5.93–5.82 (m, 1H), 5.22–5.17 (m, 2H), 5.12 (s, 2H), 4.16–4.00 (m, 5H), 2.90 (br, 2H), 2.47–2.38 (m, 1H), 2.00–1.80 (m, 3H), 1.74–1.57 (m, 5H); **^{13}C NMR** (101 MHz, $CDCl_3$): *δ* 200.3, 174.3, 155.1, 136.6, 136.5, 136.4, 133.1, 128.6 (2C), 128.42 (2C), 128.39 (2C), 127.9, 127.8 (2C), 118.2, 67.0, 64.1, 51.1, 43.1 (2C), 40.9, 28.1, 27.8 (2C), 26.2; **IR** (ATR): 3055, 2954, 2861, 2249, 1728, 1683, 1635, 1597, 1578, 1498, 1470, 1447, 1430, 1354, 1311, 1275, 1221, 1173, 1123, 1073, 1035, 1001, 953, 913, 840, 764, 730, 697, 647 cm^{-1}; **HRMS** (ESI) *m/z* : $[M+Na]^+$ Calcd for $C_{27}H_{31}NNaO_5$ 472.20999, found 472.20898. $[\boldsymbol{\alpha}]_{\boldsymbol{D}}^{\mathbf{25}}$ = +27.6 (*c* = 1.0, $CHCl_3$).

(*R*)-1,2-Diphenylbut-3-en-1-one (3al) [16]

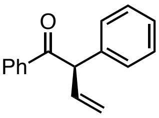

The product was isolated by silica gel column chromatography with hexane/EtOAc (99:1 to 90:10) as a colorless oil (23.3 mg, 0.11 mmol, 70% yield). The ee value (95% ee) was determined by HPLC analysis [CHIRALCEL® IE-3 column, 4.6 mm × 250 mm, Daicel Chemical Industries, hexane/2-propanol 99.0:1.0, 1.0 mL/min, 40 °C, 254 nm UV detector, retention time = 11.9 min for the *S* isomer and 12.9 min for the *R* isomer]. **^{1}H NMR** (400 MHz, $CDCl_3$): *δ* 7.97 (d, *J* = 7.6 Hz, 2H), 7.51 (t, *J* = 7.2 Hz, 1H), 7.41 (t, *J* = 7.8 Hz, 2H), 7.33–7.29 (m, 4H), 7.25–7.22 (m, 1H), 6.41–6.32 (m, 1H), 5.29 (d, *J* = 7.6 Hz, 1H), 5.23 (d, *J* = 10.0 Hz, 1H), 5.10 (d, *J* = 16.8 Hz, 1H); **^{13}C NMR** (101 MHz, $CDCl_3$): *δ* 198.5, 138.3, 137.1, 136.3, 130.0, 129.0 (2C), 128.8 (2C), 128.5 (2C), 128.3 (2C), 127.2, 117.2, 57.9; $[\boldsymbol{\alpha}]_{\boldsymbol{D}}^{\mathbf{25}}$ = –154.5 (*c* = 0.70, $CHCl_3$). Spectral data match those reported in the literature.[16]

(*R*)-2-Cyclohexyl-1-phenylbut-3-en-1-one (3am)

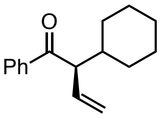

The product was isolated by silica gel column chromatography with hexane/EtOAc (99:1 to 90:10) as a colorless oil (30.8 mg, 0.14 mmol, 90% yield). The ee value (99% ee) was determined by HPLC analysis [CHIRALCEL® IE-3 column, 4.6 mm × 250 mm/IF-3 column, 4.6 mm × 250 mm, Daicel Chemical Industries, hexane/2-propanol 99.0:1.0, 1.0 mL/min, 40 °C, 254 nm UV detector, retention time = 19.2 min for the *R* isomer and 20.2 min for the *S* isomer]. **^{1}H NMR** (400 MHz, $CDCl_3$): *δ* 7.96 (d, *J* = 6.8 Hz, 2H), 7.56 (t, *J* = 7.2 Hz, 1H), 7.46 (t, *J* = 7.4 Hz, 2H), 5.91–5.81 (m, 1H), 5.16–5.11 (m, 2H), 3.85 (t, *J* = 8.8 Hz, 1H), 1.96–1.62 (m, 6H), 1.27–1.08 (m, 3H), 1.03–0.88 (m, 2H); **^{13}C NMR** (101 MHz, $CDCl_3$): *δ* 201.8, 137.5, 136.3, 132.9, 128.5 (2C), 128.3 (2C), 118.1, 58.5, 40.1, 31.9, 30.2, 26.3, 26.2 (2C); **IR** (ATR): 3062, 3027, 2924, 2852, 1679, 1635, 1597, 1580, 1495, 1447, 1413, 1342, 1293, 1200, 1180, 1075, 996, 917, 846, 832, 776, 699, 687 cm^{-1}; **HRMS** (ESI) *m/z* : $[M+Na]^+$ Calcd for $C_{16}H_{20}NaO$ 251.14118, found 251.14064; $[\alpha]_D^{25}$ = +42.7 (*c* = 1.0, $CHCl_3$).

(*S*)-2-Methyl-2-phenethyl-1-phenylbut-3-en-1-one (3an) [17]

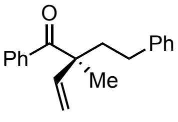

The product was isolated by silica gel column chromatography with hexane/EtOAc (99:1 to 90:10) as a colorless oil (20.6 mg, 0.078 mmol, 52% yield). The ee value (85% ee) was determined by HPLC analysis [CHIRALCEL® IE-3 column, 4.6 mm × 250 mm/OZ-H column, 4.6 mm × 250 mm, Daicel Chemical Industries, hexane/2-propanol 99.0:1.0, 1.0 mL/min, 40 °C, 254 nm UV detector, retention time = 17.2 min for the *R* isomer and 17.8 min for the *S* isomer]. **^{1}H NMR** (400 MHz, $CDCl_3$): *δ* 7.88 (d, *J* = 7.2 Hz, 2H), 7.49 (t, *J* = 7.4 Hz, 1H), 7.39 (t, *J* = 7.6 Hz, 2H), 7.25–7.21 (m, 2H), 7.15 (t, *J* = 7.4 Hz, 1H), 7.05 (d, *J* = 7.2 Hz, 2H), 6.21 (dd, *J* = 17.6, 11.2 Hz, 1H), 5.29 (d, *J* = 10.4 Hz, 1H), 5.26 (d, *J* = 17.6 Hz, 1H), 2.59 (dt, *J* = 4.9 Hz, 13.0 Hz, 1H), 2.39 (dt, *J* = 13.0, 4.3 Hz, 1H), 2.21 (dt, *J* = 13.0, 4.4 Hz, 1H), 2.05 (dt, *J* = 13.0, 4.7 Hz, 1H), 1.47 (s, 3H); **^{13}C NMR** (101 MHz, $CDCl_3$): *δ* 200.5, 142.8, 142.2, 137.6, 131.7, 129.0 (2C), 128.33 (2C), 128.27 (2C), 128.0 (2C), 125.8, 115.1, 53.6, 41.2, 30.8, 22.9; $[\alpha]_D^{25}$ = +30.4 (*c* = 1.0, $CHCl_3$). Spectral data match those reported in the literature.[17]

(*S*)-2,6-Dimethyl-1-phenyl-2-vinylhept-5-en-1-one (3ao) [6a]

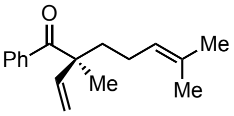

The product was isolated by silica gel column chromatography with hexane/EtOAc (99:1 to 90:10) as a colorless oil (17.1 mg, 0.071 mmol, 47% yield). The ee value (78% ee) was determined by HPLC analysis [CHIRALCEL® OJ-H column, 4.6 mm × 250 mm, Daicel Chemical Industries, hexane/2-propanol 97.0:3.0, 0.3 mL/min, 40 °C, 254 nm UV detector, retention time = 15.9 min for the *S* isomer and 17.1 min for the *R* isomer]. **^{1}H NMR** (400 MHz, $CDCl_3$): δ 7.84 (d, J = 7.6 Hz, 2H), 7.45 (t, J = 7.4 Hz, 1H), 7.36 (t, J = 7.8 Hz, 2H), 6.16 (dd, J = 17.6, 10.8 Hz, 1H), 5.27–5.18 (m, 2H), 5.01 (br, 1H), 1.94–1.88 (m, 2H), 1.77–1.73 (m, 2H), 1.72 (s, 3H), 1.43 (s, 3H), 1.36 (s, 3H); **^{13}C NMR** (101 MHz, $CDCl_3$): δ 204.7, 143.1, 137.7, 132.0, 131.5, 129.0 (2C), 127.9 (2C), 123.9, 114.8, 53.5, 38.9, 25.6, 22.93, 22.88, 17.4; $[\alpha]_D^{25}$ = +1.9 (*c* = 1.0, $CHCl_3$). Spectral data match those reported in the literature.[6a]

References

(1) Trost, B. M. Proc. Natl. Acad. Sci. U. S. A. 2004, 101, 5348-5355.

(2) (a) Trost, B. M. *Acc. Chem. Res*. **1996**, *29*, 355–364. (b) Trost, B. M.; Crawley, M. L. *Chem. Rev*. **2003**, *103*, 2921–2944. (c) Trost, B. M.; Machacek, M. R.; Aponick, A. *Acc. Chem. Res.* **2006**, *39*, 747–760.

(3) (a) Evans, P. A.; Nelson, J. D. *J. Am. Chem. Soc*. **1998**, *120*, 5581─5582. (b) Hayashi, T.; Okada, A.; Suzuka, T.; Kawatsura, M. *Org. Lett*. **2003**, *5*, 1713─1715. (c) Kazmaier, U.; Stolz, D. *Angew. Chem., Int. Ed*. **2006**, *45*, 3072─3075. (d) Sidera, M.; Fletcher, S. P. *Nat. Chem*. **2015**, *7*, 935─939. (e) Li, C.; Breit, B. *Chem. - Eur. J.* **2016**, *22*, 14655─14663. (f) Parveen, S.; Li, C.; Hassan, A.; Breit, B. *Org. Lett*. **2017**, *19*, 2326─2329. (g) Takeuchi, R.; Kashio, M. *Angew. Chem., Int. Ed. Engl*. **1997**, *36*, 263─265. (h) Miyabe, H.; Takemoto, Y. *Synlett* **2005**, 1641─1655. (i) Helmchen, G.; Dahnz, A.; Dübon, P.; Schelwies, M.; Weihofen, R. *Chem.Commun*. **2007**, 675─691. (j) Hartwig, J. F.; Stanley, L. M. *Acc. Chem. Res.* **2010**, *43*, 1461─1475. (k) Tosatti, P.; Nelson, A.; Marsden, S. P. *Org. Biomol. Chem*. **2012**, *10*, 3147─3163. (l) Hethcox, J. C.; Shockley, S. E.; Stoltz, B. M. *ACS Catal*. **2016**, *6*, 6207─6213. (m) Qu, J.; Helmchen, G. *Acc. Chem. Res*. **2017**, *50*, 2539─2555. (n) Cheng, Q.; Tu, H.-F.; Zheng, C.; Qu, J.-P.; Helmchen, G.; You, S.-L. *Chem. Rev*. **2019**, *119*, 1855─1969. (o) Belda, O.; Moberg, C. *Acc. Chem. Res.* **2004**, *37*, 159─167. (p) Trost, B. M.; Hachiya, I. *J. Am. Chem. Soc.* **1998**, *120*, 1104─1105. (q) Trost, B. M.; Zhang, Y. *J. Am. Chem. Soc*. **2007**, *129*, 14548─14549.

(4) (a) Yorimitsu, H.; Oshima, K. *Angew. Chem., Int. Ed*. **2005**, *44*, 4435─4439. (b) Falciola, C. A.; Alexakis, A. *Eur. J. Org. Chem*. **2008**, *2008*, 3765─3780. (c) Alexakis, A.; Bäckvall, J. E.; Krause, N.; Pàmies, O.; Diéguez, M. *Chem. Rev*. **2008**, *108*, 2796─2823. (d) Har- utyunyan, S. R.; den Hartog, T.; Geurts, K.; Minnaard, A. J.; Feringa, B. L. *Chem. Rev*. **2008**, *108*, 2824─2852. (e) Süsse, L.; Stoltz, B. M. *Chem. Rev*. **2021**, *121*, 4084─4099.

(5) (a) Harada, A.; Makida, Y.; Sato, T.; Ohmiya, H.; Sawamura, M. *J. Am. Chem. Soc*. **2014**, *136*, 13932─13939. (b) Ohmiya, H.; Zhang, H.; Shibata, S.; Harada, A.; Sawamura, M. *Angew. Chem., Int. Ed*. **2016**, *55*, 4777─4780. (c) Yasuda, Y.; Ohmiya, H.; Sawamura, M. *Angew. Chem., Int. Ed*. **2016**, *55*, 10816─10820. (d) Hojoh, K.; Ohmiya, H.; Sawamura, M. *J. Am. Chem. Soc*. **2017**, *139*, 2184─2187.

(6) (a) Evans, P. A.; Oliver, S. *Org. Lett.* **2013**, *15*, 5626─5629. (b) Breitler, S.; Carreira, E. M. *J. Am. Chem. Soc*. **2015**, *137*, 5296─5299. (c) Turnbull, B. W. H.; Oliver, S.; Evans, P. A. *J. Am. Chem. Soc*. **2015**, *137*, 15374─15377. (d) Yao, K.; Liu, D.; Yuan, Q.; Imamoto, T.; Liu, Y.; Zhang, W. *Org. Lett*. **2016**, *18*, 6296─6299. (e) Yuan, Y.; Zhang, X.; Qian, H.; Ma, S. *Chem. Sci*. **2020**, *11*, 9115─9121. (f) del Pozo, J.; Zhang, S.; Romiti, F.; Xu, S.; Conger, R. P.; Hoveyda, A. H. *J. Am. Chem. Soc.* **2020**, *142*, 18200─18212.

(7) (a) Brook, A. G.; Duff, J. M. *J. Am. Chem. Soc.* **1967**, *89*, 454–455. (b) Duff, J. M.; Brook, A. G. *Can. J. Chem.* **1973**, *51*, 2869–2883. (c) Bourque, R. A.; Davis, P. D.; Dalton, J. C. *J. Am. Chem. Soc.* **1981**, *103*, 697–699. (d) Ito, K.; Tamashima, H.; Iwasawa, N.; Kusama, H. *J. Am. Chem. Soc.* **2011**, *133*, 3716–3719. (e) Ishida, K.; Tobita, F.; Kusama, H. *Chem. - Eur. J.* **2018**, *24*, 543–546.

(8) (a) Hossain, A.; Bhattacharyya, A.; Reiser, O. *Science* **2019**, *364*, eaav9713. (b) Kutal, C. *Coord. Chem. Rev.* **1990**, *99*, 213–252. (c) Armaroli, N. *Chem. Soc. Rev.* **2001**, *30*, 113–124. (d) Hockin, B. M.; Li, C.; Robertson, N.; Zysman-Colman, E. *Catal. Sci. Technol.* **2019**, *9*, 889–915.

(9) (a) Giannerini, M.; Fañanás-Mastral, M.; Feringa, B. L. *J. Am. Chem. Soc.* **2012**, *134*, 4108–4111. (b) Shi, Y.; Jung, B.; Torker, S.; Hoveyda, A. H. *J. Am. Chem. Soc.* **2015**, *137*, 8948–8964. (c) Rivera-Chao, E.; Mitxelena, M.; Varela, J. A.; Fañanás-Mastral, M. *Angew. Chem., Int. Ed.* **2019**, *58*, 18230–18234. (d) Xu, G.; Fu, B.; Zhao, H.; Li, Y.; Zhang, G.; Wang, Y.; Xiong, T.; Zhang, Q. *Chem. Sci.* **2019**, *10*, 1802–1806.

(10) (a) Ye, J.-H.; Quach, L.; Paulisch, T.; Glorius, F. *J. Am. Chem. Soc.* **2019**, *141*, 16227–16231. (b) Ishida, K.; Yamazaki, H.; Hagiwara, C.; Abe, M.; Kusama, H. *Chem. - Eur. J.* **2020**, *26*, 1249–1253.

(11) Lou, S.; Fu, G. C. *J. Am. Chem. Soc.* **2010**, *132*, 5010–5011.

(12) Pangborn, A. B.; Giardello, M. A.; Grubbs, R. H.; Rosen, R. K.; Timmers, F. J. *Organometallics* **1996**, *15*, 1518–1520.

(13) (a) Linderman, R. J.; Suhr, Y. *J. Org. Chem.* **1988**, *53*, 1569–1572. (b) Lu, X.; Zhang, J.; Xu, L.; Shen, W.; Yu, F.; Ding, L.; Zhong, G. *Org. Lett.* **2020**, *22*, 5610–5616.

(14) Yasuda, Y.; Ohmiya, H.; Sawamura, M. *Synthesis* **2018**, *50*, 2235–2246.

(15) Lee, S.; Lee, S.; Lee, Y. *Org. Lett.* **2020**, *22*, 5806–5810.

(16) Chen, Q.-A.; Cruz, F. A.; Dong, V. M. *J. Am. Chem. Soc.* **2015**, *137*, 3157–3160.

(17) Evans, P. A.; Oliver, S.; Chae, J. *J. Am. Chem. Soc.* **2012**, *134*, 19314–19317.

Chapter 2

Mechanistic Investigation of Photoinduced Copper-Catalyzed Asymmetric Acylation of Allylic Phosphates with Acylsilanes

Introduction

Photoinduced catalysis enables novel molecular transformations for organic synthesis complementary to thermal catalytic reactions.[1] In particular, photoinduced transition metal catalyzed reactions based on direct excitation of chiral transition metal catalysts by visible light can be asymmetrically controlled by chiral ligands, and thus have a different appeal from commonly investigated photocatalyst-based transformation reactions.[2] In most cases, the proposed reaction mechanisms consist of intermolecular photo-induced single-electron transfer between the catalytic metal complex and the substrate followed by homolytic bond dissociation of the resulting open-shell species to liberate a highly reactive free radical, which may recombine with the metal afterward.

As described in Chapter 1, the author developed that visible-light irradiation with a blue LED lamp induced copper-catalyzed highly enantioselective umpolung acylation of γ-mono- or γ,γ-disubstituted primary allylic phosphates with acylsilanes as acyl anion equivalents. This reaction offers straightforward access to enantioenriched α-branched β,γ-unsaturated ketones, which serve as versatile chiral building blocks in organic synthesis. In this work, the author assumes that the reaction proceeds by MLCT from the copper center to the acyl group upon photoexcitation. In Chapter 2, the author describes the results of a mechanistic investigation that combines experiments and calculations to elucidate the proposed mechanism. In this process, it was supported that the allylic phosphate substrate in the excited state undergoes novel molecular activation into an allylic radical weakly bound to the copper complex (Scheme 1). Furthermore, in the mechanistic analysis, secondary allylic phosphates were found to be suitable reaction substrates.

Scheme 1. Mechanistic Investigation of Photoinduced Copper-Catalyzed Asymmetric Acylation

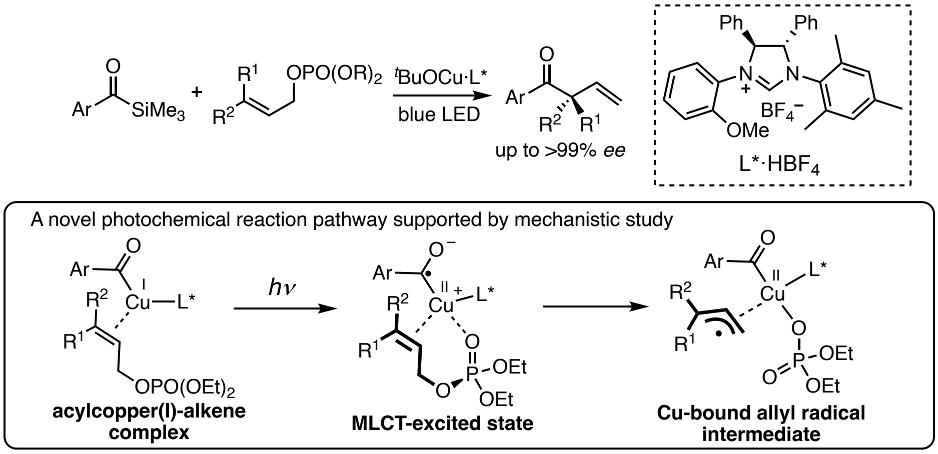

Result and Discussion

In order to gain a mechanistic insight, the effects of *trans*-stilbene (*trans*-**4**) as a triplet quencher were studied (Scheme 2).[3] When a mixture of acylsilane **1a**, methanol, and *trans*-**4** was irradiated with blue LED at r.t. for 12 h, **1a** was quantitatively converted to silylacetal **5** (Scheme 2a).[4] Thus, while the triplet quencher did not influence the photoisomerization of **1a** to the corresponding siloxycarbene, the triplet energy of **1a** was partially transferred to *trans*-**4** as indicated by the formation of *cis*-stilbene (*cis*-**4**) in 50% yield. In contrast, the copper-catalyzed allylic acylation of **2a** with **1a** was significantly suppressed by the addition of *trans*-**4** in a dose-dependent manner, the acylation product (**3aa**) being obtained in only 29% and 6% yields with 1.2 and 2.5 equivalents of *trans*-**4**, respectively (Scheme 2b). Furthermore, *trans*-**4** was sensitized to undergo double bond isomerization into *cis*-**4**. It was confirmed that most of *trans*-**4** was recovered in the absence of acylsilane **1a** and allylic phosphate **2a** (Scheme 2c). These observations are in accord with the existence of triplet photoexcited organocopper species.

Scheme 2. Effects of *trans*-stilbene triplet quencher

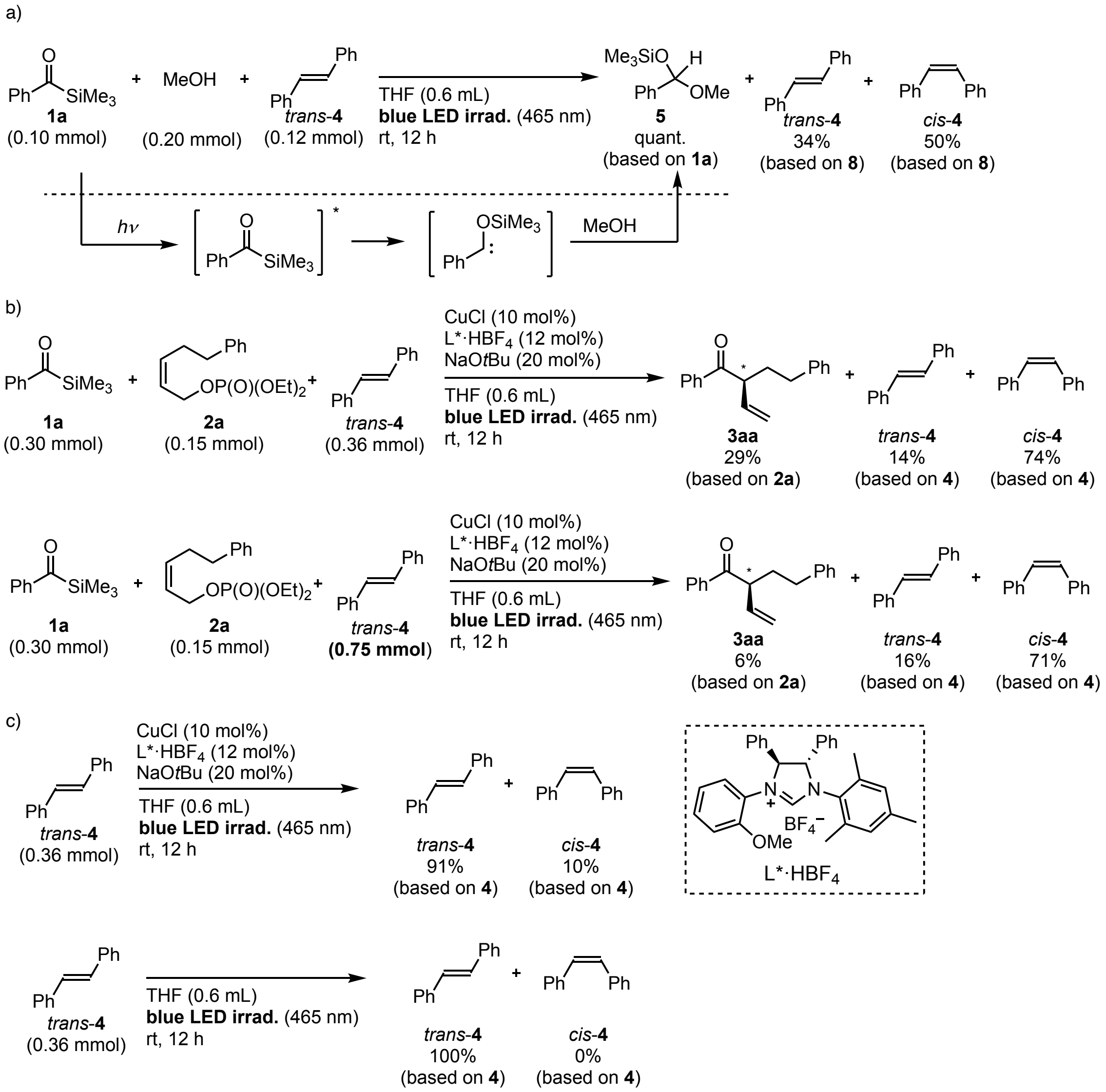

The author attempted to observe the key acylcopper intermediate by spectroscopic techniques. First, UV-vis spectra of acylsilane (1a, 300 μM) (blue line), allylic phosphate (2a, 300 μM) (green line), the mixture of L3·CuCl (300 μM) and NaOtBu (300 μM) (brown line), and the mixture of 1a (300 μM), 2a (300 μM), L3·CuCl (300 μM), and NaOtBu (300 μM) (red line) were recorded, respectively, using THF as a solvent (Figure 1). However no distinctive absorption indicative of a new organocopper species was observed upon addition of 1a and 2a.

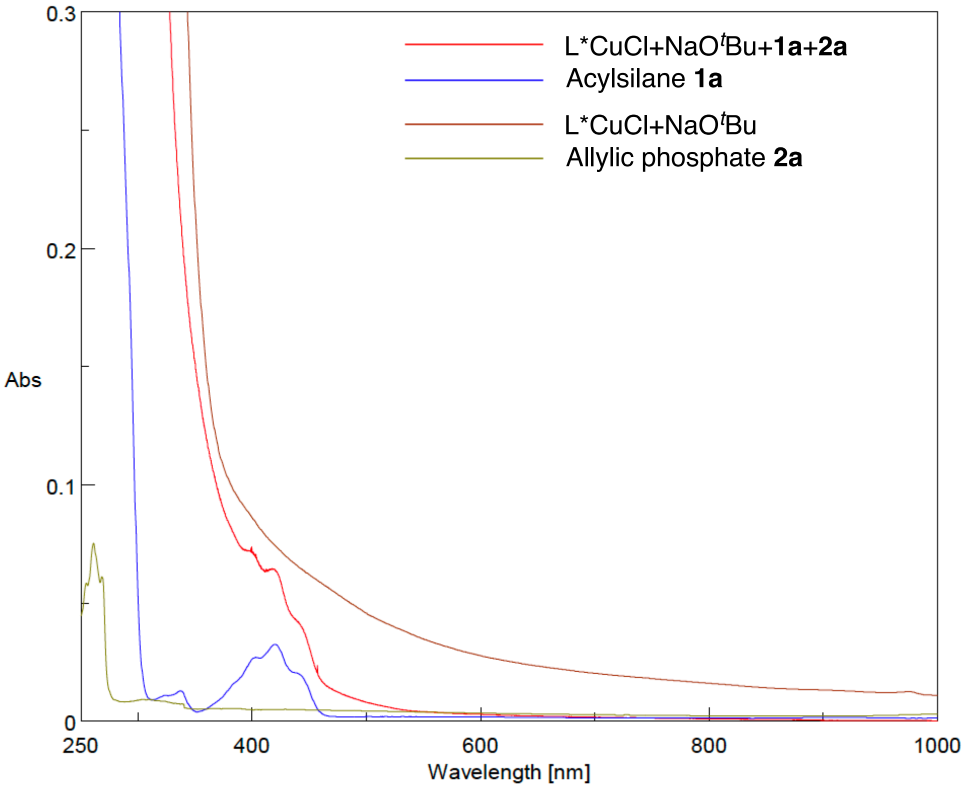

Figure 1. UV-vis absorption spectra of the reaction components.

Next, emission spectra of acylsilane (**1a**, 100 μM) (blue line) and the mixture of L*·CuCl (100 μM), NaOtBu (100 μM), **1a** (100 μM), and allylic phosphate **2a** (100 μM) (red line) were recorded at 468 nm excitation (Figure 2). While no distinctive signal indicative of a new organocopper species was observed upon addition of **1a** and **2a**, the slightly enhanced broad band emission around 610 nm and the disappearance of the 500 nm suggest the change of the existing chemical species.

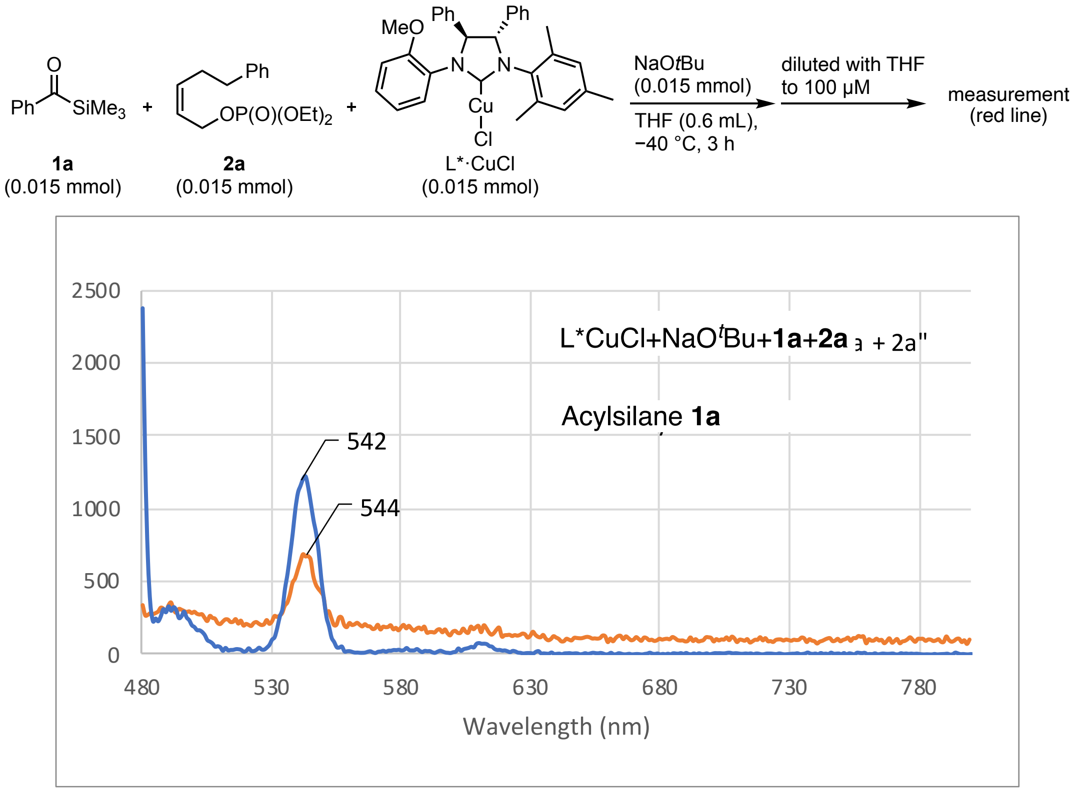

Figure 2. Emission spectra of the reaction components in THF at 468 nm excitation.

Futuremore, the author measured emission spectra of the reaction mixture after photoirradiation. Allylic carbonate **6**, which was inert to the allylic acylation reaction but could coordinate to the copper center, was used instead of **2a**. A mixture of **1a** (0.015 mmol), **6** (0.015 mmol), L*·CuCl (0.015 mmol), and NaO^{t}Bu (0.015 mmol) in THF (0.6 mL) was irradiated with blue LEDs at –40 °C for 3 h, and the mixture was diluted with THF to 100 µM and transferred to a quartz cuvette for measurement. Emission spectra of the resulting mixture were recorded at 468 nm excitation (Figure 3). Emission of acylsilane **1a** was dominant, and no distinctive signal corresponding to a new organocopper species was observed.

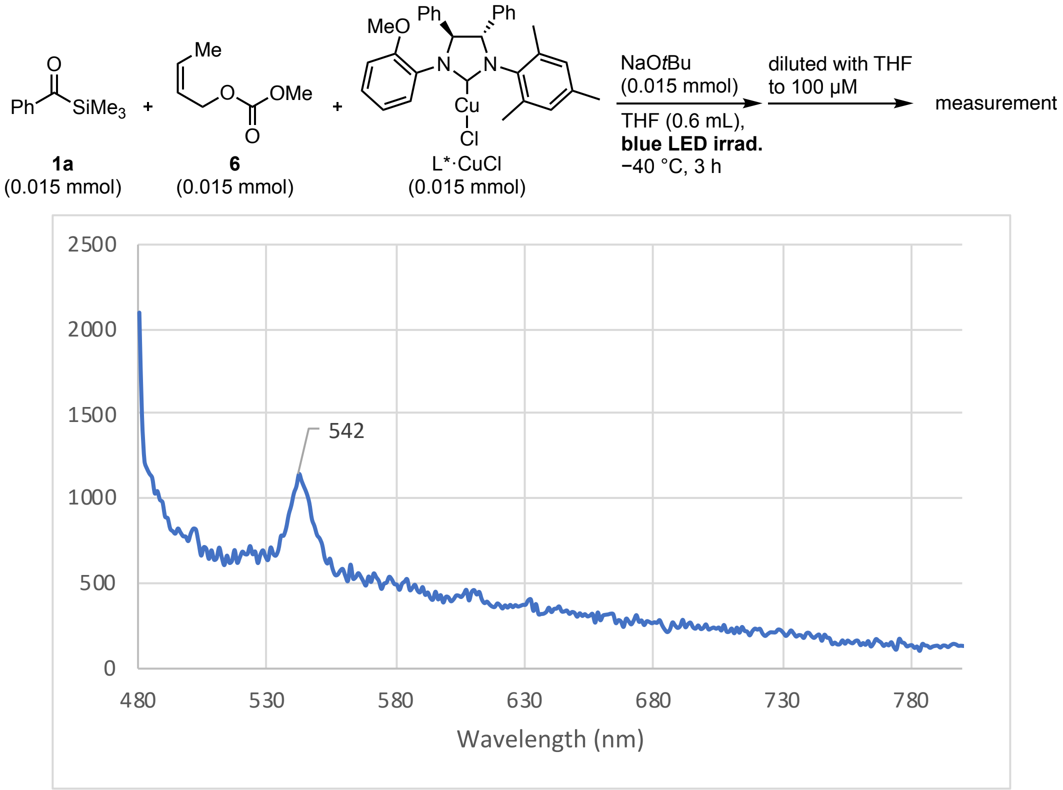

Figure 3. Emission spectra of a mixture of L*·CuCl (100 µM), NaO^{t}Bu (100 µM), **1a** (100 µM), and alkene **S1** (100 µM) in THF at 468 nm excitation after photoirradiation.

Since it was difficult to directly observe the intermediates by experimental methods, the reaction mechanism was analyzed by DFT calculations (B3LYP-D3/6-31G**). Shown in Figure 4 is a potential energy profile for generation of an acylcopper intermediate from the siloxycarbene and **L**·CuO*t*Bu. Starting from copper(I) *tert*-butoxide **7** generated by coordination of siloxycarbene to **L**·CuO*t*Bu, the *tert*-butoxide ligand of **7** attacks the silicon atom to eliminate silyl *tert*-butoxide through five-membered-ring transition state **TS**$_{7\text{-}8}$ (ΔE = 11.3 kcal/mol). This is consistent with the experimental result that the reaction proceeds at –40 ˚C.

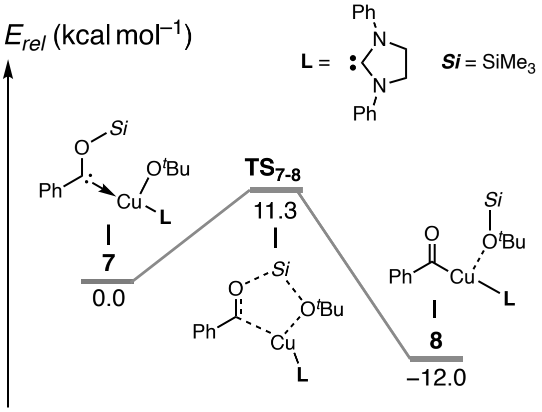

Figure 4. Energy diagrams for the generation of acylcopper intermediates from copper(I) *tert*-butoxide **7**

Calculated frontier molecular orbitals of a ground-state copper complex **9** and a triplet excited state complex **10** are shown in Figure 5. DFT calculations for the achiral model acylcopper(I) complex **9** η^2-coordinated with dimethyl (*Z*)-2-butenyl phosphate gave a rationale for the reaction design based on Cu-to-acyl MLCT photoexcitation. At ground state, HOMO (denote as HOMO_{s0}) of **9** mainly possesses a copper d-orbital character. LUMO (denote as LUMO_{s0}) and LUMO+1 (denote as LUMO+1_{s0}) have nearly equal orbital energies and are localized in the NHC ligand and the acyl group, respectively. At the triplet state, two α-SOMO orbitals are very similar to HOMO_{s0} and LUMO+1_{s0}, indicating that the electrons in the HOMO_{s0} were excited to the LUMO+1_{s0} orbital. These results indicate that photoexcitation of copper complex **9** induces electron transition from HOMO to LUMO+1, which corresponds to metal-to-ligand charge transfer (MLCT) excitation.

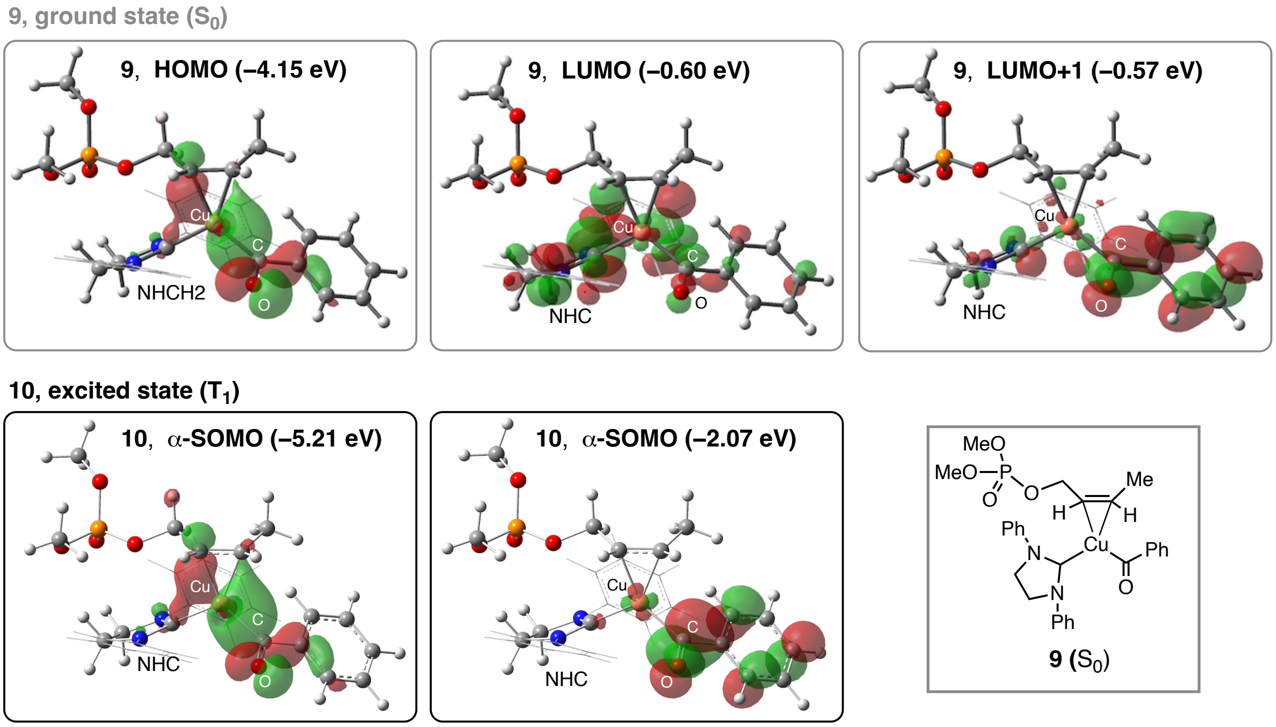

Figure 5. Frontier molecular orbitals of copper complex **9**

The calculated excited states of copper complex **9** at TD-DFT level were shown in Table 1. Both S_1 and T_1 states are below the experimental energy of blue LED (465 nm, 2.7 eV). In addition, T_2 state was located close to the LED energy. Therefore, it is proposed that copper complex **9** was excited to higher excited states and finally decays into T_1 state to form active species complex **10**. Due to the high activities and low concentration of active species **9**, it is difficult to compare the calculated data with the experimental ones.

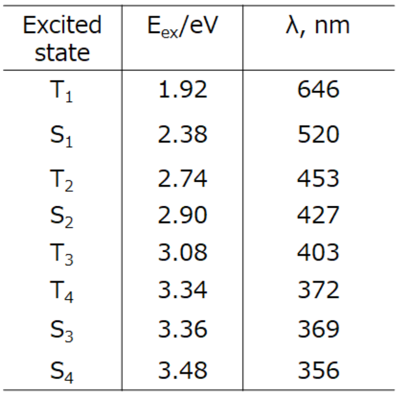

Excited state	E_{ex}/eV	λ, nm
T_1	1.92	646
S_1	2.38	520
T_2	2.74	453
S_2	2.90	427
T_3	3.08	403
T_4	3.34	372
S_3	3.36	369
S_4	3.48	356

Table 1. Excited states of copper complex **9** at TD-DFT level. E_{ex} and λ are vertical excitation energy and absorption wave length relative to S_{0min}.

Potential energy profiles at triplet state of the copper-photocatalytic allylic acylation reaction are shown in Figure 6. As shown in Figure 6, the most populated ground state of **9** (S_0, 0 kcal mol^{-1}) can be excited to S_1 state and decay into T_1 state via nonradiative processes to form active species complex **10** (46.9 kcal/mol). Subsequent geometric relaxation of **10** leads to charge-separated copper-bound ketyl radical species **11** as the T_1 local minimum (38.0 kcal mol^{-1}). This transition increases the positive charge at the copper atom (**9**, +0.74; **10**, +0.82; **11**, +0.82). The spin density of **11** is localized at the carbonyl carbon and oxygen atoms, reflecting the ketyl radical character of this species. Note that the separated charges are significantly neutralized through an O···Cu electrostatic interaction as indicated by the narrowed Cu–C–O angles (**9**, 114.4° vs. **11**, 99.3°). Intermediate **11** then alters its conformation in the allylic substrate toward coordination of the phosphate leaving group to the positively charged copper atom (**TS$_{11\text{-}12}$**). The resulting cyclic intermediate (**12**, 41.0 kcal mol^{-1}) undergoes facile C–O bond cleavage with a barrier of 5.8 kcal mol^{-1} (**TS$_{12\text{-}13}$**) to form a novel acylcopper(II) complex (**13**, 14.1 kcal mol^{-1}) with an electronically neutral allylic radical fragment (total NBO charge of the crotyl group: –0.005), which is η^2-coordinated with the Cu atom. Notably, this radical coordination is markedly weaker than the normal η^2-coordination of the allylphosphate substrate in the precursor complexes **9–12** as indicated by the elongated C–Cu atomic distances. This triplet state **13** undergoes intersystem crossing (**ISC$_{13\text{-}14}$**), forming a ground state (S_0) acyl(η^1-allyl)copper(III) phosphate (**14**, –15.4 kcal mol^{-1}). Finally, reductive elimination furnishes the α-branched β,γ-unsaturated ketone **15** (–35.0 kcal mol^{-1}).

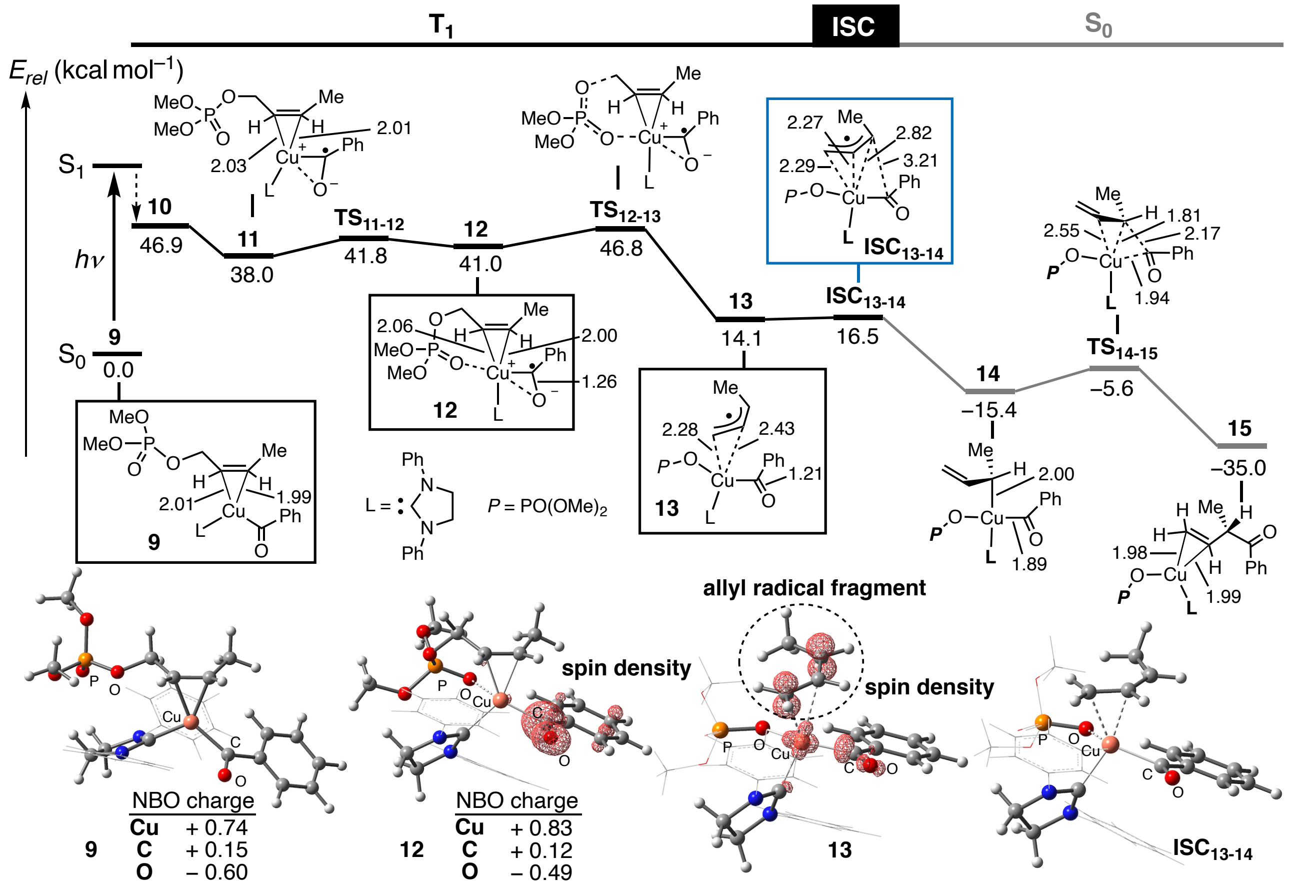

Figure 6. Energy diagram for calculated photochemical reaction of **9**. All energies are relative to **9** (kcal mol^{-1}). **TS**: transition state. **ISC**: intersystem crossing

Frontier molecular orbitals for **13**, **ISC**, and **14** are analyzed to clarify the origin of site-selectivity for C–C bond formation. As shown in Figure 7, C_α is closest to Cu with a distance of 2.28 Å in **13**. The α-SOMO with lower energy is populated at the C_α and C_γ atoms of the allylic fragment and the Cu atom, and C_α and Cu possess an anti-bonding interaction. Another α-SOMO does at the Cu and acyl group. With the geometry change from **13** to **ISC** at T_1 state, the distances of C_α–Cu and C_β–Cu become nearly equal, 2.29 Å and 2.27 Å, respectively. A bonding character appears between C_γ and the acyl carbonyl carbon atom at α-SOMO orbital (α-SOMO$_{T1}$) with a lower energy. Another α-SOMO orbital showed an anti-bonding orbital character between the allylic fragment and Cu. When the spin state changes from T_1 to S_0 at **ISC**, an electron at α-SOMO$_{T1}$ with the higher energy switches to the one with lower energy to form a doubly occupied orbital, HOMO. Therefore, the bonding character between C_γ and Cu is strengthened and **14** is formed with the Cu–C_γ bond formation.

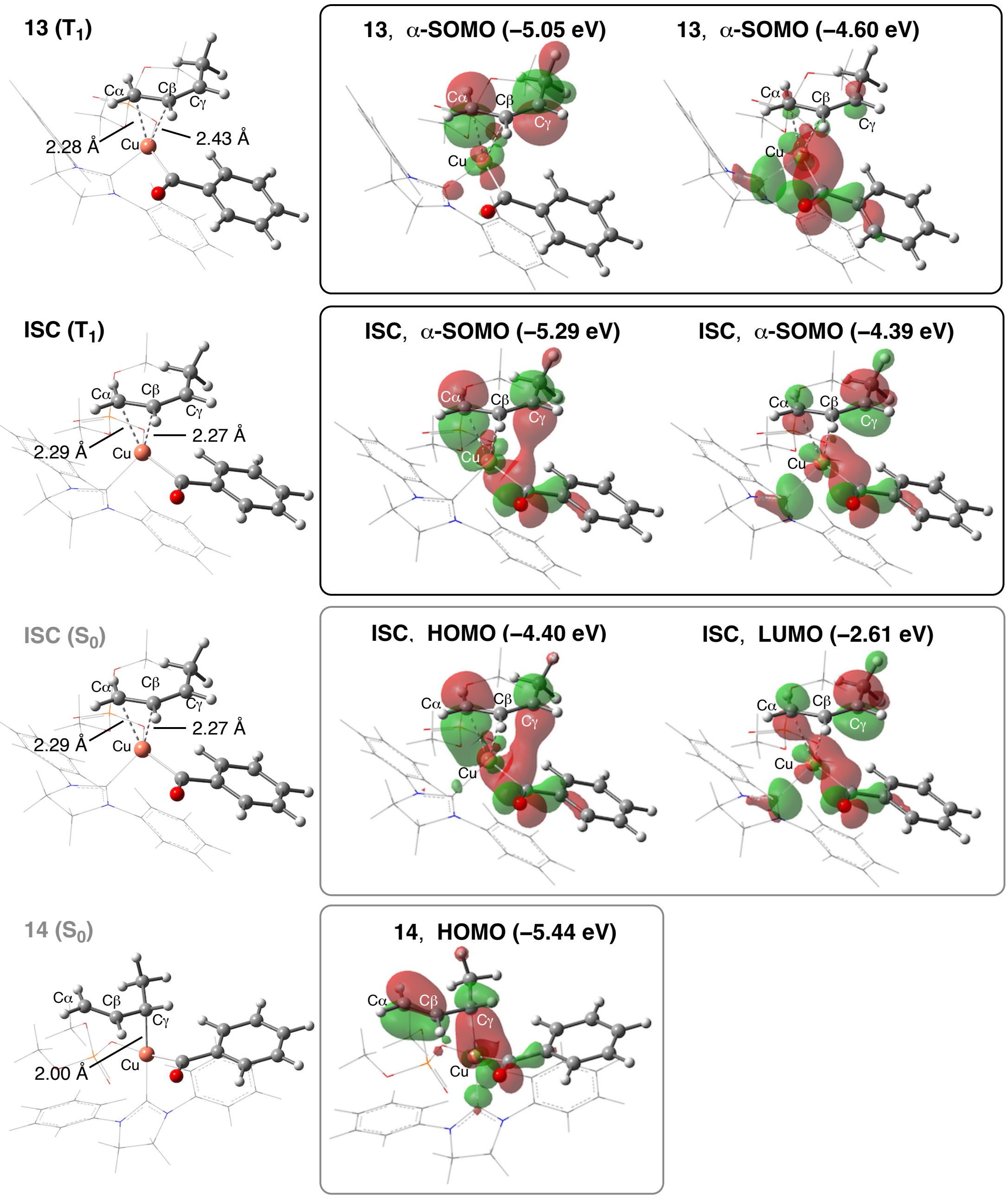

Figure 7. Molecular orbitals of copper complex **13** (triplet state), **ISC** (ground state, triplet state) and **14** (ground state)

Although the triplet-quenching experiments (Scheme 2) suggested that allylic substitution of the acylcopper(I) intermediate should go through the photoexcited reaction pathway, the author also considered potential energy profiles of copper-catalyzed allylic acylation at the ground state (Figure 8). Starting from the copper complex **9**, an oxygen atom of the phosphate group coordinates to the copper center through transition-state **TS$_{9\text{-}16}$** (4.9 kcal/mol) to produce intermediate **16** (3.9 kcal/mol). The cyclic copper complex **16** undergoes concerted C(allyl)–O bond cleavage and Cu–O bond formation to afford intermediate **14**, which is shared with the excited-state reaction pathway discussed in the Figure 6, through **TS**$_{16\text{-}14}$. The energy of this transition state is 10.2 kcal/mol higher than that of starting copper complex **9**. Thus, the photoexcitation pathway is more feasible than the ground state pathway for the present allylic acylation reaction.

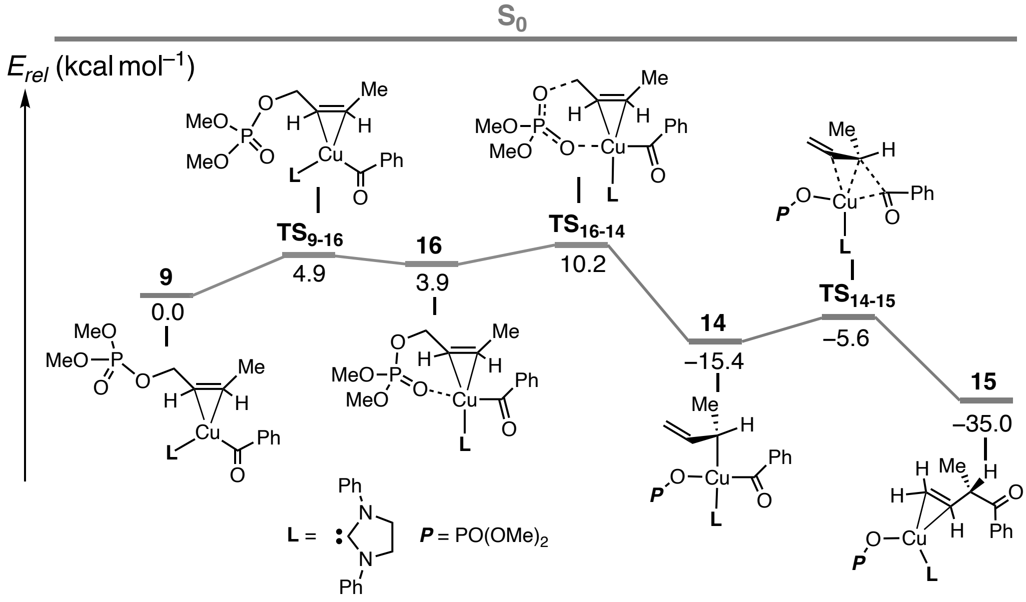

Figure 8. Calculated ground-state reaction pathway (less favorable pathway)

A proposed catalytic cycle for the photoinduced copper-catalyzed enantioselective allylic acylation involving two photoexcitation events is shown in Scheme 3. First, photoexcitation of the acylsilane (**1**) produces a singlet siloxycarbene species,[3] which leads to the acylcopper(I) intermediate (**9'**) through coordination to **L***·CuO*t*Bu,[5] followed by nucleophilic attack of the alkoxo ligand to the silicon atom. The second photoexcitation occurs with **9'** in an MLCT fashion to generate the charge-separated triplet excited state **12'**. Next, the allylic phosphate undergoes molecular activation by the charge-separated species through Lewis acid activation of the leaving group, accompanied by a shift in the electron density from the anionic acylcopper moiety to the allylic system to produce an acylcopper(II) complex bound with an allylic radical fragment (**13'**). This species undergoes regio- and stereo-controlled C–Cu bond formation under the influence of the chiral NHC ligand, resulting in the formation of the ground state (S_0) copper(III) complex (**14'**). Finally, stereoretentive reductive elimination produces enantioenriched allylic acylation product **3** and a copper(I) phosphate complex, which reenters the catalytic cycle through the reaction with the photochemically produced siloxycarbene species.

Scheme 3. A proposed catalytic cycle for photoinduced copper-catalyzed enantioselective allylic acylation.

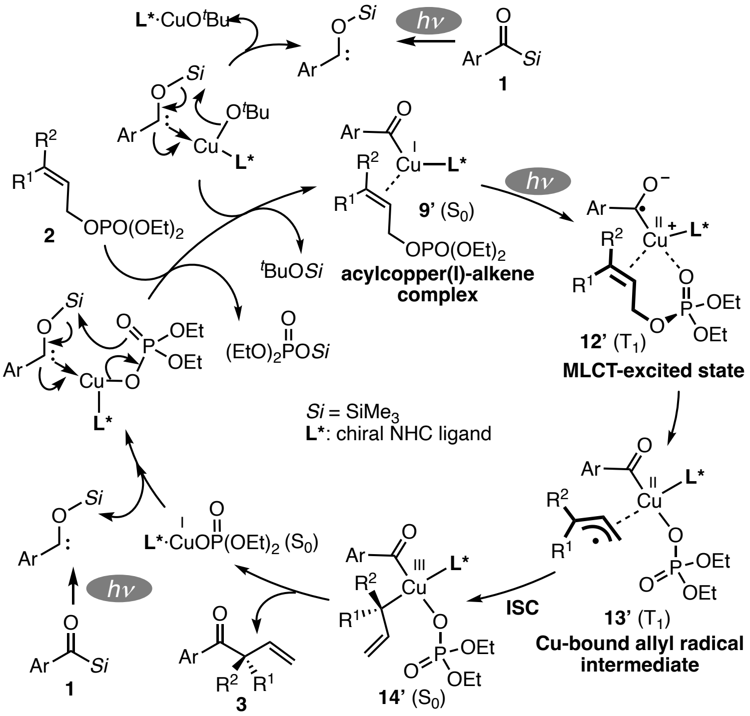

Conclusion

In summary, the author performed mechanistic investigation combined experimental and theoretical studies to elucidate the proposed mechanism. These results supported the reaction design based on copper-to-acyl metal-to-ligand charge transfer (MLCT) photoexcitation that generates a charge-separated triplet state as a highly reactive intermediate. In the process, the interesting finding that the photoexcited acyl copper activates the leaving group of the allyl phosphate substrate to generate allyl radicals, which are bound on the copper complex by dispersion force, was obtained.

Experimental Section

Instrumentation and Chemicals

NMR spectra were recorded on a JEOL ECX-400, operating at 400 MHz for ^{1}H NMR, 101 MHz for ^{13}C NMR. Chemical shift values for ^{1}H NMR and ^{13}C NMR are referenced to Me_4Si (0.00 ppm for ^{1}H NMR) and $CDCl_3$ (77.0 ppm for ^{13}C NMR). Chemical shifts are reported in δ ppm. High-resolution mass spectra were recorded at the Instrumental Analysis Division, Global Facility Center, Creative Research Institution, Hokkaido University (Thermo Fisher Scientific Exactive or JEOL JMS-T100LP for ESI-MS) and the GC–MS & NMR Laboratory, Research Faculty of Agriculture, Hokkaido University (JEOL JMS-T100GCv for FD-MS). HPLC analyses were conducted on a HITACHI ELITE LaChrom system with a HITACHI L-2455 diode array detector. Optical rotations were measured on a JASCO P-2200. TLC analyses were performed on commercial glass plates bearing 0.25-mm layer of Merck Silica gel $60F_{254}$. Silica gel (Kanto Chemical Co., Silica gel 60 N, spherical, neutral) was used for column chromatography. IR spectra were measured with a PerkinElmer Frontier instrument.

All reactions were carried out under nitrogen or argon atmosphere. Materials were obtained from commercial suppliers or prepared according to standard procedures unless otherwise noted. CuCl was purchased from Aldrich Chemical Co., stored under nitrogen, and used as received. THF was purchased from Kanto Chemical Co., and purified by passing through activated alumina under positive argon pressure as described by Grubbs *et al.*[9] NaO*t*Bu was purchased from TCI Chemical Co., stored under nitrogen, and used as received.

General procedure for mechanism analysis experiment using *trans*-4

In a N_2-filled glove box, CuCl (1.5 mg, 0.015 mmol), **L3**·HBF_4 (9.6 mg, 0.018 mmol), and NaO^{t}Bu (2.9 mg, 0.030 mmol) were placed in a vial containing a magnetic stirring bar. THF (0.6 mL) was added to the vial. The mixture was stirred at room temperature for 10 min. ***trans*-4** (64.9 mg, 0.32 mmol) was added to the vial, which was sealed with a cap and was removed from the glove box. Next, allylic phosphate **2a** (0.15 mmol) and acylsilane **1a** (0.30 mmol) were added via a syringe. After 12 h stirring at room temperature under blue LED irradiation, the reaction mixture was diluted with Et_2O and filtered through a pad of silica gel (eluting with Et_2O). The volatiles were removed under vacuum, and then an internal standard (dibenzyl) was added to determine the ^{1}H NMR yield.

Spectroscopic analysis

All UV-vis absorption spectra were recorded on a JASCO V-730 spectrophotometer using a screw-top quartz cuvette (10 × 10 mm, 3.5 mL). All emission spectra were recorded on a HITACHI fluorescence spectrophotometer F-4500 using a screw-top quartz cuvette (10 × 10 mm, 3.5 mL). In both cases, samples were prepared in a N_2-filled glove box and then taken out of the glove box.

Computational Studies

All computations in the present study were performed by Density Functional Theory implemented in Gaussian 09 program.[10] The optimizer implemented in GRRM17[11,12] were used for all the optimizations of intermediates, transition states (TSs) and intersystem crossing points. B3LYP functional with the D3 empirical dispersion correction (B3LYP-D3)[13] was selected as the exchange-correlation functional and 6-31G** basis set was used for all the atoms. The reaction pathways at excited state (triplet state, T_1) and ground state (S_0) were done by unrestricted B3LYP-D3 (UB3LYP-D3) and restricted B3LYP-D3 (RB3LYP-D3), respectively. The transition states were verified by frequency calculations and IRC calculations. Natural population analysis (NPA)[14,15] was done to calculate the natural atomic charge with Gaussian NBO Version 3.1. The intersystem crossing point was optimized to be a minimum energy crossing point (MECP) and it was confirmed by comparing the energy difference of S_0/T_1 and reaction pathway connections. The simplified computational model of achiral NHC ligand and allylic phosphate were shown below.

Cartesian coordinates of the structures optimized by calculation at the B3LYP+D3/6-31G** level of theory

7

C	1.918885133108	1.645857944869	1.949709605068
C	0.561009795343	1.476911412163	2.637562778028
H	2.768568443246	1.563344827739	2.632032674915
H	0.006211297096	2.414139135960	2.683040129500
N	1.928181281651	0.533781553527	0.974443930169
N	-0.110560268655	0.515839490228	1.738823967008
C	3.020477526931	0.347256388632	0.093296904583
C	3.217539115900	-0.884906753720	-0.548914557797
C	3.924692927297	1.395888021277	-0.133182079272
C	4.273855097452	-1.033444225063	-1.444801608272
C	4.985948265540	1.225556633328	-1.024047257968
H	3.804536615543	2.347264945138	0.371044282888
C	5.161237114138	0.016225530235	-1.694843093926
H	4.408505303084	-1.994217011516	-1.932666980842
H	5.675490652146	2.048546772379	-1.189931108488
H	5.987013260237	-0.112950279165	-2.387706631888
C	-1.479622328701	0.164632896076	1.922376094259
C	-2.455178746836	1.169802010332	1.936628684486
C	-1.839800697137	-1.174369209268	2.097221895396
C	-3.792502736579	0.820833309211	2.124499958120
C	-3.182034784031	-1.511326198141	2.273748295340
C	-4.160652386876	-0.516531058561	2.291611075459
H	-4.550183916492	1.599023488665	2.130092457661
H	-3.453205039520	-2.555546321597	2.389533587436
Cu	0.087539993234	-1.200071940103	-0.600624161589
C	0.703387250940	-0.025618618458	0.815763267246
C	0.277713048432	-3.107341653885	-0.251988120899
O	1.444129943834	-3.526633249877	-0.321398210380
C	-0.787668380644	-4.134421186426	0.062149868512
C	-2.138345569699	-3.775889987962	0.039264445059
C	-0.442107198666	-5.456485870326	0.380636627025
C	-3.133696116764	-4.711930781993	0.324934190830
H	-2.397800632848	-2.749251573218	-0.191932268485
C	-1.428376068229	-6.394513508436	0.672300112609
H	0.612172982606	-5.716536936557	0.388593231317
C	-2.778226412377	-6.023834825554	0.644248274933
H	-4.180343684359	-4.419922400938	0.300025629667
H	-1.153804624509	-7.416334912015	0.921193148036
H	-3.548146938039	-6.756605393244	0.870653564423
C	-0.746293695206	-1.035364561882	-2.404590418984
C	-0.114115121539	0.172275361070	-2.051157016700
H	-0.209184584050	-1.675312570669	-3.102619391555
H	0.877163235330	0.363583067330	-2.462625833050
C	-2.250750603911	-1.202087742890	-2.430208818197
H	-2.673118717170	-0.748776221552	-3.337856791691
H	-2.529140775505	-2.258110154905	-2.424193081982
H	-2.737478297683	-0.727899558095	-1.571046830208
C	-0.827079817624	1.429466336104	-1.653650046056
H	-1.229259333454	1.977860642132	-2.515046266906
H	-1.637303177907	1.246629707803	-0.940938500991
O	0.177176479990	2.285182972122	-1.027051287849
P	-0.148425460742	3.713907491814	-0.410043513845
O	-0.863716402531	3.801163962139	0.884822360931
O	1.323828747217	4.350419365834	-0.312730264122
O	-0.895516045570	4.440930659532	-1.643421430960
C	2.199100196018	4.312467949662	-1.462902454050
H	1.693762191175	4.721141263771	-2.342902201757
H	2.520602609430	3.286629221364	-1.656135402773
C	-1.663762045366	5.634294405104	-1.383138647495
H	-2.294743817498	5.498982615147	-0.501458321700
H	-0.997655342440	6.489454183799	-1.229634937253
H	0.639258379774	1.042747614449	3.640945911851
H	1.977571545567	2.605714092517	1.427885554334
H	2.583902727230	-1.741668821316	-0.337302798368
H	-1.073519954653	-1.940004811265	2.073449869513
H	-2.162520989680	2.201970446976	1.776728223817
H	-5.204175361117	-0.781457780282	2.433593242741
H	-2.279214619813	5.804207211029	-2.267427228983
H	3.058762612975	4.934225090987	-1.209862168250

9

C	1.932776645565	1.673389021829	2.113372169571
C	0.615970876503	1.365354985372	2.843593747479
H	2.821400718439	1.535303107324	2.735151868360
H	-0.020104612710	2.246782364825	2.930644895232
N	1.924644581876	0.683609162913	1.011605621964
N	-0.015134615461	0.383377665390	1.940839808515
C	2.989745211584	0.570241065521	0.091094231407
C	3.262202013396	-0.664053944727	-0.518099131503
C	3.780612200782	1.685435405062	-0.213242399223
C	4.278366853062	-0.755377636215	-1.467261627296
C	4.807156863289	1.574291455181	-1.151563656910
H	3.578730115006	2.640092384062	0.257503302241
C	5.053464670896	0.360145029300	-1.793828382035
H	4.476034625967	-1.715188841867	-1.934953418588
H	5.412336877297	2.446357667661	-1.383086315343
H	5.850754202785	0.279414980005	-2.526119406972
C	-1.330199051854	-0.116257171637	2.190966358478
C	-2.431530133406	0.721817998993	1.991890435525
C	-1.491808299204	-1.424555418111	2.650452878669
C	-3.711258308701	0.233118518111	2.260225523475
C	-2.776679871889	-1.906001509027	2.903156877075
C	-3.883471837104	-1.076169867275	2.716601505793
H	-4.574757401909	0.873414277842	2.104610834873
H	-2.910536040238	-2.934536393333	3.218833389723
Cu	0.154445252896	-1.100647243172	-0.563231025664
C	0.745608656562	0.027005373488	0.905904714554
C	0.010374584899	-3.024412681696	-0.031489497278
O	1.229330954034	-3.333788283381	-0.058234124854
C	-1.144365841564	-3.821248591010	0.112492012442
C	-2.465612477490	-3.278895117190	0.086602724101
C	-1.021882667932	-5.237787098430	0.310908296217
C	-3.575972140373	-4.091071813150	0.236719367336
H	-2.588626353825	-2.205764925297	-0.019245902680
C	-2.145792484373	-6.029779750838	0.463376019444
H	-0.026593890010	-5.669904900058	0.339235751907
C	-3.439411589425	-5.477632371815	0.425644747704
H	-4.566303937677	-3.641686458766	0.219611507327
H	-2.023132148171	-7.100501102463	0.612649918776

H	-4.314382375918	-6.109054354499	0.543903815678
C	-0.439662030616	-1.219422616719	-2.482076851648
C	0.215458607228	-0.004805595895	-2.267053259995
H	0.150185783662	-2.015466242175	-2.934466328311
H	1.269016734228	0.073688811518	-2.532579668826
C	-1.932902847125	-1.359939475819	-2.659500848269
H	-2.208502935174	-1.159328791053	-3.703555185810
H	-2.261975227570	-2.368828376267	-2.405954791395
H	-2.496727428149	-0.663362978827	-2.030568743445
C	-0.461675008993	1.327021755539	-2.145324755260
H	-0.729421090616	1.744646668373	-3.124224010203
H	-1.366047107640	1.279920987105	-1.531290436766
O	0.503325199670	2.239365784511	-1.548346016579
P	0.053396240085	3.442743270991	-0.610301329390
O	-0.609380128575	3.145711086048	0.680086142148
O	1.444328130086	4.217929683975	-0.402204761947
O	-0.832767962389	4.329364032057	-1.628858597586
C	2.256575862075	4.558164696142	-1.549095938541
H	1.657592526837	5.078381311908	-2.301939813480
H	2.696122400849	3.653580213646	-1.974886249057
C	-1.716576975925	5.332320940489	-1.084244437095
H	-2.276554547835	4.929631204965	-0.236861110653
H	-1.145186227811	6.209287292366	-0.763220460492
H	0.763417674792	0.915474926565	3.831444850792
H	1.930207846641	2.688972176612	1.710652738713
H	2.702524824888	-1.549247432274	-0.232415111145
H	-0.622706173515	-2.063273488190	2.758369506212
H	-2.265100628850	1.728463444297	1.622964144809
H	-4.881908799427	-1.456217604714	2.911071862447
H	-2.396995435962	5.613760542677	-1.888737458999
H	3.040813615979	5.219949076564	-1.179582358119

TS$_{9-10}$

C	2.290338281390	1.655443061553	2.107492132062
C	0.909503996135	1.531188603304	2.775853781912
H	3.113024600699	1.306905299780	2.740481218425
H	0.353371821869	2.471145413639	2.746527762995
N	2.150870077945	0.771189686828	0.932627199442
N	0.232935568568	0.528543283603	1.928223964052
C	3.233097658669	0.490344794622	0.065859165977
C	3.455101540728	-0.825581864643	-0.368382787120
C	4.085266767850	1.517233447731	-0.355282590586
C	4.490749977523	-1.089312847640	-1.262931193738
C	5.131645357681	1.236706414555	-1.233982455831
H	3.922655431635	2.533284617596	-0.011982764255
C	5.331326017277	-0.063145544818	-1.701717979922
H	4.649099446515	-2.108857380878	-1.600975978486
H	5.784224537569	2.040540082382	-1.561667925463
H	6.141714484652	-0.276633073017	-2.391719545111
C	-1.005471286338	-0.051633887966	2.341021252853
C	-2.142033555287	0.747237546915	2.479755613264
C	-1.042046609569	-1.413279832227	2.651682522193
C	-3.329847990580	0.169113016131	2.925285618758
C	-2.242234933313	-1.987450515971	3.069494537616
C	-3.382237528880	-1.197376121221	3.212724521520
H	-4.221376293464	0.781542319941	3.022649661455
H	-2.288333233814	-3.055863386261	3.250368012023
Cu	0.371325120111	-0.895511112544	-0.673879752643
C	0.945762418105	0.157449667996	0.862326779332
C	-0.059653262778	-2.747534320630	-0.055757973226
O	1.064500506415	-3.271095656085	0.139416056284
C	-1.366106092464	-3.273201178523	0.033003793353
C	-2.529572956242	-2.471162727165	-0.183494003282
C	-1.571442300464	-4.638130009328	0.423768521699
C	-3.797780171318	-3.001629788982	-0.038798486571
H	-2.407592965148	-1.416497837179	-0.418347254532
C	-2.851675936132	-5.145437363710	0.567633366345
H	-0.700196536697	-5.259310101497	0.606604052018
C	-3.984265091129	-4.345619370588	0.333685727316
H	-4.661276090187	-2.360632689768	-0.199805644108
H	-2.979550601334	-6.184608024680	0.864065680366
H	-4.983286373921	-4.754545600314	0.448128407161
C	0.211747217150	-1.283229761490	-2.630047798393
C	0.786957135597	-0.014927179464	-2.470903301213
H	0.904574922119	-2.110350349536	-2.786227583000
H	1.872788656203	0.065263172867	-2.491743673984
C	-1.191431527207	-1.548965196083	-3.119942810176
H	-1.216214120551	-1.557293524476	-4.217615325380
H	-1.541160177208	-2.516766228423	-2.757774268248
H	-1.907757768668	-0.799718520282	-2.772832182074
C	0.081082141556	1.262776806802	-2.792381695311
H	0.368258103311	1.633715645010	-3.782048116649
H	-1.003892802323	1.147447341157	-2.765570967132
O	0.487000163598	2.322097915813	-1.863174930454
P	-0.597509215910	2.856722442789	-0.824561827775
O	-1.588064022157	1.900097799596	-0.288611661630
O	0.323665978695	3.525339794327	0.319346263594
O	-1.234192213978	4.104749570330	-1.634378609690
C	1.340012404642	4.472774623776	-0.067526304064
H	0.906137656646	5.286533936904	-0.655591497833
H	2.117521102462	3.972578954679	-0.651072472452
C	-2.479499247458	4.654741596025	-1.156216351339
H	-3.199941613545	3.856734570378	-0.960266601292
H	-2.316953526364	5.235118537274	-0.241420428158
H	0.959106621417	1.175087073062	3.808720611921
H	2.499846994000	2.681588111349	1.799213342368
H	2.828095767843	-1.633456967805	-0.001835829701
H	-0.148361036476	-2.013167059286	2.526154117729
H	-2.097353287617	1.790381689068	2.191934261017
H	-4.316466630679	-1.650205855843	3.530442120664
H	-2.848797601256	5.312697506716	-1.943777218092
H	1.759749080880	4.871764536817	0.857263795218

10

C	-3.210440005015	1.283375776245	1.024516070316
C	-2.102514804257	2.289110772484	1.367607692775
H	-4.154023202205	1.750383475793	0.731741816669
H	-1.883699627653	2.326273449491	2.435917765733
N	-2.613492669199	0.549652434682	-0.105352236426
N	-0.948965323814	1.744079110498	0.624879029013
C	-3.349188473521	-0.346693779502	-0.909381272800
C	-2.989420833592	-0.519991736697	-2.256062618311
C	-4.436097151527	-1.051900611325	-0.380028620941
C	-3.689572597666	-1.431174634153	-3.042110882289
C	-5.140576301025	-1.948019647988	-1.185597533145
H	-4.719598876050	-0.920488918632	0.658852508720

C	-4.766247338199	-2.150222293341	-2.514177966083
H	-3.398224242506	-1.564747010318	-4.079453439748
H	-5.979035168837	-2.495837495748	-0.765601446277
H	-5.313497228517	-2.852141070737	-3.135613073601
C	0.303446592049	2.425324854602	0.630630295927
C	0.956719040775	2.674938525016	1.840129998822
C	0.852554272168	2.853211975421	-0.580710499877
C	2.180343575402	3.340847016199	1.829751421794
C	2.094728384694	3.488090258750	-0.582718610341
C	2.756196436748	3.736610359825	0.618871103886
H	2.698302165505	3.526859842694	2.766167090494
H	2.549403884797	3.763231303443	-1.528333282027
Cu	-0.059532746159	-0.509360811717	-1.094524026659
C	-1.275197274371	0.749149824607	-0.210815607414
C	0.951669376893	0.389272041559	-2.559507613214
O	0.082647266429	0.527201694616	-3.454713122814
C	2.335482541399	0.678724712256	-2.554213559554
C	3.151897450221	0.495119726292	-1.396003120591
C	2.951844239702	1.250070797018	-3.715493546212
C	4.490916407109	0.841712394777	-1.412629713759
H	2.696654775840	0.124300166480	-0.483046515975
C	4.293264654315	1.594881431931	-3.704101442975
H	2.341661548881	1.408791974585	-4.599116417755
C	5.087071708995	1.391815452870	-2.562171857314
H	5.084458818251	0.700254456020	-0.512277931436
H	4.737518711627	2.026999621715	-4.598506387572
H	6.137961292310	1.664442967315	-2.564250778651
C	0.526676566835	-2.367579499916	-1.545128943212
C	-0.570194084878	-2.456025362144	-0.672426204924
H	0.308293651612	-2.456667983356	-2.609383850054
H	-1.558452477392	-2.554977695008	-1.116430707326
C	1.956069973459	-2.670527481790	-1.166359859835
H	2.150092342170	-3.749978046666	-1.225350404175
H	2.639687280015	-2.160034657669	-1.846535194232
H	2.191763960956	-2.326704116329	-0.156690705897
C	-0.477933622920	-2.961163636497	0.737433545158
H	-1.174002350688	-3.788899768278	0.889926855440
H	0.525821042905	-3.312275288212	0.987037982302
O	-0.893839014610	-1.974403016047	1.757651053719
P	0.261777946475	-1.052877284249	2.358063316389
O	1.242036372577	-0.465776298938	1.417383180187
O	-0.585340635305	0.044667130535	3.180596602127
O	0.920743205725	-2.020707704741	3.472516639265
C	-1.563586465531	-0.391669449580	4.145775391078
H	-1.104883503403	-1.046931858587	4.891658717281
H	-2.379625413838	-0.920950260699	3.645784246977
C	2.254683958685	-1.716938609105	3.937780981233
H	2.907190309327	-1.474801814455	3.095848314167
H	2.231760276845	-0.874963917224	4.637322763081
H	-2.320990673563	3.303154827481	1.014031727330
H	-3.403734372397	0.596984128229	1.857637374290
H	-2.169037754047	0.053554853727	-2.677325816078
H	0.326031379675	2.653850385303	-1.505866603867
H	0.528915724649	2.307866653311	2.766165130147
H	3.724242607066	4.228184491295	0.612301311365
H	2.611547433973	-2.610071057797	4.451903650642
H	-1.941838099343	0.510309649155	4.628963327927

TS$_{10-11}$

C	-3.229712556148	1.147168740389	1.140739202210
C	-2.203283926714	2.237339658115	1.477647979029
H	-4.235064143259	1.530879778837	0.952370585824
H	-1.938140434587	2.245377482798	2.535334844013
N	-2.648761613320	0.552023736775	-0.076049027953
N	-1.047947410198	1.825462143823	0.655755662144
C	-3.344745492848	-0.367603952473	-0.888107394175
C	-3.001812266892	-0.484959393412	-2.245064322686
C	-4.376819892587	-1.149679163172	-0.358194895650
C	-3.670210289500	-1.406694759602	-3.045452283518
C	-5.048438066915	-2.059511659507	-1.176983542445
H	-4.641722768094	-1.068577161173	0.690345113007
C	-4.696348874927	-2.198000345232	-2.519274856721
H	-3.390829074247	-1.497419859465	-4.090729550682
H	-5.844026202901	-2.667143033938	-0.755871117027
H	-5.218614090991	-2.909329961481	-3.151448139178
C	0.190370924179	2.524960310056	0.692755362049
C	0.820407600236	2.780055670756	1.913747699262
C	0.770661540995	2.948215117158	-0.506908504904
C	2.042404870307	3.449542909100	1.926840842972
C	2.007344077546	3.591576803473	-0.484656079902
C	2.643063200051	3.848755365948	0.729865727885
H	2.538611519578	3.638424987899	2.874422360567
H	2.473241675564	3.881514917513	-1.420613111421
Cu	0.011247825149	-0.397203391938	-0.968223358545
C	-1.334374762387	0.847371603373	-0.216226869467
C	0.943436819292	0.445070462309	-2.503462256479
O	0.174109538482	0.442789829825	-3.473443849259
C	2.382984213008	0.585474861620	-2.517977619250
C	3.155366487012	0.535718279631	-1.330935174608
C	3.037321858420	0.898430706107	-3.739141865750
C	4.520640857297	0.779347565022	-1.372226092860
H	2.667495391699	0.322920981431	-0.385637042184
C	4.402766186057	1.149654633883	-3.760502576215
H	2.444765876041	0.943602563708	-4.647099680644
C	5.158782749736	1.089547155245	-2.582233677490
H	5.096145594407	0.738613162568	-0.451130396476
H	4.888182444940	1.389686701715	-4.703380813862
H	6.226474762944	1.286450875202	-2.605218849579
C	0.652234610667	-2.239735368547	-1.511387484347
C	-0.573404901693	-2.496844138474	-0.841828401147
H	0.590252371562	-2.244938180751	-2.598966079277
H	-1.484111399724	-2.481406436391	-1.432948213031
C	1.995114651607	-2.640410831566	-0.954220818378
H	2.154625293931	-3.721545225991	-1.070826019377
H	2.799595062956	-2.120642941138	-1.478695931617
H	2.086874155685	-2.390147016660	0.104608452035
C	-0.706225267940	-3.046673259336	0.483559645749
H	-1.610184967964	-3.619932072740	0.658521370032
H	0.176235442166	-3.505027485688	0.922551169703
O	-1.069022492161	-1.871296485688	1.734127082995
P	0.161791551708	-1.039478714833	2.200915015011
O	1.020715679398	-0.384100215771	1.168062976092
O	-0.438151803333	0.070272121609	3.228008344271
O	1.013898795280	-2.055152324232	3.137232104085
C	-1.262916487200	-0.385393096837	4.315994875880
H	-0.718280184431	-1.098311124730	4.942604743599

H	-2.171919117204	-0.861172483405	3.935643887442
C	2.362570562208	-1.678051116704	3.476514162117
H	2.931732172974	-1.433692268542	2.575897619420
H	2.364028932750	-0.813625983186	4.149745030360
H	-2.530032963924	3.240972086813	1.181509530634
H	-3.276901445421	0.386524803013	1.929130867844
H	-2.203604943330	0.125263739289	-2.656009503487
H	0.264529325829	2.743971053403	-1.442439100033
H	0.383425269868	2.406363115369	2.832119813943
H	3.604926290529	4.352251072781	0.744364108882
H	2.806395262312	-2.535832530592	3.983974288862
H	-1.520521942442	0.497818593722	4.903371361026

11

C	-3.079915447751	1.269206613786	1.194236478960
C	-2.006567252751	2.339253434581	1.467716171249
H	-4.076744302199	1.682276090281	1.024061423569
H	-1.675461747251	2.340497780158	2.507263252248
N	-2.559607092943	0.625767683145	-0.030015685566
N	-0.906863007552	1.897419975250	0.584371946744
C	-3.271713856121	-0.355752052877	-0.762666402291
C	-3.136324450636	-0.377270076871	-2.157292888245
C	-4.078166755170	-1.291631269080	-0.110744780971
C	-3.811566915766	-1.346555851751	-2.896400828776
C	-4.761224740606	-2.246071253928	-0.864877825556
H	-4.110193689792	-1.312618106839	0.971568083586
C	-4.633728067315	-2.277435972855	-2.255150427822
H	-3.696318344555	-1.369061387378	-3.975844699039
H	-5.378648965485	-2.981894966338	-0.358491944727
H	-5.164431616818	-3.026960313726	-2.834384571610
C	0.348816145160	2.566194119572	0.521931107023
C	1.161189481847	2.652723821645	1.655704742352
C	0.758127535812	3.129261983350	-0.690650764484
C	2.386923798472	3.311098990845	1.565617514441
C	1.992242222820	3.771944645262	-0.773905321440
C	2.805965035367	3.869057685742	0.354913476150
H	3.027104648035	3.369875043619	2.441040430397
H	2.322242092945	4.178287880021	-1.724435202713
Cu	0.028057111478	-0.470324450149	-0.839014913992
C	-1.262698150060	0.899865601749	-0.234421667119
C	0.714461611873	0.306341005722	-2.487852895550
O	0.015988011028	0.522710409374	-3.463344329191
C	2.166868324038	0.711233128884	-2.477652395338
C	2.958951503309	0.479914434635	-1.345346786037
C	2.719771544111	1.352714565157	-3.595554004177
C	4.290542383767	0.890617337202	-1.329784601396
H	2.527757937924	0.011502028297	-0.464528501759
C	4.049913143036	1.761976556722	-3.578066767395
H	2.083712570854	1.523653348547	-4.458428351386
C	4.836682582578	1.531101191089	-2.443845121127
H	4.897501486923	0.721947988671	-0.445418972244
H	4.477686011344	2.261450479435	-4.442976194054
H	5.874003335436	1.853900895803	-2.429842719991
C	1.792880604884	-3.011805203653	-1.323941632997
C	0.534935904616	-2.643676208757	-1.811440079515
H	2.621499591323	-2.970625322856	-2.027117959251
H	0.488067405976	-2.390293873863	-2.868635393705
C	2.111365898628	-3.457016784187	0.063864363190
H	2.400881154447	-4.517885881715	0.070979247231
H	2.970356677604	-2.896740914183	0.452674744535
H	1.284930997858	-3.315544682129	0.758606978650
C	-0.679774934830	-2.616229125697	-1.114869951446
H	-1.605183934546	-2.482138189868	-1.661402697018
H	-0.770858844711	-2.936048385302	-0.083617417676
O	-1.681254205285	-1.499778375759	2.031810326962
P	-0.249560569574	-1.131210864412	2.246141628508
O	0.661766480360	-0.803321691846	1.060142202775
O	-0.118902976915	0.180627403522	3.244897073278
O	0.475428182811	-2.302262672294	3.129400081840
C	-0.860812904263	0.116614556396	4.467886741191
H	-0.465841291182	-0.665813401336	5.126215636568
H	-1.918178480251	-0.092125339142	4.272963825580
C	1.847372189739	-2.110947190117	3.490400646168
H	2.460914905361	-1.914165786723	2.605916225259
H	1.954507039994	-1.271946821167	4.188294827756
H	-2.324084258871	3.350861211074	1.188755752116
H	-3.110293105910	0.520049087993	1.990025948538
H	-2.471307959194	0.330997091160	-2.641711064259
H	0.117758203425	3.032263561765	-1.560989509417
H	0.850271532883	2.159475185533	2.568754425306
H	3.768962815497	4.366262659465	0.288891094136
H	2.181939440048	-3.031331722982	3.974155918033
H	-0.757518794094	1.087430116622	4.959488440974

ISC$_{11-12}$

C	-3.182725901	1.281462413	1.057174160
C	-2.111788146	2.357888854	1.298643952
H	-4.178258201	1.686845177	0.862582262
H	-1.816649938	2.427091958	2.347536484
N	-2.649233240	0.593366482	-0.135947043
N	-0.987754240	1.850841975	0.483618575
C	-3.365821533	-0.389921584	-0.850554814
C	-3.087494475	-0.574213156	-2.214075369
C	-4.336477051	-1.171396823	-0.218104805
C	-3.762673909	-1.561978857	-2.925791349
C	-5.017169625	-2.147062033	-0.948121462
H	-4.524870235	-1.050546590	0.842169432
C	-4.732479980	-2.350691545	-2.298930233
H	-3.535557299	-1.708397562	-3.977554245
H	-5.761760253	-2.760807203	-0.450001781
H	-5.261425483	-3.115335494	-2.859362284
C	0.251747020	2.550114821	0.390352075
C	1.089181566	2.650085662	1.503457495
C	0.607273793	3.142893816	-0.824669496
C	2.288117349	3.352706995	1.390489634
C	1.813878245	3.833555916	-0.930472452
C	2.653250920	3.943577584	0.177995216
H	2.950220951	3.419661273	2.248736248
H	2.102923142	4.268178113	-1.881848447
Cu	-0.028434902	-0.561677453	-0.822254460
C	-1.334283601	0.823280944	-0.302629020
C	0.869663134	0.252420091	-2.367416178
O	0.255319705	0.409178274	-3.405189664
C	2.305507358	0.673314979	-2.235988269
C	2.982765286	0.530793452	-1.017733283
C	2.962109165	1.233148549	-3.343317134

C	4.307133437	0.952586633	-0.910477979
H	2.469352546	0.125915684	-0.151083373
C	4.284733388	1.649481272	-3.230809306
H	2.413554128	1.334982898	-4.274303979
C	4.958477143	1.510199251	-2.012050289
H	4.826334171	0.855892852	0.038258549
H	4.793439974	2.083654322	-4.087022583
H	5.989938529	1.839935868	-1.923380165
C	1.522251830	-2.791407825	-1.567400848
C	0.140899210	-2.628122173	-1.746676307
H	2.150789641	-2.643856252	-2.441879848
H	-0.192077675	-2.432443550	-2.764981796
C	2.213392788	-3.148453739	-0.294609542
H	2.753908912	-4.098592774	-0.407166364
H	2.959852842	-2.385264742	-0.041871823
H	1.528740513	-3.227585188	0.548810133
C	-0.848454325	-2.698949915	-0.761402140
H	-1.891260613	-2.667838612	-1.045165512
H	-0.632167302	-2.988283700	0.259117541
O	-1.550571098	-1.101004580	2.166138686
P	-0.065540310	-0.992150016	2.298031005
O	0.809630299	-0.692537833	1.080799931
O	0.355324624	0.156196656	3.407248567
O	0.495040505	-2.365542547	2.999903796
C	-0.353128159	0.119382519	4.651017306
H	-0.106532312	-0.787677097	5.215783865
H	-1.434957231	0.142863649	4.483372931
C	1.884523297	-2.416692629	3.339031402
H	2.510289591	-2.151318362	2.480730528
H	2.111082474	-1.731097690	4.164102767
H	-2.408694660	3.352660347	0.944674685
H	-3.206655376	0.563783798	1.881354424
H	-2.325658620	0.033743976	-2.692344711
H	-0.052392077	3.034264857	-1.679347805
H	0.822327568	2.134632885	2.418370956
H	3.596389095	4.474760322	0.093528759
H	2.102303186	-3.441587031	3.648471051
H	-0.044118668	0.996980888	5.224459226

12

C	-2.914233841430	1.576597443906	0.658323703715
C	-1.850724376410	2.681116004095	0.754117410066
H	-3.839531821220	1.893282070963	0.169936443761
H	-1.584360583147	2.891628458339	1.791167522766
N	-2.234409894195	0.547286550218	-0.159346263644
N	-0.686216270513	2.060567513938	0.084087021626
C	-2.886676024466	-0.653245298817	-0.541107400872
C	-2.522695555836	-1.299620450697	-1.728725028174
C	-3.907567839837	-1.182278650528	0.257700644018
C	-3.146181530015	-2.494355736380	-2.083625628900
C	-4.537213204558	-2.366383917325	-0.120881665352
H	-4.177963936707	-0.704270451891	1.190301444719
C	-4.155742673311	-3.034214628716	-1.286006534705
H	-2.847036606569	-2.992332450272	-3.001046046899
H	-5.321414820606	-2.774342269838	0.509987528778
H	-4.645770682828	-3.959815324402	-1.572010027957
C	0.606719335476	2.657994432124	0.222909916193
C	1.415669544229	2.306413511904	1.306453495446
C	1.009370768353	3.635145540696	-0.689458503099
C	2.651085844277	2.937289624839	1.461806832106
C	2.240915877884	4.265517499221	-0.519999128296
C	3.060975993342	3.917432377164	0.555818698142
H	3.288082564720	2.667873051144	2.298965227794
H	2.567277726906	5.012329104116	-1.236531793944
Cu	0.409865386401	-0.580431968289	-0.704347496014
C	-0.928627636764	0.819120524524	-0.334902275728
C	0.823864836832	0.059717632243	-2.433624857342
O	0.073184791759	-0.188510224201	-3.356391190459
C	2.024808509204	0.932158174316	-2.611052083043
C	3.023817574017	1.003102951422	-1.635141423766
C	2.153064430112	1.673656826939	-3.795090159482
C	4.153001210044	1.789772174382	-1.845872756100
H	2.912731492142	0.446722887535	-0.711229138899
C	3.273295001351	2.474346198522	-3.996329990286
H	1.368581409352	1.600425927847	-4.540979864766
C	4.277942555065	2.527379405937	-3.024691634601
H	4.924587356862	1.839611357636	-1.084724129096
H	3.371031631718	3.050630843113	-4.911764115934
H	5.155743105402	3.146567517998	-3.186157116192
C	1.611595308699	-2.063890658949	-1.311773685285
C	0.541925094422	-3.025872966298	-1.651537039041
H	2.176627601589	-1.806095000131	-2.210956582685
H	0.007052338146	-2.802592555734	-2.574100827579
C	2.565363716109	-2.433048553494	-0.185575435521
H	3.084831847347	-3.369005506489	-0.433221671604
H	3.327670907931	-1.660471790171	-0.047186927396
H	2.042650354519	-2.559240951350	0.762475837520
C	0.159466130394	-4.088236607165	-0.927473555810
H	-0.663400116978	-4.718975368791	-1.249195370133
H	0.645487135734	-4.352501738230	0.005935546983
O	-0.888662190611	0.495766141978	2.674923724446
P	-0.530096132139	-0.926884996784	2.374928922474
O	0.168285129292	-1.307957725618	1.061588080649
O	0.467315333367	-1.567400382864	3.497378035142
O	-1.885418484751	-1.824871833539	2.504244174713
C	0.137126308633	-1.321129032834	4.869651973598
H	-0.797554645902	-1.824943215502	5.144165221029
H	0.030881345272	-0.247809295737	5.056868702036
C	-1.840035220335	-3.185470516529	2.048148063004
H	-1.613028295405	-3.230104095846	0.980045781325
H	-1.086109696415	-3.755749153096	2.603257216096
H	-2.129238587528	3.608487452544	0.243474361066
H	-3.124521460758	1.165054328712	1.646918639744
H	-1.772615554427	-0.864999384894	-2.379956927433
H	0.365912153340	3.877521433005	-1.528964211599
H	1.045042839433	1.571442065889	2.012941952757
H	4.021875020244	4.407235111818	0.683408736278
H	-2.828568079997	-3.610822414357	2.231664363984
H	0.954854557919	-1.724627169149	5.470894090224

TS_{12-13}

C	-0.923636690509	-0.025664412402	-3.403848895324
C	0.358411417587	0.821463377098	-3.412394346698
H	-1.002119461857	-0.703791620864	-4.256646264307
H	0.168081189376	1.872060985282	-3.639077154685
N	-0.772435547409	-0.781059264558	-2.144850715856

N	0.827597200459	0.692490775206	-2.012245826843
C	-1.788663365346	-1.670726734297	-1.663381000242
C	-1.463757186331	-3.007485627837	-1.425720840272
C	-3.076038670321	-1.187279572085	-1.407394274636
C	-2.434891121674	-3.866362083527	-0.908733006856
C	-4.038976816523	-2.056100779475	-0.896479836598
H	-3.290567238630	-0.135807128116	-1.556773688381
C	-3.722040674586	-3.393976790166	-0.646148962420
H	-2.180014727181	-4.902581855678	-0.708046555013
H	-5.033278400691	-1.678741426536	-0.677849144245
H	-4.475015746023	-4.064905889741	-0.242703115533
C	1.768298768303	1.613250722447	-1.477337516203
C	1.457740277595	2.367441904344	-0.340642939762
C	2.989578891022	1.801890380173	-2.132267697507
C	2.381780994654	3.290592682237	0.147021477544
C	3.902653970577	2.734749007573	-1.643674572668
C	3.602794796846	3.481842345107	-0.502217379710
H	2.132064901944	3.871232522989	1.030022906889
H	4.853083373776	2.870624842778	-2.150891010503
Cu	0.020050864013	-0.580618770344	0.554987061183
C	0.128259810707	-0.220066793059	-1.324607592246
C	1.390572954844	-1.941584389849	0.769104855554
O	1.157351485160	-3.026665766093	0.234548596645
C	2.785927415571	-1.381101481839	0.758304038622
C	3.093289860747	-0.079075003283	1.170858251844
C	3.813282526734	-2.202893895531	0.271701724803
C	4.402569812790	0.394139180029	1.106818512013
H	2.311283046147	0.584073892541	1.518779015940
C	5.122381511832	-1.733563013176	0.212698160980
H	3.556275007392	-3.204306706686	-0.055888860535
C	5.420141881983	-0.433081686471	0.630445423483
H	4.618194672784	1.413251412156	1.408641013135
H	5.912009543604	-2.379083847172	-0.161308764644
H	6.441021434180	-0.065219244095	0.579897305403
C	0.474388228316	-1.759464051946	2.316794599255
C	-0.898481424689	-2.342979087190	2.148850886918
H	1.130691971039	-2.564922935900	2.661862945020
H	-0.950218602277	-3.148570259930	1.421883418037
C	0.618376870935	-0.620888483003	3.334385318637
H	0.325176605346	-0.998844408731	4.321252908338
H	1.657079534860	-0.295944133946	3.408414409135
H	-0.012382663994	0.241081635029	3.107400173824
C	-1.999425465978	-1.980153060168	2.812816512200
H	-2.948540454722	-2.466915050886	2.612426543239
H	-2.000143802050	-1.178987483508	3.544356710630
O	-1.927941435762	1.819518970881	-1.128129652479
P	-2.090147163116	1.739994881881	0.357149683018
O	-1.255255217765	0.755213483699	1.191839100387
O	-1.771850798587	3.173705823980	1.082315843918
O	-3.667797014316	1.477223447480	0.678333015888
C	-2.284257280524	4.349681382653	0.444209630110
H	-3.380771130690	4.357141216128	0.457858439321
H	-1.940626485086	4.407683956830	-0.593248649343
C	-4.040871961571	1.125881168816	2.015624656781
H	-3.614237849791	0.157488093193	2.289805373402
H	-3.704468972404	1.883791338047	2.733018721683
H	1.114836475267	0.434425060962	-4.104155972864
H	-1.815472106247	0.602541545725	-3.332894644812
H	-0.449795370921	-3.346576854885	-1.597749319183
H	3.227384001012	1.206648284750	-3.008146040761
H	0.507182237040	2.228088355330	0.154288181173
H	4.314946045274	4.209700512481	-0.124958655058
H	-5.131933912882	1.071770257320	2.035325633845
H	-1.911181819230	5.206728150873	1.009697851343

13

C	-0.076367867213	-0.372544172849	-2.934415349079
C	0.994868140524	0.675974545557	-2.628149423271
H	0.256054676302	-1.145199035182	-3.630682690287
H	0.824517749519	1.616981309074	-3.154549714343
N	-0.316187684380	-0.933556314740	-1.593261674514
N	0.833241221224	0.866691849004	-1.171137755454
C	-1.287166865987	-1.968534542831	-1.379095205421
C	-0.852135542363	-3.277237211423	-1.169053474841
C	-2.648196575633	-1.647379152124	-1.378621781568
C	-1.793468286121	-4.278081350021	-0.924770031471
C	-3.580295445216	-2.658333431573	-1.141037054365
H	-2.941147092483	-0.614626449837	-1.540636530564
C	-3.155722193906	-3.969742310710	-0.911101195169
H	-1.457855311206	-5.292965221759	-0.735788183702
H	-4.638932134897	-2.417146342042	-1.127347333912
H	-3.885885569496	-4.750367387614	-0.718047876324
C	1.466052386040	1.932757403175	-0.501556270928
C	1.093016801246	2.307830147210	0.798654342183
C	2.487560072778	2.650197137319	-1.145062245001
C	1.751643924232	3.347624062395	1.445792279372
C	3.135178778234	3.697481909273	-0.488369037043
C	2.780622201063	4.048694805017	0.813089607091
H	1.433489097360	3.624886251686	2.445964943500
H	3.924006731383	4.236978794209	-1.004422819314
Cu	-0.742332268158	-0.248161000216	1.128457572874
C	0.076400825487	-0.108838290628	-0.615965764088
C	1.898061074442	-2.744433776069	1.145433099412
O	1.485409894860	-3.871595923927	0.894046959531
C	2.933936095533	-2.141727992400	0.244033044152
C	3.250541012731	-0.777405582733	0.183994621782
C	3.594489461241	-3.026662525185	-0.629699188682
C	4.205738729518	-0.311500280370	-0.720995524338
H	2.741615611466	-0.061762221291	0.810764149199
C	4.549816168877	-2.563519326823	-1.526604583981
H	3.336001675494	-4.078668241800	-0.584671975926
C	4.859146171419	-1.200294875211	-1.574335878680
H	4.427272975352	0.749677356354	-0.754719321429
H	5.054796270295	-3.261104204925	-2.188240787522
H	5.607523407259	-0.835027244599	-2.272005344982
C	1.288709034002	-2.074342161377	2.397959223002
C	-0.201164676376	-1.874774789603	2.138091323667
H	1.339567262152	-2.901774244491	3.121144272724
H	-0.645691133099	-2.718144690239	1.610358492925
C	1.982621037631	-0.870010373220	3.042833147662
H	1.654689456494	-0.772453938192	4.081594046596
H	3.069480078195	-0.982730094254	3.046681957036
H	1.731173079711	0.067824621650	2.538555781306
C	-1.044850538777	-1.074382975284	2.905889463338
H	-2.103111034150	-1.312599395984	2.979142096006
H	-0.659387528580	-0.435883430449	3.698033284759

O	-2.187647411047	1.536941822835	-1.511364478610
P	-2.439127812133	2.015790011893	-0.115562226831
O	-2.093432305709	1.128697264397	1.096370807425
O	-1.639497046883	3.406600452386	0.207775589288
O	-4.008149955319	2.424126731930	0.025656424315
C	-1.385803634076	4.328625705976	-0.854768202953
H	-2.258083033581	4.969773138908	-1.030788211266
H	-1.139800486862	3.798833412917	-1.779658778757
C	-4.486515765004	2.836808289212	1.310969589864
H	-4.367149050205	2.034536472818	2.045870995807
H	-3.949419964994	3.726000814434	1.661473127990
H	2.007599506284	0.312504303627	-2.841989630055
H	-1.004313560435	0.088848971116	-3.286360190053
H	0.208742356777	-3.496789793969	-1.151996888995
H	2.793499042010	2.389916648958	-2.150950029365
H	0.247361182517	1.831553736725	1.271399854361
H	3.286121313897	4.863878698662	1.320851967699
H	-5.545572779049	3.076991670957	1.192295960272
H	-0.537314871127	4.943951913931	-0.545175366132

TS$_{7-14}$

C	2.297333063831	1.539756045616	2.070560646490
C	0.904484695309	1.477817159302	2.722108312148
H	3.093778717242	1.144883579173	2.709607488515
H	0.418979497969	2.455567126195	2.757050520901
N	2.127198824742	0.680424189170	0.883843475655
N	0.161588404406	0.584036062934	1.809387963979
C	3.204192731564	0.364166996901	0.018696347100
C	3.393919507586	-0.961816453756	-0.398063316571
C	4.073166126787	1.369160168150	-0.418746226088
C	4.423151302581	-1.256187110892	-1.291155574732
C	5.112200309029	1.056860207169	-1.295330912031
H	3.925761895372	2.393923128156	-0.093760127798
C	5.284185769431	-0.253776395978	-1.744057456120
H	4.558007895474	-2.282509542598	-1.618970149390
H	5.778638124183	1.843126284839	-1.637597893095
H	6.088379224765	-0.493070061187	-2.433144697951
C	-1.099560329846	0.056126937148	2.222420783747
C	-2.198793297330	0.904150589344	2.374308821259
C	-1.195521462366	-1.297864322795	2.552108522188
C	-3.403642224949	0.382748837550	2.842924092628
C	-2.409510221763	-1.815844205838	3.000888443990
C	-3.512974077164	-0.975819151310	3.151718916097
H	-4.264536014058	1.036360702798	2.949115314562
H	-2.491825830434	-2.877437228548	3.210116903671
Cu	0.346156010781	-0.912571858201	-0.760529215450
C	0.880779747305	0.170217989488	0.755173349522
C	0.096834549791	-2.725738964493	-0.112964982982
O	1.115512797985	-3.353635621011	0.212278268901
C	-1.234441714735	-3.419325341555	0.074589684688
C	-2.417796896018	-2.749369753982	-0.250290486466
C	-1.308544254176	-4.706144200462	0.625365908754
C	-3.658763319968	-3.348141198940	-0.036621775520
H	-2.354597315414	-1.737764641881	-0.642286310995
C	-2.544236967234	-5.309253531411	0.846100670517
H	-0.376387270760	-5.202697509318	0.879192405987
C	-3.722821325968	-4.630223639954	0.513332069367
H	-4.571750962224	-2.813677011357	-0.283525991213
H	-2.597444343123	-6.306039368884	1.276712822256
H	-4.687509942124	-5.099705870191	0.687141931233
C	0.201935446279	-1.176120942048	-2.704747438686
C	0.761640797417	0.102709248476	-2.454999060188
H	0.908483650420	-1.962032210080	-2.972089550102
H	1.845809640838	0.190720045567	-2.514000856556
C	-1.195156380697	-1.412603921955	-3.236354718601
H	-1.219735086481	-1.313484272316	-4.330305989867
H	-1.536625170546	-2.417853135058	-2.979089059482
H	-1.924948581152	-0.709434655661	-2.824320438207
C	0.047038618897	1.380364215901	-2.741459428918
H	0.340484659706	1.808063195660	-3.706500777892
H	-1.037064144239	1.254760303446	-2.730353479305
O	0.422132034840	2.415027029951	-1.758645865631
P	-0.704506300936	2.972083428305	-0.788634924680
O	-1.791720665855	2.064760346985	-0.365252620507
O	0.158278014854	3.552832061953	0.450212254131
O	-1.206046393901	4.291749838337	-1.586587518092
C	1.251315346981	4.448739155633	0.169883553383
H	0.908869746576	5.305341451000	-0.418067883816
H	2.038859369635	3.922987341512	-0.377302928970
C	-2.422508800490	4.921015259619	-1.139036190929
H	-3.221933157076	4.182568735630	-1.036912024277
H	-2.266188518806	5.424406900094	-0.178225922711
H	0.921727064216	1.048908781218	3.728814092525
H	2.565630772993	2.557737491842	1.778135111300
H	2.750435221216	-1.756895569410	-0.026399061158
H	-0.329823048224	-1.937816657582	2.425294617070
H	-2.111994637515	1.941916991793	2.079244958842
H	-4.459199387690	-1.379673118146	3.499590227681
H	-2.686365804155	5.659817539117	-1.897103906069
H	1.627067221741	4.792640102639	1.135022352873

14

C	-3.161879402747	1.247200736198	0.945315961874
C	-2.025845642478	2.208277752068	1.318637014869
H	-4.080371447677	1.749569782126	0.632334596429
H	-1.854206217149	2.268634030430	2.395013231411
N	-2.561994372005	0.496374388169	-0.169508058063
N	-0.864783077214	1.590608533630	0.645003592533
C	-3.305427914180	-0.371302110650	-1.001061584795
C	-2.916820147886	-0.541375451482	-2.340275380420
C	-4.426206442191	-1.045486706511	-0.504962528029
C	-3.625699161647	-1.424735677341	-3.150293369417
C	-5.138543685520	-1.912131035758	-1.335482071436
H	-4.730013225181	-0.914311301799	0.528289335611
C	-4.736390719214	-2.114518980999	-2.655757249599
H	-3.312613003408	-1.558789623369	-4.181210126886
H	-6.003866161879	-2.437147949334	-0.941609332168
H	-5.289062588923	-2.794151822440	-3.297054657607
C	0.375334075461	2.301094225913	0.620909177329
C	1.081737269669	2.515368750630	1.806598813789
C	0.829382631491	2.844381574057	-0.583103089588
C	2.259472329254	3.259558732255	1.775957592604
C	2.018064318425	3.572093177874	-0.607928291198
C	2.733515670005	3.782961329863	0.570303883051
H	2.818222786480	3.415751258327	2.694153086701
H	2.391661386995	3.950368783758	-1.553791702834

Cu	-0.072328136739	-0.632853242457	-1.162829308918
C	-1.211558008247	0.611109319457	-0.209176322568
C	0.805233421011	0.285752931398	-2.618433150028
O	0.118643070772	0.588880283195	-3.604095139254
C	2.258413583671	0.699688423726	-2.611766167559
C	3.033788862985	0.486018708381	-1.465589301572
C	2.831249677622	1.340315853529	-3.719168762548
C	4.363559571138	0.904447348984	-1.425340435724
H	2.577656945982	0.031413164925	-0.589922473404
C	4.159722783783	1.756480900887	-3.683779575541
H	2.203853832846	1.504657888318	-4.590585896891
C	4.928636045130	1.538014264801	-2.534195072011
H	4.953385610128	0.749446732150	-0.526195266891
H	4.601479622041	2.252046291589	-4.544732030853
H	5.964633351284	1.865722758988	-2.504243115106
C	0.482376054922	-2.473715520758	-1.535623223448
C	-0.604484313915	-2.509705494827	-0.616679046219
H	0.240102672903	-2.685844069666	-2.577185227465
H	-1.594673579553	-2.664954945659	-1.041255144646
C	1.912817282422	-2.787213891548	-1.156098934344
H	2.087634465229	-3.872303603490	-1.140376407292
H	2.602975165084	-2.343642307913	-1.877281148599
H	2.169524171996	-2.381524919965	-0.174073054548
C	-0.476692121740	-2.985369165554	0.794138759019
H	-1.192404295137	-3.781742570514	1.009719593763
H	0.524346911740	-3.358731907390	1.021816994483
O	-0.820725990078	-1.953947084395	1.814404088108
P	0.388827597657	-1.138869537709	2.444435663101
O	1.437238542167	-0.590867496789	1.554388270569
O	-0.383842408748	-0.001346707159	3.292204138451
O	0.954034100591	-2.183050361166	3.547737177343
C	-1.433597368012	-0.385580938687	4.199753990644
H	-1.071079395146	-1.121969816059	4.922994554387
H	-2.279394348566	-0.804315483008	3.646932658009
C	2.284426052892	-1.975474934447	4.063194965002
H	2.982158117520	-1.764679318951	3.249226431821
H	2.294331732728	-1.144294020693	4.776688174618
H	-2.181825281387	3.220714230199	0.927363070180
H	-3.398758815624	0.565427667055	1.771792103018
H	-2.073923798815	0.012077092691	-2.748014716434
H	0.270142490914	2.661863645942	-1.493534502872
H	0.723401513573	2.072078748200	2.727399111429
H	3.661911472146	4.345712407998	0.548803895734
H	2.565516731938	-2.897179071819	4.574652774938
H	-1.739053430669	0.523258563396	4.720764269049

TS_{14-12}

C	-3.048356580098	1.108906699871	1.128549148114
C	-1.965494167515	2.162629366914	1.393042005580
H	-4.046367609788	1.526164741668	0.977776340022
H	-1.668546211492	2.207983669605	2.441326038073
N	-2.544595570855	0.470948590253	-0.099191391180
N	-0.848806918614	1.655985272369	0.568598826875
C	-3.300057655671	-0.442464789068	-0.863948729463
C	-3.049030590072	-0.550823130915	-2.241180624660
C	-4.292116391224	-1.226761070791	-0.268020322864
C	-3.768248581742	-1.469963576595	-3.000132582838
C	-5.016699375609	-2.132839635766	-1.044056053112
H	-4.475683813456	-1.154663011316	0.798278466466
C	-4.755408694852	-2.263836787910	-2.408266959089
H	-3.560859337991	-1.556786468753	-4.062347730597
H	-5.780130366174	-2.745640980352	-0.573756149461
H	-5.318587503696	-2.973148409389	-3.006731781852
C	0.381671165393	2.375220295420	0.501565668371
C	1.165822014502	2.528670650717	1.647304061983
C	0.763912324597	2.963318558306	-0.706512616201
C	2.343143713351	3.270208397621	1.572218262166
C	1.950791311792	3.691528192286	-0.774947312945
C	2.740035941346	3.848961037619	0.363640146577
H	2.963340243775	3.380071283485	2.457008186621
H	2.265425409404	4.113681510980	-1.723636136430
Cu	-0.047823076803	-0.601163097489	-1.170169553989
C	-1.217206632654	0.676193346998	-0.266729055809
C	0.920983189175	0.293603944932	-2.565892223590
O	0.279981659274	0.596467784492	-3.569827779139
C	2.365157866259	0.692811310393	-2.453497065021
C	3.059996378330	0.484218876370	-1.255914775349
C	3.008895979389	1.319585122599	-3.530477865004
C	4.385421740694	0.900629822949	-1.136950587457
H	2.549800018023	0.034889872265	-0.409560745352
C	4.333920278920	1.729176629805	-3.412916124402
H	2.442815474501	1.478819907763	-4.443322524286
C	5.023977468304	1.520275172874	-2.212942457499
H	4.915514037068	0.751919602730	-0.200613009918
H	4.832758206840	2.212515266895	-4.248891259759
H	6.057205437077	1.844100554620	-2.118844565789
C	0.555656874043	-2.379293916540	-1.621370072973
C	-0.657996474650	-2.581374763354	-0.859936923912
H	0.439294110662	-2.546908376050	-2.692628990464
H	-1.587741499452	-2.638575787934	-1.419197071506
C	1.915776439018	-2.766553317426	-1.087113778423
H	2.051365852932	-3.856288332087	-1.126821172624
H	2.705155444269	-2.304545325736	-1.684312917596
H	2.050502317109	-2.433662691895	-0.055867822593
C	-0.724415788703	-3.082869023396	0.466809927197
H	-1.617063495758	-3.631154436985	0.743376454225
H	0.181524757651	-3.465704200182	0.927121235049
O	-1.106582551458	-1.806932744452	1.763786523711
P	0.184049557447	-1.125454589536	2.279821453730
O	1.172042415631	-0.574106002446	1.306395471863
O	-0.315060576370	0.057355527006	3.295076564470
O	0.862196223451	-2.230102951693	3.270406974392
C	-1.209532522516	-0.300852613759	4.359760240254
H	-0.742613351431	-1.028973538420	5.030683457943
H	-2.135369922670	-0.727987840255	3.961267365049
C	2.209493751178	-1.988141312697	3.707389328543
H	2.860844142249	-1.779118421533	2.854314195701
H	2.246737492149	-1.140542314697	4.402051316849
H	-2.250879651786	3.165116062144	1.051861864697
H	-3.080411357981	0.364294332604	1.932071203268
H	-2.282615927003	0.066103190796	-2.702331200003
H	0.149514445159	2.815086326944	-1.587870208100
H	0.868455268439	2.036195563346	2.565079457698
H	3.667848279949	4.410051577154	0.307515307465
H	2.540753997916	-2.891889218346	4.222384684565
H	-1.429199391172	0.616474282952	4.910015965240

15

C	-0.187520597233	-3.858374987328	-1.157212363825
C	-1.475392319186	-3.734700614629	-0.349678334039
H	-0.384129388916	-3.870910322337	-2.236283825736
H	-1.447244305162	-4.331086008779	0.570752388685
N	0.522999063179	-2.624475933813	-0.781368501974
N	-1.493961649157	-2.297548537842	-0.015024372805
C	1.903836207471	-2.472448179461	-1.058045766459
C	2.488278090003	-3.198690758191	-2.105282777009
C	2.699845551738	-1.642300238996	-0.256756414682
C	3.856772606083	-3.087369812108	-2.350763728349
C	4.063439165207	-1.537230175754	-0.518978865837
H	2.250771553123	-1.093431940051	0.564189508801
C	4.651652149481	-2.256433210483	-1.561341713473
H	4.297689342223	-3.651937824223	-3.167049366567
H	4.666590728511	-0.888743658339	0.108159519407
H	5.716988835724	-2.173940790661	-1.753074948308
C	-2.604456562928	-1.742054211273	0.663780241854
C	-2.680592947510	-0.367534016864	0.936490014377
C	-3.662992199197	-2.569157263924	1.073387655401
C	-3.778594922670	0.160242731285	1.604864980641
C	-4.760881019595	-2.027544418000	1.743094148071
C	-4.828913034665	-0.662779321042	2.015612229221
H	-3.806554269247	1.227512833918	1.801354561988
H	-5.564949548112	-2.687579007844	2.054983411213
Cu	0.158666851350	0.150685925167	0.170678399018
C	-0.280147009292	-1.694824072873	-0.208758113812
C	-0.078112677370	1.616500688210	-0.993858008590
C	-1.296697289531	1.852506808870	-1.799594550817
C	-2.142334717759	0.773959729051	-2.114829673828
C	-1.660688271266	3.143576092269	-2.231855043696
C	-3.313720873047	0.974354722739	-2.839185995398
H	-1.852798201252	-0.221616626692	-1.799834093289
C	-2.840524030442	3.346407262582	-2.939558392786
H	-1.011033613822	3.977453682036	-1.990059160129
C	-3.669311495061	2.261927797650	-3.247111135070
H	-3.952233476980	0.129737387942	-3.080521551864
H	-3.118939739019	4.347882163473	-3.255113499276
H	-4.589147524144	2.422052561503	-3.802504230371
H	-2.361295137587	-4.016803847659	-0.923052706932
H	0.403396620800	-4.740337582258	-0.900195563854
H	1.883803861042	-3.840518323955	-2.736922802363
H	-3.641868032578	-3.636099597147	0.888496534454
H	-1.882200640262	0.287413743787	0.611526143985
H	-5.684172730527	-0.246729265013	2.538325459421
O	1.015341994240	0.439611228187	1.831491454959
O	0.801684610225	2.582801943376	-1.228037447445
Si	2.076040678849	3.136555607981	-0.184734141937
C	3.369717297417	1.813286231577	0.054624418626
H	3.612686995228	1.296792275762	-0.877954471325
H	4.290291006461	2.254791232030	0.454047711724
H	2.977113140560	1.093048218449	0.777919118996
C	2.728929433968	4.602008062570	-1.162421705664
H	1.944655925594	5.346290904352	-1.333973559308
H	3.545839530241	5.092550099535	-0.621434755911
H	3.114130995643	4.285369085860	-2.137311276671
C	1.258429795543	3.595689927358	1.428059228848
H	1.974332926183	4.061328866547	2.115063166103
H	0.418544220884	4.283905926727	1.288689886761
H	0.908751455092	2.654830102123	1.872418177503
C	0.861779124227	-0.155841173341	3.088731141087
C	-0.284275288346	0.541333793837	3.849214385117
C	2.189270018008	0.039567457030	3.848628570231
H	3.000405187033	-0.460445779611	3.307696494688
H	2.426601800703	1.106901053334	3.899298093139
H	2.151394204293	-0.360812144758	4.868756337155
H	-0.072977263532	1.612057747309	3.936483778888
H	-0.430394767481	0.131796163508	4.856457977031
H	-1.218281507783	0.423601969773	3.289800110104
C	0.552266061234	-1.664938673203	2.988404639943
H	-0.414800069125	-1.820293671406	2.500937265059
H	1.319892648493	-2.171874184214	2.394240325056
H	0.513829244739	-2.137948447877	3.976670076500

TS$_{15\text{-}16}$

C	-0.154209417787	-4.163891414157	-0.689454858823
C	-1.365589519508	-3.982273822509	0.220334720973
H	-0.448059334757	-4.372295926677	-1.725960190374
H	-1.205472769207	-4.423323428872	1.212133834420
N	0.497740096414	-2.847500306139	-0.598313294855
N	-1.457810534886	-2.516417954773	0.324180527774
C	1.785245522278	-2.637882904898	-1.143186988615
C	2.336098769637	-3.592841719625	-2.011702728983
C	2.536343957214	-1.497132405759	-0.814079159011
C	3.611268603396	-3.405415857387	-2.544561096831
C	3.808158824481	-1.326552041046	-1.352105632764
H	2.145165756270	-0.770669258631	-0.112458338315
C	4.355267711283	-2.272698829010	-2.220637653966
H	4.017865920608	-4.153588246579	-3.218609636678
H	4.380762703966	-0.449233797253	-1.072192471206
H	5.349475793560	-2.130563418447	-2.631985444322
C	-2.605545113934	-1.907942809042	0.882084689593
C	-2.847165410685	-0.535179365848	0.720432960950
C	-3.538303504345	-2.681606514809	1.590233544172
C	-3.987298842502	0.048148565953	1.259247573026
C	-4.680499154589	-2.084921897210	2.125813561970
C	-4.914796641924	-0.720150778982	1.966549879390
H	-4.148273437541	1.112387466072	1.116653128501
H	-5.387672250280	-2.699252321760	2.675314833143
Cu	0.054975916257	-0.040614501898	-0.050584812005
C	-0.318650364998	-1.880809332053	-0.087667458666
C	-0.235608894762	1.645524033566	-0.912525593006
C	-1.271291018930	2.023228682636	-1.901744951542
C	-2.003612925506	0.993581118235	-2.511005795478
C	-1.554210373841	3.359597053960	-2.238289036512
C	-3.003015365415	1.283742911611	-3.437374380519
H	-1.763720698111	-0.030541453287	-2.238122397749
C	-2.552221837862	3.651423233188	-3.161106840777
H	-0.979717468778	4.147487176882	-1.762494179293
C	-3.277844944340	2.614047951957	-3.760969991023
H	-3.565481852262	0.480801564022	-3.904583109678
H	-2.771072876125	4.683679155632	-3.419250044229
H	-4.056904782371	2.846533787109	-4.481842271656
H	-2.281172038145	-4.402236497147	-0.202867840461
H	0.518502373940	-4.956207879073	-0.353075069608

H	1.776554159365	-4.478276697045	-2.289538123724
H	-3.380187270235	-3.742913820895	1.741862555404
H	-2.130231796357	0.061593565608	0.172017603673
H	-5.804840948226	-0.262067473229	2.385866100832
O	1.042518103288	1.034337782217	1.387685217126
O	0.401526849047	2.644157597761	-0.432528260897
Si	1.920446512389	2.638148688204	0.689985746164
C	3.607331160945	1.729661123848	0.858670349891
H	3.857972448597	1.350216458621	-0.139369805237
H	4.392739671305	2.454139506357	1.106358589290
H	3.661978607129	0.893783690268	1.554341596036
C	2.631349601532	3.819778174581	-0.689839908639
H	1.932020204828	4.616050092719	-0.965022908143
H	3.560950339969	4.289317595168	-0.342203435930
H	2.875203778609	3.270992978407	-1.609094327031
C	1.361725312066	3.902388954120	1.985475594573
H	2.143561472805	4.112636040377	2.722159514915
H	1.127755884324	4.840070624732	1.472562896617
H	0.466694563982	3.574840001976	2.519228672755
C	1.105769410188	0.460825682400	2.714799600285
C	-0.345026385117	0.314644150677	3.202342422755
C	1.872294322583	1.315538430566	3.744590341305
H	2.887087688593	1.549166410304	3.420767016277
H	1.353290428591	2.248387185215	3.962632739261
H	1.944637979471	0.754432107622	4.681968801924
H	-0.846593597668	1.285720156966	3.159562044992
H	-0.389168293477	-0.061686949758	4.230392670691
H	-0.899619242471	-0.376594859673	2.563098804289
C	1.767797090526	-0.926746532582	2.644679747715
H	1.234196523304	-1.561440864850	1.934136780350
H	2.808906017280	-0.854675084765	2.319802965897
H	1.747763826938	-1.415836733851	3.624174409556

16

C	-0.719944441081	-3.681214053080	-1.215550888611
C	-1.658415824293	-3.765691417813	-0.017639224265
H	-1.267423978527	-3.467654805733	-2.143636493010
H	-1.289535274951	-4.477259914460	0.732732617126
N	0.118508307313	-2.534360803653	-0.835319196021
N	-1.598621560547	-2.387598532250	0.503894647901
C	1.298780174308	-2.218885279388	-1.536332235877
C	1.498080610546	-2.696941171802	-2.839940095179
C	2.292620215885	-1.429542846595	-0.934614256730
C	2.664735741406	-2.374536964731	-3.533630179970
C	3.451731164706	-1.116061823133	-1.639753026900
H	2.165984406996	-1.083279767096	0.082596601571
C	3.646321578531	-1.579603765852	-2.942455666276
H	2.798495501888	-2.744401967125	-4.545893982064
H	4.210747034860	-0.505646934829	-1.159371483216
H	4.551759687131	-1.329194839916	-3.485802732145
C	-2.578804830171	-1.928149628546	1.416407399560
C	-2.938495838032	-0.573789080337	1.472723675423
C	-3.234776976938	-2.848284182765	2.248710083096
C	-3.919920450063	-0.151302902155	2.365501459627
C	-4.222788034145	-2.413108071239	3.131707809565
C	-4.569326289593	-1.063380159867	3.199494441327
H	-4.178058940973	0.902825538912	2.391021463009
H	-4.717749619316	-3.137241541708	3.772371107584
Cu	-0.116360517415	0.145129675959	0.168063388976
C	-0.500972218831	-1.701578445924	0.064290812786
C	-1.056607512331	1.561146523956	-0.719087142345
C	-1.025165986575	1.784475718331	-2.219752491445
C	-0.276702828329	0.921304140126	-3.027521252438
C	-1.722285096260	2.843450159518	-2.817295529088
C	-0.222294133622	1.101674646922	-4.408790063173
H	0.268015704042	0.109312362817	-2.552875219644
C	-1.668018831544	3.033777360212	-4.195916640453
H	-2.298861067035	3.498689159434	-2.170491203848
C	-0.918474610530	2.161728743455	-4.994775826730
H	0.363583941276	0.422794968216	-5.022997786414
H	-2.207427129151	3.858083545571	-4.655844300622
H	-0.876796730626	2.311621858411	-6.070518132300
H	-2.682193910925	-4.036388794077	-0.284497970194
H	-0.115712133172	-4.579584875472	-1.360012220254
H	0.739246845696	-3.299886640601	-3.325762681038
H	-2.971164473714	-3.900019186811	2.222310762550
H	-2.454814873723	0.148256973599	0.829545273914
H	-5.338911229345	-0.728730187900	3.888176965219
O	1.476344580880	0.841778578809	1.521534545471
O	-1.835810221658	2.279583837614	-0.064682562584
Si	2.069676572803	2.376793289152	1.017487657181
C	3.824163516524	2.685716386015	1.656790519377
H	4.454903450997	1.798750344553	1.528532210778
H	4.265900013681	3.486989481329	1.052794973599
H	3.878279697459	2.993328022393	2.703023506127
C	2.201845937408	2.336128640343	-0.854895197400
H	1.292542344914	2.697895318700	-1.335213342715
H	3.032893666155	2.979690480886	-1.167722139679
H	2.392297043162	1.332283638691	-1.240132371514
C	0.877222486890	3.708605669228	1.583272937364
H	0.840267828616	3.814129647636	2.672313463148
H	1.170521639531	4.679571545260	1.167019792213
H	-0.128049030836	3.471445669365	1.219637608954
C	1.289152797555	0.360926138918	2.900415597403
C	-0.169160026566	0.612930602158	3.291995148153
C	2.226425706544	1.057217607880	3.891854731601
H	3.274631693098	0.903986728024	3.627418756085
H	2.027330736239	2.129944950699	3.959002266025
H	2.064023166866	0.631458266955	4.886510006543
H	-0.429065130442	1.665612246094	3.159145050453
H	-0.342130116053	0.333721948579	4.335951660420
H	-0.844347315205	0.019495947059	2.675282885815
C	1.604033022268	-1.135879501654	2.869513131351
H	0.974559457827	-1.630998743368	2.127366534968
H	2.653353161615	-1.300420739271	2.605890079283
H	1.414393178298	-1.586387770845	3.848382225248

17

C	-1.114403919476	4.272876903339	-0.182197873900
C	-2.470666004307	3.738892266754	0.290331761525
H	-0.731535222367	5.075021643581	0.451626152311
H	-3.313555191395	4.092811758027	-0.307491678559
N	-0.272414505554	3.062653254804	-0.095698576965
N	-2.290835243698	2.283258537839	0.133498159270
C	1.100212385200	3.091657531600	-0.468140616995
C	1.969689687369	3.998265360502	0.149596047667

C	1.578100710055	2.207206166260	-1.442346704074
C	3.318646467501	4.011383504745	-0.202796921051
C	2.932936957586	2.213039153422	-1.769562684761
H	0.908324152937	1.500470781575	-1.918144244383
C	3.804681363919	3.115497845792	-1.159571938833
H	3.992384472698	4.710941357915	0.282877607359
H	3.291431527047	1.492654819118	-2.495657419750
H	4.858334453806	3.119988180177	-1.422159821780
C	-3.384808749929	1.386008265910	0.160927015264
C	-3.351136239886	0.222351720144	-0.620704309734
C	-4.506451084221	1.667703136908	0.950151033848
C	-4.421310176005	-0.667759517362	-0.570478893714
C	-5.577876579002	0.775249588443	0.977515808765
C	-5.536985384585	-0.400289632175	0.226322851767
H	-4.380169524993	-1.572928045422	-1.167738429800
H	-6.440958651167	0.997438143895	1.597986180585
Cu	-0.206616352190	0.168870872102	0.166493161969
C	-0.987598161526	1.920532967667	0.031480137665
C	0.676231081279	-0.961494811099	1.377010434061
C	2.144846972213	-0.940796851890	1.514102206049
C	2.877630707608	-2.088583952181	1.869806629825
C	2.834602128730	0.245113781913	1.219448946792
C	4.266308557365	-2.042067326682	1.925936996105
H	2.341454910402	-3.009617233704	2.065193531481
C	4.223921045917	0.297135168774	1.293420462744
H	2.267073116229	1.123222080544	0.936903422832
C	4.941620981106	-0.848447057330	1.643355282600
H	4.828974990785	-2.934891879873	2.183133212382
H	4.738858339276	1.224794178351	1.065076378308
H	6.026828347839	-0.816966833045	1.689231995810
H	-2.657747732480	3.988005475029	1.342114848310
H	-1.138844783224	4.630215029557	-1.219248653469
H	1.596748488036	4.667607518705	0.918593718245
H	-4.536484685470	2.565341010741	1.558750580992
H	-2.501149715866	0.024393559248	-1.265216801339
H	-6.370029214095	-1.095817400749	0.253566395160
O	0.159269427580	-1.963625734876	2.063722654128
Si	-1.506450112983	-2.449250146345	2.041139203834
C	-1.929678860851	-3.015457515147	0.315483787227
H	-1.882185719506	-2.182548172620	-0.388074303762
H	-1.195239315760	-3.746704466308	-0.030824617181
H	-2.935598264346	-3.449457573940	0.285683652498
C	-1.533054176507	-3.854588312787	3.280919649190
H	-1.181230938465	-3.523410512732	4.263169431931
H	-2.548853737637	-4.247672396180	3.400512689230
H	-0.891825878474	-4.676722964967	2.947513449534
C	-2.470794404296	-0.947532844623	2.611712105443
H	-3.540445196117	-1.028408169685	2.398806697913
H	-2.330508443883	-0.758448686432	3.680517016455
H	-2.085557693995	-0.086861910305	2.057821282493
O	0.945508499906	-2.868311244633	-1.008009795082
P	0.797372983974	-1.699744821641	-1.919655910709
O	-0.263610085424	-0.608402621706	-1.659840812875
O	2.190978398243	-0.825052418224	-2.018156008183
O	0.575322114018	-2.217462084595	-3.452450472244
C	3.432901686868	-1.520446098921	-1.862500675294
H	3.683240088651	-2.080115877695	-2.772200809049
H	3.386968671666	-2.207879762251	-1.015071157914
C	0.360487676256	-1.231082567729	-4.464066398527
H	-0.539755367988	-0.644034529366	-4.253349859174
H	1.218628188619	-0.551394127821	-4.538755355356
H	0.240487977563	-1.764079772257	-5.410406936119
H	4.198282856685	-0.763348045981	-1.675800744904

TS$_{17-18}$

C	-0.898644524826	4.387794117116	-0.397314941266
C	-2.234652512706	3.978228175892	0.233775984235
H	-0.402683920884	5.184297299555	0.160776192793
H	-3.106310225810	4.340673835119	-0.316301295715
N	-0.140238078828	3.124266410709	-0.341262408115
N	-2.161083308756	2.506029289011	0.185582283000
C	1.219194550690	3.030561711561	-0.737145565710
C	2.149904733666	3.978411102887	-0.293699208459
C	1.643949783553	1.950759413234	-1.523654521398
C	3.499297642353	3.826947927996	-0.612504403209
C	2.998176999852	1.794248579190	-1.811087787858
H	0.924315610159	1.239442357785	-1.908742123141
C	3.931025768381	2.727567410749	-1.358506690622
H	4.216642612556	4.561319892513	-0.258175740870
H	3.308385409307	0.930030986231	-2.389035809133
H	4.985432830504	2.603323624261	-1.584831933362
C	-3.289705731891	1.696349217385	0.457568685495
C	-3.395129501114	0.420482815990	-0.115100718064
C	-4.320672997597	2.181115395641	1.272996495248
C	-4.513076749516	-0.364931746589	0.153862746855
C	-5.439362150563	1.387199715739	1.525050209535
C	-5.539119932498	0.110488884414	0.972711520549
H	-4.577821778530	-1.353747228571	-0.286690021957
H	-6.230103566398	1.770314906489	2.163360694911
Cu	-0.184993333603	0.285834109688	0.120776467331
C	-0.907968333868	2.044993839456	-0.040299426287
C	0.816536299764	-0.887320940325	1.249264085863
C	2.104842933623	-0.482830279015	1.883131456989
C	2.957138365139	-1.407852816427	2.513135024043
C	2.502549444430	0.858635235027	1.804458312322
C	4.175260711127	-0.994688167006	3.042639780356
H	2.644591423209	-2.445324140811	2.570883320237
C	3.723032306156	1.275885692172	2.330587105474
H	1.840918299800	1.565200348775	1.319070574019
C	4.562001943648	0.348294616867	2.950318356207
H	4.830114323115	-1.714107359549	3.526693722680
H	4.017874082568	2.317682565336	2.248276680986
H	5.516567229315	0.666477957173	3.360736241761
H	-2.312039120459	4.320962795426	1.272700735156
H	-1.002557657068	4.709612701647	-1.440612507806
H	1.829986471269	4.808912544882	0.327053994110
H	-4.250212979979	3.165361393307	1.723287940428
H	-2.617096163666	0.061151239465	-0.778631513412
H	-6.409365072244	-0.506422488101	1.173531915340
O	0.548185007596	-2.124638751333	1.442860565047
Si	-0.986785573429	-3.078588669686	0.749064787731
C	-2.404158003834	-3.289321249673	-0.526607506196
H	-2.574599422627	-2.353208006350	-1.069449197287
H	-2.163438652591	-4.052776238732	-1.271992363891
H	-3.339587810003	-3.561127750555	-0.023894478288
C	-0.462742033676	-4.770672594195	1.374623454598

H	0.222822905188	-4.684211167859	2.222359326543
H	-1.343530712838	-5.334378964203	1.701736852974
H	0.031633988157	-5.341037113246	0.583059574050
C	-1.970913704938	-2.119599075472	2.086894595762
H	-3.000452458959	-2.482743367949	2.169844742815
H	-1.485498338097	-2.179994821412	3.066021706527
H	-2.024556611652	-1.057232978423	1.821876621464
O	0.185878426680	-2.992698935215	-0.823705922377
P	0.376498630504	-1.879032084677	-1.852059201123
O	-0.480434643808	-0.632127590663	-1.741593549100
O	1.924481490971	-1.383934696692	-1.822550507801
O	0.200241442781	-2.586083937689	-3.292771249017
C	2.940065393206	-2.240516801407	-1.268620294733
H	3.080062338190	-3.132051251308	-1.888767256534
H	2.674622718524	-2.536527265381	-0.252285892832
C	0.285207529500	-1.752313348091	-4.459940386788
H	-0.469179348811	-0.960639942092	-4.422875590190
H	1.281676610380	-1.304060033341	-4.543300354330
H	0.103220396350	-2.399921565086	-5.318949589114
H	3.858998303850	-1.652316741590	-1.254420797398

18

C	-0.818845219781	4.505898639839	-0.768417638015
C	-2.103073150257	4.235387566999	0.024144266933
H	-0.218830363488	5.299174594575	-0.313758159383
H	-3.011063081251	4.503577188375	-0.523521056184
N	-0.117967784983	3.211810085086	-0.702198615722
N	-2.040470917907	2.783128752453	0.247006775158
C	1.151393483030	3.041401637712	-1.296158895559
C	1.846401074453	4.145098493761	-1.816676021277
C	1.742463150036	1.769909068703	-1.383575634347
C	3.105117736291	3.972640910861	-2.395317934042
C	3.001352965665	1.613156865211	-1.949474086958
H	1.210800776087	0.907744867530	-1.008745285738
C	3.695398167513	2.711344618119	-2.463095971869
H	3.625242481765	4.840150731598	-2.791089984214
H	3.427180117937	0.614956075299	-1.982704990904
H	4.676803602649	2.586083882282	-2.909614455898
C	-3.105125219528	2.082477084161	0.852933353168
C	-3.159765472655	0.679338291862	0.795714496997
C	-4.130852957086	2.781970227904	1.505364612827
C	-4.209153641011	-0.000715731743	1.403432239883
C	-5.182517397892	2.085990393295	2.102404084908
C	-5.226805946982	0.693358529212	2.061588570908
H	-4.227613952221	-1.083913722443	1.348956160929
H	-5.966463083829	2.643347321691	2.606758661494
Cu	-0.251689192332	0.498631278624	0.365768631064
C	-0.847876582771	2.230181831162	-0.096634240270
C	0.603038243653	-0.701024476250	1.604265102203
C	1.897583572028	-0.363936048428	2.319609766840
C	2.533768273507	-1.293236063886	3.155936715830
C	2.498056449802	0.882464121695	2.114063113230
C	3.744364847266	-0.982824736107	3.768719136851
H	2.051233668044	-2.255157887795	3.304644942231
C	3.716250417884	1.198069425780	2.716402766088
H	1.995286041721	1.594036728882	1.464452065147
C	4.340472464001	0.264812942465	3.546625457164
H	4.230164567656	-1.705777446370	4.419391517998
H	4.177025926941	2.166453370243	2.540744224947
H	5.287636920214	0.506608106317	4.021742825661
H	-2.109531502120	4.768554832861	0.981703635433
H	-1.011223317332	4.777212948893	-1.812782679678
H	1.422211234432	5.141316823922	-1.775064475798
H	-4.112717353215	3.864115135334	1.565109843257
H	-2.399400915269	0.131241517044	0.252419896758
H	-6.045604743246	0.155693015244	2.529232016702
O	0.193810015708	-1.872830655188	1.750767779011
Si	-1.153439282955	-4.131464548641	-0.376637250728
C	-1.831303268824	-5.337784550103	-1.646516003614
H	-2.232564741494	-4.805510377397	-2.515214871705
H	-1.051079290790	-6.019733646701	-1.999725280460
H	-2.639518319870	-5.941667959657	-1.218549521539
C	-0.351706605516	-4.999010726788	1.071786966625
H	0.067167718350	-4.248732953551	1.747981916516
H	-1.086090490965	-5.596462315129	1.623860387598
H	0.446977894951	-5.670791759233	0.740197063312
C	-2.415057297257	-2.856361956875	0.141120221756
H	-2.770676369290	-2.263947217455	-0.706260760343
H	-3.273809897210	-3.345665398724	0.615341568691
H	-1.930847307462	-2.192023005833	0.861632915359
O	0.144385967570	-3.350356833336	-1.207142326516
P	0.490829509472	-1.902635325564	-1.685253578276
O	-0.469071806678	-0.799239546237	-1.363118482270
O	1.966089656357	-1.579529993738	-1.142122447359
O	0.669870614339	-2.098967325691	-3.272053336568
C	2.709851016990	-2.491718172998	-0.301156023677
H	3.006062939188	-3.376337170863	-0.871579452699
H	2.112667106570	-2.772794924936	0.566580241566
C	0.869879435138	-0.913398262050	-4.069723970092
H	0.040237149273	-0.215122500202	-3.930161176077
H	1.808755109884	-0.418488486829	-3.801911514632
H	0.911692659516	-1.247279779894	-5.107039787183
H	3.589425132991	-1.938273333853	0.026375190504

References

(1) (a) Shaw, M. H.; Twilton, J.; MacMillan, D. W. C. *J. Org. Chem.* **2016**, *81*, 6898−6926. (b) Marzo, L.; Pagire, S. K.; Reiser, O.; König, B. *Angew. Chem., Int. Ed.* **2018**, *57*, 10034−10072. (c) Narayanam, J. M. R.; Stephenson, C. R. J. *Chem. Soc. Rev.* **2011**, *40*, 102−113. (d) Huang, X.; Meggers, E. *Acc. Chem. Res.* **2019**, *52*, 833−847. (e) Schultz, D. M.; Yoon, T. P. *Science*, **2014**, *343*, 1239176. (f) Romero, N. A.; Nicewicz, D. A. *Chem. Rev.* **2016**, *116*, 10075−10166.

(2) (a) Sumino, S.; Fusano, A.; Fukuyama, T.; Ryu, I. *Acc. Chem. Res.* **2014**, *47*, 1563−1574. (b) Parasram, M.; Gevorgyan, V. *Chem. Soc. Rev.* **2017**, *46*, 6227−6240. (c) Chuentragool, P.; Kurandina, D.; Gevorgyan, V. *Angew. Chem. Int. Ed.* **2019**, *58,* 11586−11598. (d) Hossain, A.; Bhattacharyya, A.; Reiser, O. *Science*, **2019**, *364*, eaav9713. (e) Cheng, W.-M.; Shang, R. Recent Developments and Future Perspectives. *ACS Catal.* **2020**, *10*, 9170−9196. (f) Shing Cheung, K. P.; Sarkar, S.; Gevorgyan, V. Chem. Rev. **2022**, *122*, 1543−1625. (g) Brimioulle, R.; Lenhart, D.; Maturi, M. M.; Bach, T. *Angew. Chem. Int. Ed.* **2015**, *54*, 3872–3890. (h) Jiang, C.; Chen, W.; Zheng, W.-H.; Lu, H. *Org. Biomol. Chem.* **2019**, *17*, 8673–8689. (i) Lipp, A.; Badir, S. O.; Molander, G. A. *Angew. Chem. Int. Ed.* **2021**, *60*, 1714–1726.

(3) (a) Ye, J.-H.; Quach, L.; Paulisch, T.; Glorius, F. *J. Am. Chem. Soc.* **2019**, *141*, 16227–16231. (b) Fan, Z.; Yi, Y.; Chen, S.; Xi, C. *Org. Lett.* **2021**, *23*, 2303–2307.

(4) (a) Brook, A. G.; Duff, J. M. *J. Am. Chem. Soc.* **1967**, *89*, 454−455. (b) Bourque, R. A.; Davis, P. D.; Dalton, J. C. *J. Am. Chem. Soc.* **1981**, *103*, 697−699.

(5) Takeuchi, T.; Aoyama, T.; Orihara, K.; Ishida, K.; Kusama, H. *Org. Lett.* **2021**, *23*, 9490−9494.

(6) Lou, S.; Fu, G. C. *J. Am. Chem. Soc.* **2010**, *132*, 5010−5011.

(7) Makida, Y.; Ohmiya, H.; Sawamura, M. *Angew. Chem. Int. Ed.* **2012**, *51*, 4122−4127.

(8) Ohmiya, H.; Yokobori, U.; Makida, Y.; Sawamura, M. *J. Am. Chem. Soc.* **2010**, *132*, 2895−2897.

(9) Pangborn, A. B.; Giardello, M. A.; Grubbs, R. H.; Rosen, R. K.; Timmers, F. J. *Organometallics* **1996**, *15*, 1518–1520.

(10) Frisch, M. J.; Trucks, G. W.; Schlegel, H. B.; Scuseria, G. E.; Robb, M. A.; Cheeseman, J. R.; Scalmani, G.; Barone, V.; Mennucci, B.; Petersson, G. A.; Nakatsuji, H.; Caricato, M.; Li, X.; Hratchian, H. P.; Izmaylov, A. F.; Bloino, J.; Zheng, G.; Sonnenberg, J. L.; Hada, M.; Ehara, M.; Toyota, K.; Fukuda, R.; Hasegawa, J.; Ishida, M.; Nakajima, T.; Honda, Y.; Kitao, O.; Nakai, H.; Vreven, T.; Montgomery, J. A., Jr.; Peralta, J. E.; Ogliaro, F.; Bearpark, M.; Heyd, J. J.; Brothers, E.; Kudin, K. N.; Staroverov, V. N.; Kobayashi, R.; Normand, J.; Raghavachari, K.; Rendell, A.; Burant, J. C.; Iyengar, S. S.; Tomasi, J.; Cossi, M.; Rega, N.; Millam, J. M.; Klene, M.; Knox, J. E.; Cross, J. B.; Bakken, V.; Adamo, C.; Jaramillo, J.; Gomperts, R.; Stratmann, R. E.; Yazyev, O.; Austin, A. J.; Cammi, R.; Pomelli, C.; Ochterski, J. W.; Martin, R. L.; Morokuma, K.; Zakrzewski, V. G.; Voth, G. A.; Salvador, P.; Dannenberg, J. J.; Dapprich, S.; Daniels, A. D.; Farkas, Ö.; Foresman, J. B.; Ortiz, J. V.; Cioslowski, J.; Fox, D. J. *Gaussian 09* (Gaussian, Inc., Wallingford CT, 2009).

(11) Maeda, S.; Harabuchi, Y.; Sumiya, Y.; Takagi, M.; Suzuki, K.; Hatanaka, M.; Osada, Y.; Taketsugu, T.; Morokuma, K.; Ohno, K. GRRM17, see http://iqce.jp/GRRM/index_e.shtml (accessed date 27 October, 2021).

(12) Maeda, S.; Ohno, K.; Morokuma, K. Systematic Exploration of the Mechanism of Chemical Reactions: The Global Reaction Route Mapping (GRRM) Strategy by the ADDF and AFIR Methods. *Phys. Chem. Chem. Phys.* **2013**, *15*, 3683–3701.

(13) Grimme, S.; Antony, J.; Ehrlich, S.; Krieg, H. A consistent and accurate *ab initio* parametrization of density functional dispersion correction (DFT-D) for the 94 elements H-Pu. *J. Chem. Phys.* **2010***,* *132*, 154104.

(14) Reed, A. E.; Weinhold, F. Natural bond orbital analysis of near-Hartree–Fock water dimer. *J. Chem. Phys.* **1983**, *78*, 4066–4073.

(15) Reed, A. E.; Weinstock, R. B.; Weinhold, F. Natural population analysis. *J. Chem. Phys.* **1985**, *83*, 735–746.

(16) (a) Ito, K.; Tamashima, H.; Iwasawa, N.; Kusama, H. *J. Am. Chem. Soc*. **2011**, *133*, 3716─3719. (b) Ishida, K.; Tobita, F.; Kusama, H. *Chem. - Eur. J.* **2018**, *24*, 543─546. (c) Linderman, R. J.; Suhr, Y. *J. Org. Chem.* **1988**, *53*, 1569–1572. (d) Lu, X.; Zhang, J.; Xu, L.; Shen, W.; Yu, F.; Ding, L.; Zhong, G. *Org. Lett.* **2020**, *22*, 5610–5616.

(17) (a) Ohmiya, H.; Yokokawa, N.; Sawamura, M. *Org. Lett.* **2010**, *12*, 2438−2440. (b) Li, D.; Ohmiya, H.; Sawamura, M. *J. Am. Chem. Soc*. **2011**, *133,* 5672−5675. (c) Nagao, K.; Yokobori, U.; Makida, Y.; Ohmiya, H.; Sawamura, M. *J. Am. Chem. Soc.* **2012**, *134*, 8982−8987. (d) Makida, Y.; Takayama, Y.; Ohmiya, H.; Sawamura, M. *Angew. Chem. Int. Ed.* **2013**, *52,*5350–5354. (e) Yasuda,Y.; Nagao, K.; Shido, Y.; Mori, S.; Ohmiya, H.; Sawamura, M. *Chem. Eur. J.* **2015**, *21*, 9666–9670.

Chapter 3

Photoinduced Copper-Catalyzed Asymmetric Conjugate Addition Reaction of Acylsilanes to α,β-Unsaturated Ketones and Aldehydes

Introduction

Chiral 1,4-dicarbonyl compounds are important synthetic intermediates for a variety of natural products and pharmaceuticals.[1] A convenient method for their synthesis is the 1,4-addition reaction of an acyl anion (or its equivalent) to an *α,β*-unsaturated carbonyl compound. In 2008, Henser and co-workers reported the asymmetric intermolecular Stetter reaction catalyzed by a novel triazolium-derived N-heterocyclic carbene (NHC) (Scheme 1a).[2a] The Breslow intermediate, which is catalytically generated in situ from aldehyde and NHC, acts as an acyl anion equivalent, and stereoselectively synthesizes chiral 1,4-dicarbonyl compounds under the influence of chirality on the NHC catalyst. In 2019, Melchiorre and co-workers reported the synthetic method for chiral 1,4-dicarbonyl compounds using visible light (Scheme 1b).[3] In this reaction, an acyl radical photochemically generated from 4-acyl-1,4-dihydropyridines attacks the alkene moiety of an *α,β*-unsaturated aldehyde activated by an asymmetric organocatalyst to afford enantioenriched products. Although these methods are pioneering examples of access to chiral 1,4-dicarbonyl compounds,[4] the enantiomeric excess of the products remains less than 80%.

Scheme 1. Synthesis of chiral 1,4-dicarbonyl compounds by 1,4-addition reaction

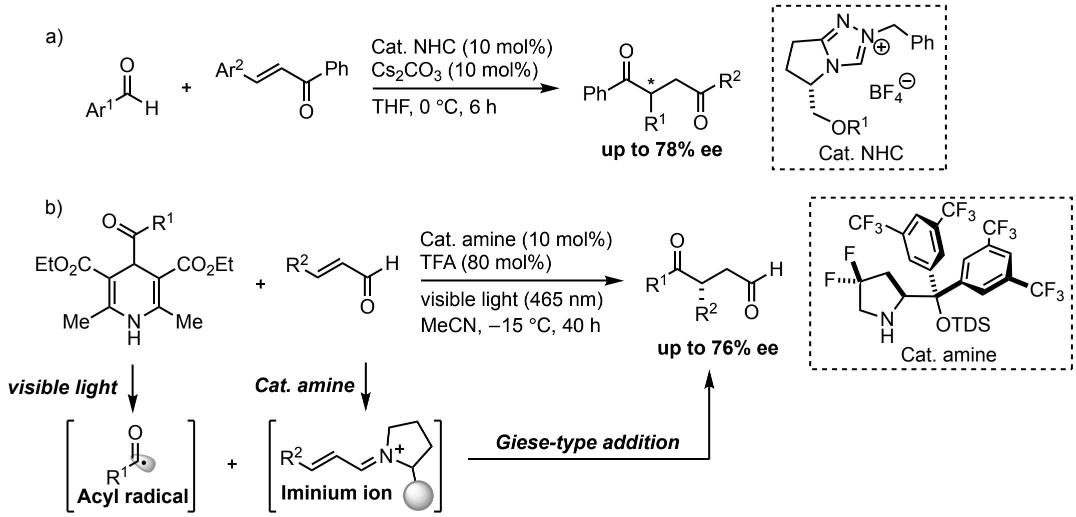

As described in Chapters 1 and 2, the author developed the asymmetric allylic acylation of allylic phosphates with acylsilanes using a blue LED and a chiral copper catalyst. In this method, acylcopper, which has low nucleophilicity in its ground state, is excited upon photoirradiation and utilized in the acylation reaction with high enantioselectivity. Based on this finding, the author thought that 1,4-dicarbonyl compounds could be synthesized stereoselectively by replacing allylic phosphates with *α,β*-unsaturated carbonyl compounds. Chapter 3 describes the development of a photoinduced copper-catalyzed asymmetric conjugate addition reaction of acylsilanes to α,β-unsaturated ketones or aldehydes for the synthesis of chiral 1,4-dicarbonyl compounds (Scheme 2). The proposed photoexcitation of an acyl copper intermediate enabled the desired asymmetric conjugate addition reaction with both high yield and high enantioselectivity (up to 92%).

Scheme 2. Photoinduced Cu-catalyzed asymmetric conjugate addition reaction of acylsilanes

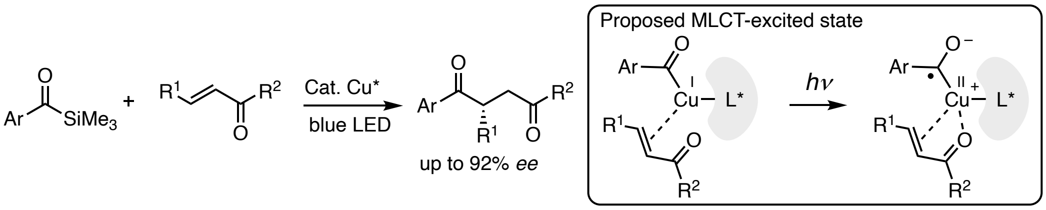

Working Hypothesis

The proposed reaction mechanism is shown in Scheme 3. First, siloxycarbene generated by photoisomerization of acylsilane **1** reacts with CuOtBu to generate acylcopper(I) complex **4** as is the case of the previous chapters. Then, coordination of the *α,β*-unsaturated ketone **2** onto the metal center of **4** affords the copper complex **5**, which undergoes metal-to-ligand charge transfer (MLCT) from the copper(I) center to the acyl ligand upon photoexcitation, resulting in an excited state copper intermediate **6**. The cationic copper center of **6** acts as a Lewis acid, and activating the carbonyl group of the α,β-unsaturated ketone, and the 1,4-addition reaction of the acyl substituent proceeds to form the *β*-acylated copper enolate **7**. Subsequently, the copper enolate **7** reacts with the siloxycarbene generated from the acylsilane under visible light irradiation to afford the chiral silyl enol ether **8** and regenerate the acyl copper(I) complex **4**, completing the catalytic cycle. The desired chiral 1,4-dicarbonyl compound can be obtained by hydrolysis of this silyl enol ether with an acid.

Scheme 3. Proposed reaction mechanism

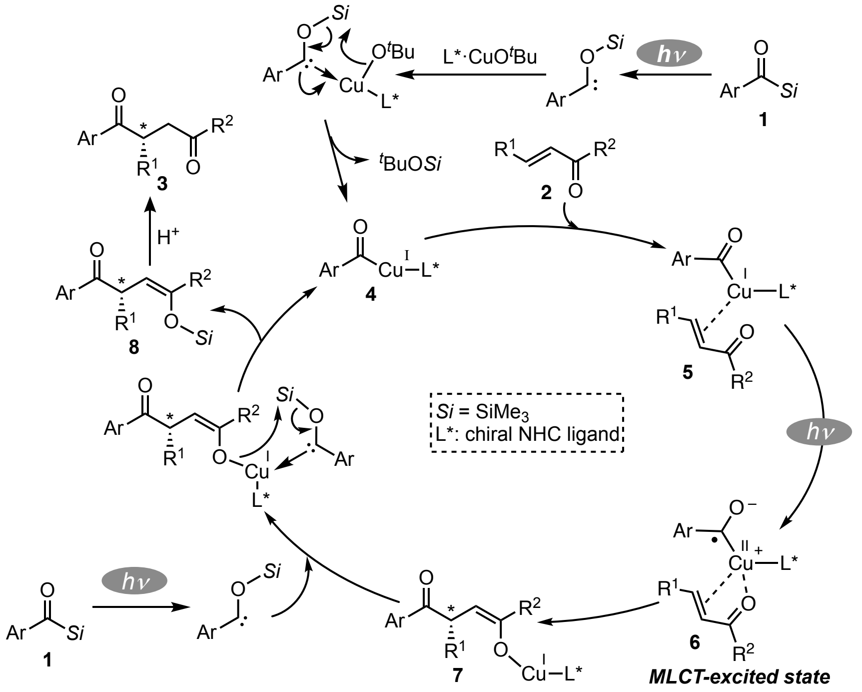

Results and Discussion

Based on the working hypothesis, the effect of chiral NHC ligands was investigated in the coupling reaction between benzoyltrimethylsilane (**1a**, 0.30 mmol) and *trans-α,β*-unsaturated ketone **2a** (0.15 mmol) with a combination of CuCl (10 mol %), chiral NHC ligands (12 mol %), and NaOtBu (20 mol %) in THF at –20 °C under blue LED photoirradiation (465 nm) for 12 h (Table 1). After photoirradiation, the reaction was treated with acetic acid to obtain the desired 1,4-dicarbonyl compound. As expected, 1,4-diketone **3aa** was obtained in 75% yield, 74% ee using NHC ligand **L1**·HBF_4, which has a mesityl group and a *o*-MeO-Ph group on the nitrogen atoms of an imidazolidine ring (entry 1). To improve the enantioselectivity, the author explored other ligands. Changing the N-mesityl group of **L1**·HBF_4 to *o*-F-Ph group (**L2**·HBF_4) or *o*-difluoro-Ph group (**L3**·HBF_4) decreased both yield and enantiomeric excess of **3aa** (entry 3, 4). On the other hand, the use of ligand **L4**·HBF_4, having a 2-biphenyl group, resulted in the enhancement of enantioselectivity (entry 4, 80% ee). Hence, the author demonstrated further ligand modifications based on 2-biphenyl-substituted NHC ligands. NHC ligands having a combination of sterically hindered mesityl group (**L5**·HBF_4) or compact *o*-F-Ph group (**L6**·HBF_4) with 2-biphenyl groups did not give better results (entry 5, 6). Ligand **L7**·HBF_4, bearing a 2-(*o*-tolyl)phenyl group instead of the 2- biphenyl group also showed no significant changes in yield and enantioselectivity from **L4**·HBF_4 (entry 7). In contrast to these C_2-asymmetric ligands, C_2-symmetric *N,N'*-di-2-biphenyl NHC ligand (**L8** · HBF_4) gave a good yield (60%) and enantioselectivity (81% ee) (entry 8). The best result was given by the C_2-symmetric ligand bearing 2-(3,5-dimethylphenyl)phenyl groups (**L9**·HBF_4) (entry 9, 83% yield, 86% ee). When the four methyl groups of ligand **L9**·HBF_4 was replaced with F (**L10**·HBF_4), OMe (**L11**·HBF_4), or ^{t}Bu (**L12**·HBF_4), however, yield and/or enantioselectivity dropped (entry 12-14).

Table 1. Chiral NHC ligand screening of photoinduced copper-catalyzed asymmetric conjugate addition reaction [a]

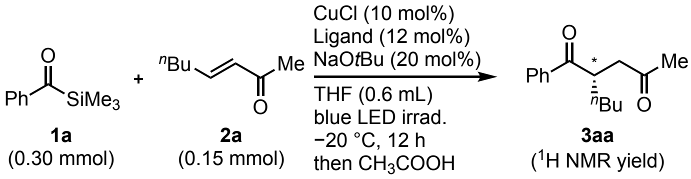

entry	ligand	3aa	
		yield, %[b]	ee, %[c]
1	**L1**·HBF_4/NaO*t*Bu	75	74
2	**L2**·HBF_4/NaO*t*Bu	35	72
3	**L3**·HBF_4/NaO*t*Bu	68	50
4	**L4**·HBF_4/NaO*t*Bu	72	80
5	**L5**·HBF_4/NaO*t*Bu	29	34
6	**L6**·HBF_4/NaO*t*Bu	45	78
7	**L7**·HBF_4/NaO*t*Bu	52	82

8	**L8**·HBF_4/NaO*t*Bu	60	81
9	**L9**·HBF_4/NaO*t*Bu	**83**	**86**
12	**L10**·HBF_4/NaO*t*Bu	71	84
13	**L11**·HBF_4/NaO*t*Bu	50	88
14	**L12**·HBF_4/NaO*t*Bu	34	76

[a] Conditions: **1a** (0.30 mmol), **2a** (0.15 mmol), CuCl (10 mol%), Ligand (12 mol%), NaOtBu (20 mol%), THF (0.60 mL), blue LED irradiation, −20 ℃, 12 h. [b] Yield determined by ^{1}H NMR analysis. [c] Enantiomeric excess determined by chiral HPLC analysis.

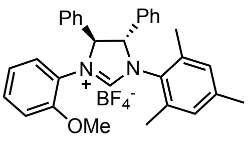

L1·HBF$_4$

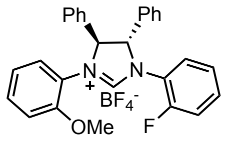

L2·HBF$_4$

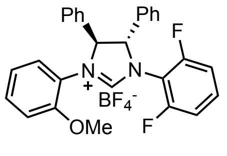

L3·HBF$_4$

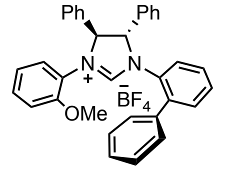

L4·HBF$_4$

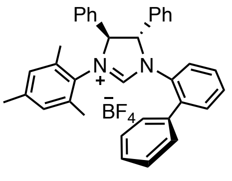

L5·HBF$_4$

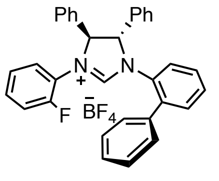

L6·HBF$_4$

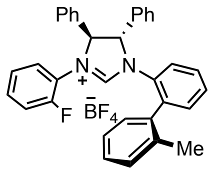

L7·HBF$_4$

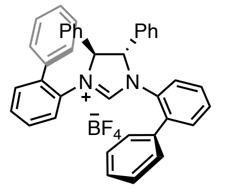

L8·HBF$_4$

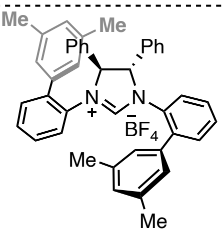

L9·HBF$_4$

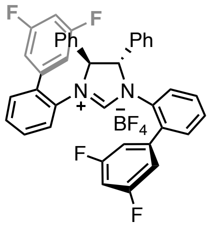

L10·HBF$_4$

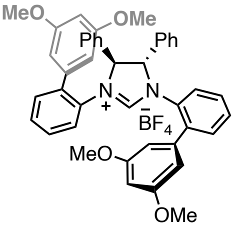

L11·HBF$_4$

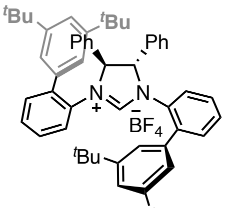

L12·HBF$_4$

Next, using L9•HBF_4 as a ligand, the effect of base, reaction temperature, and reaction time was investigated (Table 2). First, when potassium carbonate (K_2CO_3) was used as a base instead of NaO^{t}Bu, the yield of **3aa** decreased significantly (entry1, 2). On the other hand, the use of stoichiometric amounts of K_2CO_3 rather than catalytic amounts improved the product yield without affecting the enantioselectivity (entry 3). Therefore, further reaction optimization was carried out with stoichiometric amounts of weak bases. Potassium salts such as a potassium fluoride (KF) and potassium hydrogen carbonate ($KHCO_3$) gave the similar result as K_2CO_3 in yield and enantioselectivity (entry 4, 5). Lithium carbonate (Li_2CO_3) or sodium carbonate (Na_2CO_3) did not give the target product at all probably due to low solubility in THF (entry 6, 7). Cesium carbonate (Cs_2CO_3), which is more basic and more soluble in organic solvent than K_2CO_3, gave the best result, and the desired products were obtained in 83% yield (entry 8). Further improvement in enantioselectivity was achieved at lower temperature without affecting reactivity (84% yield, 89% ee) (entry 9). This result is in contrast to the fact that the use of a catalytic amount of NaO^{t}Bu at –40 °C decreased the product yield (entry 10).

Table 3. Effect of base, reaction temperature and reaction time [a]

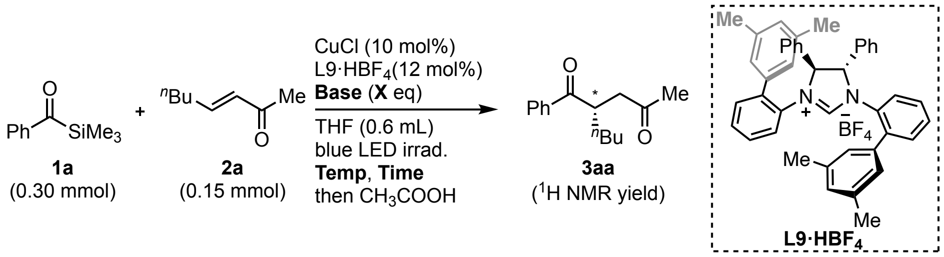

entry	Base (X eq)	Temp (°C)	Time (h)	yield, %[b]	ee, %[c]
1	NaO^{t}Bu (0.2)	−20	12	83	86
2	K_2CO_3 (0.2)	−20	12	27	-
3	K_2CO_3 (2.0)	−20	12	82	86
4	KF (2.0)	−20	12	61	87
5	$KHCO_3$ (2.0)	−20	12	76	86
6	Li_2CO_3 (2.0)	−20	12	0	-
7	Na_2CO_3 (2.0)	−20	12	0	-
8	Cs_2CO_3 (2.0)	−20	12	83	86
9	Cs_2CO_3 (2.0)	−40	20	75 (84) [d]	89
10	NaO^{t}Bu (0.2)	−40	20	60	89

[a] Conditions: **1a** (0.30 mmol), **2a** (0.15 mmol), CuCl (10 mol%), L9•HBF_4 (12 mol%), Base (X eq), THF (0.60 mL), blue LED irradiation. [b] Yield determined by ^{1}H NMR analysis. [c] Enantiomeric excess determined by chiral HPLC analysis. [d] Yield of isolated product.

With the optimized conditions in hand, the substrate scope was examined (table 4). First, the scope of *α,β*-unsaturated ketone **2** was investigated in the reaction with **1a** as a coupling partner. The *α,β*-unsaturated ketone with a *β*-$^nC_5H_{11}$ substituent (**2b**) reacted cleanly with **1a** to afford desired 1,4-diketone **3ab** in 90% yield with 90% ee. The *S* configuration of **3ab** was determined by comparing the specific rotation with the literature data[5] and was used as the basis of configuration assignment for the other 1,4-dicarbonyl products. The reaction also proceeded when alkyl chains at the β-position were changed to a methyl group (**3ac)** or a phenylethyl group (**3ad**). However, the reaction of the *α,β*-unsaturated ketone with the bulkier cyclohexyl group (**3ae**) resulted in a slight decrease of enantioselectivity (82% ee). Next, the substituent adjacent to the carbonyl group (**R^2**) was examined. Ethyl ketone (**3af**) was found to be a suitable substrate. The bulky phenyl group (**3ag**) and cyclohexyl group (**3ah**) afforded the desired products, albeit with slightly decrease in enantioselectivity (79% ee, 72% ee). A broad functional group compatibility of the present method was demonstrated by the preparation of **3ai**–**3ao**. For instance, *α,β*-unsaturated ketones bearing benzoyloxy (**2i**), siloxy (**2j**), and benzyloxy (**2k**) groups reacted with **1a** to afford the corresponding 1,4-diketones (**3ai**–**3ak**) in good to high yields with good enantioselectivities (83–90% ee). Functional groups such as fluoro (-

F), bromo (-Br), trifluoromethyl (-CF_3), and methoxy (-OMe) substitutions were tolerated on the aromatic ring of benzyloxy-substituted *α,β*-unsaturated ketone substrates (**2l**–**2o**).

Next, the author explored the generality of acylsilanes (**1**) in the reaction with *α,β*-unsaturated ketone **2b**. Benzoyltrimethylsilanes with electron-withdrawing fluoro (**1b**) or electron-donating methoxy (**1c**) substituents at the para position gave the products (**3bb**–**3cb**) in high yields with excellent enantioselectivities. Disubstituted benzoylsilane **1e** served as a suitable substrate to give the corresponding product (**3eb**). The protocol was also applicable to an acylsilane with a more extended π system (**3fb**).

Table 5. Substrate Scope [a]

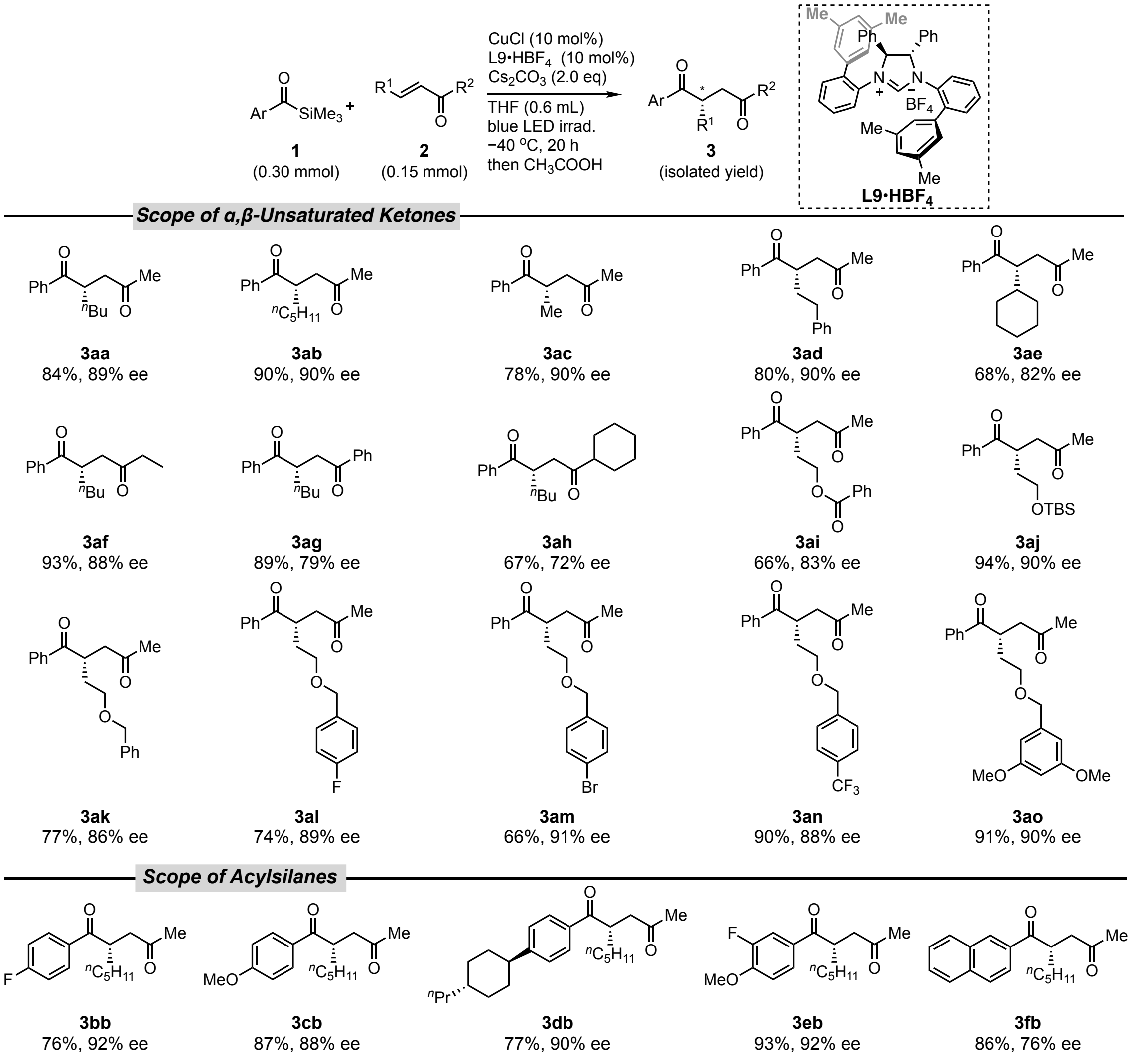

[a] Conditions: **1a**–**1f** (0.30 mmol), **2a**–**2o** (0.15 mmol), CuCl (10 mol%), **L9**·HBF_4 (12 mol%), Cs_2CO_3 (2.0 equiv), THF (0.60 mL), blue LED irradiation (465 nm), −40 °C, 12 h. Yields of isolated products (**3**) are reported.

This protocol can also be applied to *α,β*-unsaturated aldehydes instead of *α,β*-unsaturated ketones (Scheme 4). Under the optimized conditions, the asymmetric 1,4-addition reaction of acylsilane **1a** to unsaturated aldehyde **2p** proceeds efficiently to give the corresponding 1,4-dicarbonyl compound (**3ap**).

Scheme 4. Application to *α,β*-unsaturated aldehydes

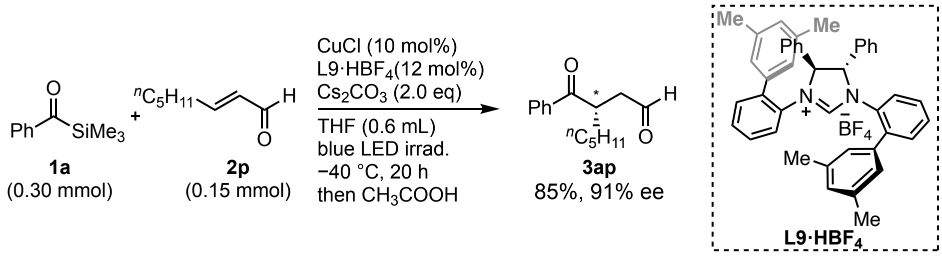

The produced chiral 1,4-dicarbonyl compounds are amenable to further derivatization as shown in Scheme 5. Reduction of both carbonyl groups of **3ap** with $NaBH_4$ proceeded in a diastereoselective manner (d.r. = 9:1)[6] to obtain the corresponding 1,4-diol (**9**) in 85% yield with retaining its enantiomeric excess.

Scheme 5. Derivation of the resulting chiral 1,4-dicarbonyl compounds

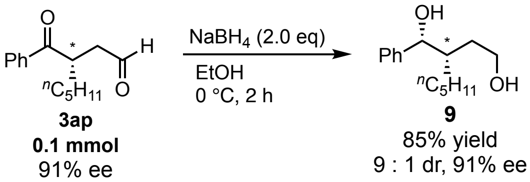

Conclusion

In summary, the author developed a photoinduced copper-catalyzed asymmetric conjugate addition reaction of acylsilanes to α,β-unsaturated ketones or aldehydes for the synthesis of chiral 1,4-dicarbonyl compounds. The proposed photoexcitation of an acyl copper intermediate enabled the desired asymmetric conjugate addition reaction under mild reaction conditions with readily available blue LEDs. The combination of C_2-symmetric *N*,*N*'-di-2-(3,5-dimethylphenyl)phenyl imidazolidinium ligand and a stoichiometric amount of cesium carbonate was crucial for high reaction efficiency and high enantioselectivity. These results demonstrate that the photoinduced copper-catalyzed strategy is applicable to asymmetric acylation reactions with a wide range of electrophiles.

Experimental Section

Instrumentation and Chemicals

NMR spectra were recorded on a JEOL ECX-400, operating at 400 MHz for ^{1}H NMR, 101 MHz for ^{13}C NMR. Chemical shift values for ^{1}H NMR and ^{13}C NMR are referenced to Me_4Si (0.00 ppm for ^{1}H NMR) and $CDCl_3$ (77.0 ppm for ^{13}C NMR). Chemical shifts are reported in δ ppm. High-resolution mass spectra were recorded at the Instrumental Analysis Division, Global Facility Center, Creative Research Institution, Hokkaido University (Thermo Fisher Scientific Exactive or JEOL JMS-T100LP for ESI-MS) and the GC–MS & NMR Laboratory, Research Faculty of Agriculture, Hokkaido University (JEOL JMS-T100GCv for FD-MS). HPLC analyses were conducted on a HITACHI ELITE LaChrom system with a HITACHI L-2455 diode array detector. Optical rotations were measured on a JASCO P-2200. TLC analyses were performed on commercial glass plates bearing 0.25-mm layer of Merck Silica gel 60F_{254}. Silica gel (Kanto Chemical Co., Silica gel 60 N, spherical, neutral) was used for column chromatography. IR spectra were measured with a PerkinElmer Frontier instrument.

All reactions were carried out under nitrogen or argon atmosphere. Materials were obtained from commercial suppliers or prepared according to standard procedures unless otherwise noted. CuCl was purchased from Aldrich Chemical Co., stored under nitrogen, and used as received. THF was purchased from Kanto Chemical Co., and purified by passing through activated alumina under positive argon pressure as described by Grubbs *et al.*[7] NaO*t*Bu was purchased from TCI Chemical Co., stored under nitrogen, and used as received.

Preparation of Substrates and Ligands

Acylsilanes[8] and *α,β*-unsaturated carbonyl compounds[9] were synthesized according to the literature methods. The preparation of the chiral NHC ligands was previously reported.[10] See the section for reaction optimization for the variants of this ligand system.

Substrate Scope

General Procedure for the Cu-Catalyzed Asymmetric Conjugate Addition Reaction.

In a N_2-filled glove box, CuCl (1.5 mg, 0.015 mmol), **L9**•HBF_4 (9.6 mg, 0.018 mmol), and Cs_2CO_3 (97.7 mg, 0.30 mmol) were placed in a vial containing a magnetic stirring bar. THF (0.6 mL) was added to the vial, which was sealed with a cap and was removed from the glove box. The mixture was stirred at room temperature for 10 min. Next, *α,β*-unsaturated carbonyl compound **2** (0.15 mmol) and acylsilane **1** (0.30 mmol) were added *via* a syringe. After 20 h stirring at –40 °C under blue LED irradiation, acetic acid was added to the reaction mixture, which was stirred for 30 minutes. The reaction mixture was diluted with Et_2O and filtered through a pad of silica gel (eluting with Et_2O). The volatiles were removed under vacuum, and then an internal standard (dibenzyl) was added to determine the ^1H NMR yield. The crude product was purified by silica gel column chromatography. Enantiomeric excess of the products was determined by HPLC analysis with a chiral stationary phase column.

(*S*)-2-butyl-1-phenylpentane-1,4-dione (3aa)

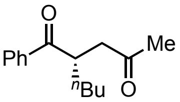

The product was isolated by silica gel column chromatography with hexane/EtOAc (90:10 to 70:30) as a colorless oil (29.3 mg, 0.13 mmol, 84% yield). The ee value (89% ee) was determined by HPLC analysis [CHIRALCEL® IC-3 column, 4.6 mm × 250 mm, Daicel Chemical Industries, hexane/2-propanol 90.0:10.0, 1.0 mL/min, 40 °C, 254 nm UV detector, retention time = 9.1 min for the *S* isomer and 16.2 min for the *R* isomer]. **^{1}H NMR** (400 MHz, $CDCl_3$): δ 7.99 (d, J = 7.3 Hz, 2H), 7.56 (t, J = 7.3 Hz, 1H), 7.47 (t, J = 7.6 Hz, 2H), 3.96–3.89 (m, 1H), 3.16 (dd, J = 9.2Hz, 8.7 Hz, 1H), 2.61 (dd, J = 17.9 Hz, 4.1 Hz, 1H), 2.17 (s, 3H), 1.71–1.60 (m, 2H), 1.48–1.41 (m, 1H), 1.26 (t, J = 3.4 Hz, 3H), 0.84 (t, J = 6.9 Hz, 3H); **^{13}C NMR** (101 MHz, $CDCl_3$): δ 207.4, 203.3, 136.7, 132.9, 128.6 (2C), 128.4 (2C), 45.0, 41.1, 32.0, 30.1, 29.3, 22.7, 13.8; **IR** (ATR): 3061, 2957, 2931, 2860, 1715, 1678, 1597, 1580, 1448, 1398, 1358, 1240, 1195, 1166, 1104, 1074, 1002, 979, 936, 849, 777, 700, 654 cm^{-1}; **HRMS** (ESI) *m/z* : $[M+Na]^+$ Calcd for $C_{15}H_{20}NaO_2$ 255.13555, found 255.13509; $[\boldsymbol{\alpha}]_{\boldsymbol{D}}^{\mathbf{21}} = -58.8$ (c = 0.81, $CHCl_3$).

(*S*)-2-pentyl-1-phenylpentane-1,4-dione (3ab)

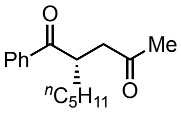

The product was isolated by silica gel column chromatography with hexane/EtOAc (90:10 to 70:30) as a colorless oil (35.2 mg, 0.14 mmol, 90% yield). The ee value (90% ee) was determined by HPLC analysis [CHIRALCEL® IC-3 column, 4.6 mm × 250 mm, Daicel Chemical Industries, hexane/2-propanol 95.0:5.0, 1.0 mL/min, 40 °C, 254 nm UV detector, retention time = 12.1 min for the *S* isomer and 23.1 min for the *R* isomer]. ^{1}**H NMR** (400 MHz, CDCl$_3$): δ 7.99 (d, J = 8.2 Hz, 2H), 7.56 (t, J = 6.9 Hz, 1H), 7.48–7.45 (m, 2H), 3.96–3.89 (m, 1H), 3.16 (dd, J = 9.6 Hz, 8.7 Hz, 1H), 2.61 (dd, J = 17.9, 4.1 Hz, 1H), 2.16 (s, 3H), 1.70–1.62 (m, 1H), 1.45–1.18 (m, 5H), 0.92–0.82 (m, 5H); ^{13}**C NMR** (101 MHz, CDCl$_3$): δ 207.4, 203.3, 136.7, 132.8, 128.5 (2C), 128.3 (2C), 45.0, 41.2, 32.2, 31.7, 30.0, 26.8, 22.3, 13.9; $[\alpha]_D^{25}$ = −49.1 (c = 0.5, CHCl$_3$). Spectral data match those reported in the literature.[5]

(*S*)-2-methyl-1-phenylpentane-1,4-dione (3ac)

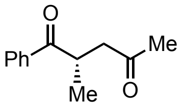

The product was isolated by silica gel column chromatography with hexane/EtOAc (90:10 to 70:30) as a colorless oil (34.9 mg, 0.14 mmol, 90% yield). The ee value (90% ee) was determined by HPLC analysis [CHIRALCEL® IC-3 column, 4.6 mm × 250 mm, Daicel Chemical Industries, hexane/2-propanol 90.0:10.0, 1.0 mL/min, 40 °C, 254 nm UV detector, retention time = 11.4 min for the *S* isomer and 22.3 min for the *R* isomer]. ^{1}**H NMR** (400 MHz, CDCl$_3$): δ 7.99 (d, J = 7.3 Hz, 2H), 7.56 (t, J = 7.3 Hz, 1H), 7.47 (t, J = 7.8 Hz, 2H), 4.02–3.93 (m, 1H), 3.17 (dd, J = 9.6 Hz, 8.2 Hz, 1H), 2.56 (dd, J = 17.9 Hz, 5.0 Hz, 1H), 2.18 (s, 3H), 1.19 (d, J = 7.3 Hz, 3H); ^{13}**C NMR** (101 MHz, CDCl$_3$): δ 207.1, 203.2, 135.6, 132.9, 128.6 (2C), 128.4 (2C), 46.7, 36.2, 30.1, 17.7; $[\alpha]_D^{23}$ = −19.2 (c = 0.40, CHCl$_3$). Spectral data match those reported in the literature.[11]

(*S*)-2-phenethyl-1-phenylpentane-1,4-dione (3ad)

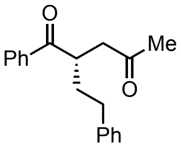

The product was isolated by silica gel column chromatography with hexane/EtOAc (90:10 to 70:30) as a colorless oil (33.6 mg, 0.12 mmol, 80% yield). The ee value (90% ee) was determined by HPLC analysis [CHIRALCEL® IC-3 column, 4.6 mm × 250 mm, Daicel Chemical Industries, hexane/2-propanol 95.0:5.0, 1.0 mL/min, 40 °C, 254 nm UV detector, retention time = 16.9 min for the *S* isomer and 26.9 min for the *R* isomer]. **^{1}H NMR** (400 MHz, $CDCl_3$): δ 7.89 (d, J = 7.3 Hz, 2H), 7.57–7.53 (m, 1H), 7.43 (t, J = 7.6 Hz, 2H), 7.29–7.24 (m, 2H), 7.21–7.17 (m, 1H), 7.09 (d, J = 6.9 Hz, 2H), 4.08–3.93 (m, 1H), 3.20 (dd, J = 9.2 Hz, 8.7 Hz, 1H), 2.69–2.53 (m, 3H), 2.17 (s, 3H), 2.05–1.96 (m, 1H), 1.84–1.72 (m, 1H); **^{13}C NMR** (101 MHz, $CDCl_3$): δ 207.1, 202.9, 141.0, 136.4, 133.0, 128.6 (2C), 128.4 (4C), 128.3 (2C), 126.1, 45.0, 40.6, 33.7, 33.3, 30.0; $[\alpha]_D^{23}$ = −44.2 (*c* = 0.77, $CHCl_3$). Spectral data match those reported in the literature.[12]

(*R*)-2-cyclohexyl-1-phenylpentane-1,4-dione (3ae)

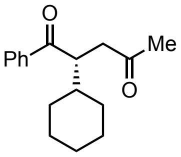

The product was isolated by silica gel column chromatography with hexane/EtOAc (90:10 to 70:30) as a colorless oil (26.4 mg, 0.10 mmol, 68% yield). The ee value (82% ee) was determined by HPLC analysis [CHIRALCEL® IC-3 column, 4.6 mm × 250 mm, Daicel Chemical Industries, hexane/2-propanol 90.0:10.0, 1.0 mL/min, 40 °C, 254 nm UV detector, retention time = 10.1 min for the *R* isomer and 16.2 min for the *S* isomer]. **^{1}H NMR** (400 MHz, $CDCl_3$): δ 7.99 (d, *J* = 6.9 Hz, 2H), 7.56 (t, *J* = 7.1 Hz, 1H), 7.47 (t, *J* = 7.8 Hz, 2H), 3.86–3.82 (m, 1H), 3.21 (dd, *J* = 18.1 Hz, 10.3 Hz, 1H), 2.61 (dd, *J* = 18.3 Hz, 3.2 Hz, 1H), 2.16 (s, 3H), 1.70–1.55 (m, 6H), 1.25–0.83 (m, 5H); **^{13}C NMR** (101 MHz, $CDCl_3$): δ 207.8, 203.3, 137.5, 132.7, 128.5 (2C), 128.4 (2C), 46.5, 42.3, 40.0, 31.7, 30.0, 29.4, 26.5, 26.3, 26.1; **IR** (ATR): 3057, 2921, 2852, 1721, 1670, 1596, 1579, 1449, 1392, 1357, 1315, 1241, 1195, 1164, 1109, 1077, 1030, 1003, 976, 938, 860, 810, 775, 737, 711, 687, 657, 617 cm^{-1}; **HRMS** (ESI) *m/z* : $[M+Na]^+$ Calcd for $C_{17}H_{22}NaO_2$ 281.15120, found 281.15082; $[\alpha]_D^{22}$ = −87.6 (*c* = 0.74, $CHCl_3$)

(*S*)-2-butyl-1-phenylhexane-1,4-dione (3af)

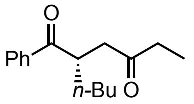

The product was isolated by silica gel column chromatography with hexane/EtOAc (90:10 to 70:30) as a colorless oil (34.3 mg, 0.14 mmol, 93% yield). The ee value (88% ee) was determined by HPLC analysis [CHIRALCEL® IC-3 column, 4.6 mm × 250 mm, Daicel Chemical Industries, hexane/2-propanol 90.0:10.0, 1.0 mL/min, 40 °C, 254 nm UV detector, retention time = 6.5 min for the *S* isomer and 9.5 min for the *R* isomer]. **^{1}H NMR** (400 MHz, $CDCl_3$): δ 8.00 (d, J = 7.3 Hz, 2H), 7.58-7.54 (m, 1H), 7.47 (t, J = 7.6 Hz, 2H), 3.98-3.91 (m, 1H), 3.13 (dd, J = 17.9, 9.6 Hz, 1H), 2.59 (dd, J = 17.9, 4.1 Hz, 1H), 2.49-2.44 (m, 2H), 1.71-1.64 (m, 1H), 1.48-1.39 (m, 1H), 1.30-1.21 (m, 4H), 1.03 (t, J = 7.3 Hz, 3H), 0.84 (t, J = 6.9 Hz, 3H); **^{13}C NMR** (101 MHz, $CDCl_3$): δ 210.2, 203.5, 136.7, 132.8, 128.5 (2C), 128.3 (2C), 43.9, 41.1, 35.9, 32.0, 29.3, 22.6, 13.8, 7.6; **IR** (ATR): 3062, 2957, 2933, 2860, 1713, 1678, 1597, 1581, 1448, 1411, 1377, 1357, 1317, 1279, 1233, 1179, 1114, 1071, 1002, 991, 944, 860, 759, 699, 644, 687, 657, 617 cm^{-1}; **HRMS** (ESI) *m/z* : $[M+Na]^+$ Calcd for $C_{16}H_{22}NaO_2$ 269.15120, found 269.15083; $[\alpha]_D^{22} = -49.2$ (*c* = 0.96, $CHCl_3$)

(*S*)-2-butyl-1,4-diphenylbutane-1,4-dione (3ag)

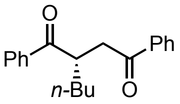

The product was isolated by silica gel column chromatography with hexane/EtOAc (90:10 to 70:30) as a colorless oil (36.7 mg, 0.12 mmol, 89% yield). The ee value (79% ee) was determined by HPLC analysis [CHIRALCEL® IC-3 column, 4.6 mm × 250 mm, Daicel Chemical Industries, hexane/2-propanol 90.0:10.0, 1.0 mL/min, 40 °C, 254 nm UV detector, retention time = 8.0 min for the *S* isomer and 9.3 min for the *R* isomer]. **^{1}H NMR** (400 MHz, $CDCl_3$): δ 8.03 (dd, J = 33.9, 7.8 Hz, 4H), 7.60−7.44 (m, 6H), 4.17−4.10 (m, 1H), 3.73 (dd, J = 9.2 Hz, 8.7 Hz, 1H), 3.18 (dd, J = 18.1, 3.9 Hz, 1H), 1.80−1.73 (m, 1H), 1.40−1.23 (m, 5H), 0.86 (t, J = 7.1 Hz, 3H); **^{13}C NMR** (101 MHz, $CDCl_3$): δ 203.4, 198.7, 136.8, 136.6, 133.1, 132.9, 128.6 (2C), 128.5 (2C), 128.4 (2C), 128.1 (2C), 41.1, 40.7, 32.2, 29.4, 22.7, 13.8; **IR** (ATR): 3061, 2957, 2930, 2860, 1676, 1597, 1581, 1448, 1398, 1378, 1350, 1277, 1216, 1178, 1159, 1102, 1074, 1001, 952, 927, 876, 845, 758, 741, 703, 687, 644, 616 cm^{-1}; **HRMS** (ESI) *m/z* : $[M+Na]^+$ Calcd for $C_{20}H_{22}NaO_2$ 317.15120, found 317.15081; $[\alpha]_D^{23} = -81.2$ (*c* = 0.92, $CHCl_3$)

(*S*)-2-butyl-4-cyclohexyl-1-phenylbutane-1,4-dione (3ah)

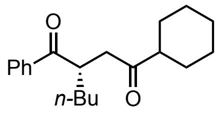

The product was isolated by silica gel column chromatography with hexane/EtOAc (90:10 to 70:30) as a colorless oil (30.2 mg, 0.10 mmol, 67% yield). The ee value (72% ee) was determined by HPLC analysis [CHIRALCEL® IC-3 column, 4.6 mm × 250 mm, Daicel Chemical Industries, hexane/2-propanol 90.0:10.0, 1.0 mL/min, 40 °C, 254 nm UV detector, retention time = 5.5 min for the *S* isomer and 7.2 min for the *R* isomer]. **^{1}H NMR** (400 MHz, $CDCl_3$): *δ* 8.00 (d, *J* = 8.2 Hz, 2H), 7.55 (t, *J* = 7.3 Hz, 1H), 7.46 (t, *J* = 7.6 Hz, 2H), 3.97−3.90 (m, 1H), 3.16 (dd, *J* = 9.6 Hz, 8.7 Hz, 1H), 2.61 (dd, *J* = 18.1, 4.4 Hz, 1H), 2.38 (d, *J* = 11.0 Hz, 1H), 1.86−1.64 (m, 8H), 1.47−1.18 (m, 8H), 0.92−0.82 (m, 3H); **^{13}C NMR** (101 MHz, $CDCl_3$): *δ* 212.8, 203.6, 136.8, 132.8, 128.5 (2C), 128.3 (2C), 50.6, 42.4, 40.9, 32.0, 29.3, 28.3, 25.8 (2C), 25.6 (2C), 22.7, 13.8; **IR** (ATR): 2928, 2855, 1705, 1679, 1597, 1581, 1448, 1396, 1376, 1334, 1231, 1196, 1179, 1146, 1067, 1002, 949, 787, 698, 650, 617 cm^{-1}; **HRMS** (ESI) *m/z* : $[M+Na]^+$ Calcd for $C_{20}H_{28}NaO_2$ 323.19815, found 323.19777; $[\alpha]_D^{23}$ = −38.1 (*c* = 1.0, $CHCl_3$)

(*S*)-3-benzoyl-5-oxohexyl benzoate (3ai)

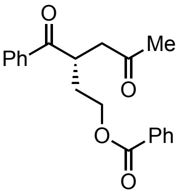

The product was isolated by silica gel column chromatography with hexane/EtOAc (90:10 to 70:30) as a colorless oil (32.1 mg, 0.10 mmol, 66% yield). The ee value (83% ee) was determined by HPLC analysis [CHIRALCEL® IC-3 column, 4.6 mm × 250 mm, Daicel Chemical Industries, hexane/2-propanol 90.0:10.0, 1.0 mL/min, 40 °C, 254 nm UV detector, retention time = 27.3 min for the *S* isomer and 33.7 min for the *R* isomer]. **^{1}H NMR** (400 MHz, $CDCl_3$): *δ* 8.02-7.93 (m, 4H), 7.59−7.52 (m, 2H), 7.42 (q, *J* = 7.5 Hz, 4H), 4.40−4.25 (m, 2H), 4.20−4.10 (m, 1H), 3.23 (q, *J* = 9.0 Hz, 1H), 2.73 (dd, *J* = 18.3, 4.6 Hz, 1H), 2.27−2.16 (m, 4H), 1.97−1.89 (m, 1H); **^{13}C NMR** (101 MHz, $CDCl_3$): *δ* 206.5, 202.2, 166.2, 136.1, 133.1, 129.8, 129.5 (2C), 129.4 (2C), 128.6, 128.45 (2C), 128.36 (2C), 62.4, 45.2, 38.1, 31.0, 29.9; **IR** (ATR): 2959, 2115, 1708, 1673, 1595, 1580, 1493, 1465, 1450, 1397, 1377, 1360, 1316, 1270, 1256, 1196, 1178, 1166, 1112, 1097, 1070, 1057, 1025, 1002, 991, 978, 935, 856, 803, 790, 736, 702, 686, 675, 654, 617 cm^{-1}; **HRMS** (ESI) *m/z* : $[M+Na]^+$ Calcd for $C_{20}H_{20}NaO_4$ 347.12538, found 347.12518; $[\alpha]_D^{23}$ = −74.6 (*c* = 1.0, $CHCl_3$)

(*S*)-2-(2-((*tert*-butyldimethylsilyl)oxy)ethyl)-1-phenylpentane-1,4-dione (3aj)

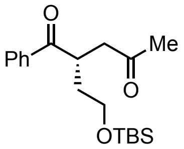

The product was isolated by silica gel column chromatography with hexane/EtOAc (90:10 to 70:30) as a colorless oil (47.2 mg, 0.14 mmol, 94% yield). The ee value (90% ee) was determined by HPLC analysis [CHIRALCEL® IC-3 column, 4.6 mm × 250 mm, Daicel Chemical Industries, hexane/2-propanol 90.0:10.0, 1.0 mL/min, 40 °C, 254 nm UV detector, retention time = 6.8 min for the *S* isomer and 9.3 min for the *R* isomer]. **^{1}H NMR** (400 MHz, $CDCl_3$): *δ* 8.05−8.03 (m, 2H), 7.54 (t, *J* = 8.0 Hz, 1H), 7.45 (t, *J* = 7.6 Hz, 2H), 4.17−4.10 (m, 1H), 3.63−3.57 (m, 2H), 3.20−3.10 (m, 1H), 2.70−2.61 (m, 1H), 2.16 (s, 3H), 2.00−1.86 (m, 1H), 1.62−1.54 (m, 1H), 0.89−0.85 (m, 9H), −0.00−−0.16 (m, 6H); **^{13}C NMR** (101 MHz, $CDCl_3$): *δ* 207.1, 203.1, 136.4, 132.9, 128.6 (2C), 128.4 (2C), 60.3, 45.0, 38.0, 35.0, 29.9, 25.8(3C), 18.2, −5.55, −5.57; **IR** (ATR): 3065, 2954, 2929, 2857, 1717, 1682, 1597, 1581, 1472, 1448, 1398, 1360, 1251, 1193, 1162, 1095, 1003, 980, 939, 834, 809, 775, 736, 698, 662 cm^{-1}; **HRMS** (ESI) *m/z* : $[M+Na]^+$ Calcd for $C_{19}H_{30}NaO_3Si$ 357.18564, found 357.18532; $[\boldsymbol{\alpha}]_{\boldsymbol{D}}^{\mathbf{23}} = -57.9$ (*c* = 1.1, $CHCl_3$)

(*S*)-2-(2-(benzyloxy)ethyl)-1-phenylpentane-1,4-dione (3ak)

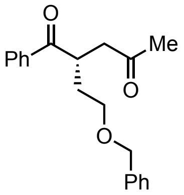

The product was isolated by silica gel column chromatography with hexane/EtOAc (90:10 to 70:30) as a colorless oil (35.6 mg, 0.12 mmol, 77% yield). The ee value (86% ee) was determined by HPLC analysis [CHIRALCEL® IC-3 column, 4.6 mm × 250 mm, Daicel Chemical Industries, hexane/2-propanol 90.0:10.0, 1.0 mL/min, 40 °C, 254 nm UV detector, retention time = 14.3 min for the *S* isomer and 19.1 min for the *R* isomer]. **^{1}H NMR** (400 MHz, $CDCl_3$): *δ* 8.03 (d, *J* = 6.9 Hz, 2H), 7.58–7.53 (m, 1H), 7.45 (t, *J* = 7.6 Hz, 2H), 7.35–7.29 (m, 3H), 7.28–7.26 (m, 2H), 4.38 (s, 2H), 4.19–4.12 (m, 1H), 3.51–3.38 (m, 2H), 3.14 (dd, *J* = 9.6 Hz, 8.7 Hz, 1H), 2.63 (dd, *J* = 18.1, 4.4 Hz, 1H), 2.13 (s, 3H), 2.05–1.96 (m, 1H), 1.77–1.69 (m, 1H); **^{13}C NMR** (101 MHz, $CDCl_3$): *δ* 207.0, 203.2, 138.1, 136.6, 132.9 (2C), 128.5 (4C), 128.3 (2C), 127.6 (2C) , 72.9, 67.4, 45.4, 38.3, 32.3, 29.9; **IR** (ATR): 3063, 2859, 1714, 1678, 1596, 1579, 1496, 1448, 1397, 1359, 1243, 1200, 1164, 1099, 1077, 1027, 1002, 978, 912, 783, 736, 697, 648 cm^{-1}; **HRMS** (ESI) *m/z* : $[M+Na]^+$ Calcd for $C_{20}H_{22}NaO_3$ 333.14612, found 333.14575; $[\boldsymbol{\alpha}]_{\boldsymbol{D}}^{\mathbf{23}} = -62.1$ (*c* = 1.1, $CHCl_3$)

(*S*)-2-(2-((4-fluorobenzyl)oxy)ethyl)-1-phenylpentane-1,4-dione (3al)

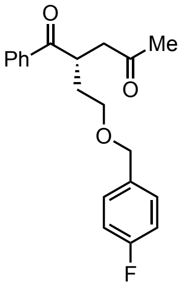

The product was isolated by silica gel column chromatography with hexane/EtOAc (90:10 to 70:30) as a colorless oil (36.5 mg, 0.11 mmol, 74% yield). The ee value (89% ee) was determined by HPLC analysis [CHIRALCEL® IC-3 column, 4.6 mm × 250 mm, Daicel Chemical Industries, hexane/2-propanol 90.0:10.0, 1.0 mL/min, 40 °C, 254 nm UV detector, retention time = 15.1 min for the *S* isomer and 20.7 min for the *R* isomer]. **^{1}H NMR** (400 MHz, $CDCl_3$): *δ* 8.01 (d, J = 7.3 Hz, 2H), 7.55 (t, J = 7.4 Hz, 1H), 7.45 (t, J = 7.8 Hz, 2H), 7.24–7.18 (m, 2H), 7.00 (t, J = 8.7 Hz, 2H), 4.32 (s, 2H), 4.18–4.10 (m, 1H), 3.48–3.37 (m, 2H), 3.14 (dd, J = 9.2 Hz, 9.2 Hz, 1H), 2.63 (dd, J = 18.1, 4.4 Hz, 1H), 2.14 (s, 3H), 2.03–1.96 (m, 1H), 1.78–1.67 (m, 1H); **^{13}C NMR** (101 MHz, $CDCl_3$): *δ* 207.1, 203.2, 163.1 (d, *J* = 436 Hz), 136.5, 133.8, 133.1 (d, *J* = 34.5 Hz, 2C), 132.0, 128.6 (2C), 128.4 (2C), 115.1 (d, *J* = 11.5 Hz, 2C), 72.9, 67.4, 45.4, 38.3, 32.3, 29.9; **IR** (ATR): 3066, 2864, 1715, 1678, 1602, 1580, 1509, 1448, 1398, 1272, 1157, 1002, 978, 824, 768, 700, 647 cm^{-1}; **HRMS** (ESI) *m/z* : $[M+Na]^+$ Calcd for $C_{20}H_{21}NaO_3F$ 351.13669, found 351.13653; $[\alpha]_D^{23} = -41.4$ (*c* = 0.69, $CHCl_3$).

(*S*)-2-(2-((4-bromobenzyl)oxy)ethyl)-1-phenylpentane-1,4-dione (3am)

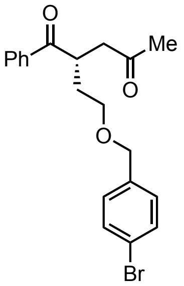

The product was isolated by silica gel column chromatography with hexane/EtOAc (90:10 to 70:30) as a colorless oil (38.8 mg, 0.10 mmol, 66% yield). The ee value (91% ee) was determined by HPLC analysis [CHIRALCEL® IC-3 column, 4.6 mm × 250 mm, Daicel Chemical Industries, hexane/2-propanol 90.0:10.0, 1.0 mL/min, 40 °C, 254 nm UV detector, retention time = 15.9 min for the *S* isomer and 22.1 min for the *R* isomer]. **^{1}H NMR** (400 MHz, $CDCl_3$): *δ* 8.01 (d, *J* = 7.8 Hz, 2H), 7.56 (t, *J* = 7.3 Hz, 1H), 7.44 (t, *J* = 8.0 Hz, 4H), 7.12 (d, *J* = 7.8 Hz, 2H), 4.31 (s, 2H), 4.19–4.10 (m, 1H), 3.51–3.37 (m, 2H), 3.14 (dd, *J* = 9.2, 8.7 Hz, 1H), 2.63 (dd, *J* = 18.1, 4.4 Hz, 1H), 2.14 (s, 3H), 2.04-1.94 (m, 1H), 1.78–1.70 (m, 1H); **^{13}C NMR** (101 MHz, $CDCl_3$): *δ* 206.9, 203.1, 137.1 (2C), 136.6 (2C), 133.0, 131.5, 129.3, 128.5 (2C), 128.4 (2C), 121.4, 72.1, 67.6, 45.4, 38.3, 32.2, 29.9; **IR** (ATR): 2863, 1714, 1678, 1596, 1579, 1488, 1448, 1397, 1359, 1240, 1199, 1164, 1095, 1070, 1010, 978, 802, 700, 643 cm^{-1}; **HRMS** (ESI) *m/z* : $[M+Na]^+$ Calcd for $C_{20}H_{21}NaO_3Br$ 411.05663, found 411.05656; $[\alpha]_D^{23} = -54.1$ (*c* = 1.2, $CHCl_3$).

(*S*)-1-phenyl-2-(2-((4-(trifluoromethyl)benzyl)oxy)ethyl)pentane-1,4-dione (3an)

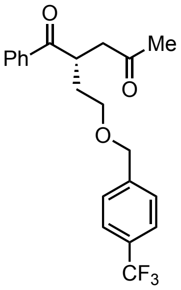

The product was isolated by silica gel column chromatography with hexane/EtOAc (90:10 to 70:30) as a colorless oil (51.1 mg, 0.14 mmol, 90% yield). The ee value (88% ee) was determined by HPLC analysis [CHIRALCEL® IC-3 column, 4.6 mm × 250 mm, Daicel Chemical Industries, hexane/2-propanol 90.0:10.0, 1.0 mL/min, 40 °C, 254 nm UV detector, retention time = 11.0 min for the *S* isomer and 15.1 min for the *R* isomer]. **^{1}H NMR** (400 MHz, $CDCl_3$): δ 8.01 (dd, *J* = 8.5, 1.1 Hz, 2H), 7.55 (t, *J* = 8.2 Hz, 3H), 7.43 (t, *J* = 7.8 Hz, 2H), 7.35 (d, *J* = 8.2 Hz, 2H), 4.40 (s, 2H), 4.20–4.11 (m, 1H), 3.52–3.40 (m, 2H), 3.15 (dd, *J* = 18.1, 8.9 Hz, 1H), 2.64 (dd, *J* = 17.9, 4.6 Hz, 1H), 2.14–2.09 (m, 3H), 2.07–1.96 (m, 1H), 1.81–1.73 (m, 1H); **^{13}C NMR** (101 MHz, $CDCl_3$): δ 206.9, 203.0, 133.6 (q, *J* = 565 Hz), 133.0, 129.6 (q, *J* = 32 Hz, 2C), 128.5 (2C), 128.4 (2C), 127.4, 125.2, 125.1, 124.1 (q, *J* = 272 Hz, 2C), 72.0, 67.9, 45.5, 38.2, 32.3, 29.9; **IR** (ATR): 2866, 1716, 1679, 1622, 1597, 1581, 1449, 1421, 1400, 1361, 1244, 1118, 1103, 1018, 978, 782, 757, 700, 641 cm^{-1}; **HRMS** (ESI) *m/z* : $[M+Na]^+$ Calcd for $C_{21}H_{21}NaO_3F_3$ 401.13350, found 401.13242; $[\alpha]_D^{23} = -40.3$ (*c* = 1.1, $CHCl_3$)

(*S*)-2-(2-((3,5-dimethoxybenzyl)oxy)ethyl)-1-phenylpentane-1,4-dione (3ao)

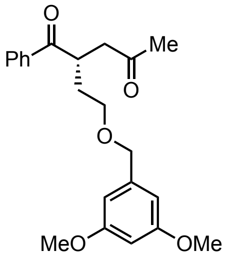

The product was isolated by silica gel column chromatography with hexane/EtOAc (90:10 to 70:30) as a colorless oil (50.6 mg, 0.14 mmol, 91% yield). The ee value (90% ee) was determined by HPLC analysis [CHIRALCEL® IC-3 column, 4.6 mm × 250 mm, Daicel Chemical Industries, hexane/2-propanol 85.0:15.0, 1.0 mL/min, 40 °C, 254 nm UV detector, retention time = 22.2 min for the *S* isomer and 29.9 min for the *R* isomer]. **^{1}H NMR** (400 MHz, $CDCl_3$): δ 8.03 (dd, *J* = 8.2, 1.4 Hz, 2H), 7.55 (t, *J* = 7.3 Hz, 1H), 7.45 (t, *J* = 7.6 Hz, 2H), 6.44 (d, *J* = 2.3 Hz, 2H), 6.38 (t, *J* = 2.3 Hz, 1H), 4.35 (d, *J* = 11.9 Hz, 1H), 4.30 (d, *J* = 12.4 Hz, 1H), 4.20–4.12 (m, 1H), 3.77 (s, 6H), 3.49–3.38 (m, 2H), 3.14 (dd, *J* = 18.1, 9.4 Hz, 1H), 2.64 (dd, *J* = 18.1, 4.4 Hz, 1H), 2.13 (s, 3H), 2.05-1.97 (m, 1H), 1.76–1.68 (m, 1H); **^{13}C NMR** (101 MHz, $CDCl_3$): δ 206.9, 203.1, 160.7 (2C), 140.5, 136.5, 132.9, 128.5 (2C), 128.4 (2C), 105.2 (2C), 99.5, 72.7, 67.4, 55.2 (2C), 45.2, 38.3, 32.1, 29.9; **IR** (ATR): 2939, 2841, 1714, 1678, 1596, 1542, 1449, 1397, 1320, 1296, 1203, 1151, 1055, 978, 833, 782, 699 cm^{-1}; **HRMS** (ESI) *m/z* : [M+Na]$^+$ Calcd for $C_{22}H_{26}NaO_5$ 393.16725, found 393.16680; $[\alpha]_D^{23}$ = −52.1 (*c* = 0.70, $CHCl_3$)

(*S*)-1-(4-fluorophenyl)-2-pentylpentane-1,4-dione (3bb)

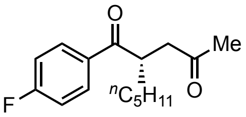

The product was isolated by silica gel column chromatography with hexane/EtOAc (90:10 to 70:30) as a colorless oil (30.1 mg, 0.11 mmol, 76% yield). The ee value (92% ee) was determined by HPLC analysis [CHIRALCEL® IC-3 column, 4.6 mm × 250 mm, Daicel Chemical Industries, hexane/2-propanol 90.0:10.0, 1.0 mL/min, 40 °C, 254 nm UV detector, retention time = 7.0 min for the *S* isomer and 7.9 min for the *R* isomer]. **^{1}H NMR** (400 MHz, $CDCl_3$): *δ* 8.04–8.00 (m, 2H), 7.14 (t, *J* = 8.7 Hz, 2H), 3.90–3.84 (m, 1H), 3.16 (dd, *J* = 17.9, 9.8 Hz, 1H), 2.62 (dd, *J* = 18.1, 3.9 Hz, 1H), 2.16 (s, 3H), 1.66–1.59 (m, 1H), 1.49–1.38 (m, 1H), 1.29–1.16 (m, 6H), 0.84 (t, J = 6.6 Hz, 3H); **^{13}C NMR** (101 MHz, $CDCl_3$): *δ* 207.4, 201.9, 165.6 (d, J = 254 Hz), 133.2, 131.0 (d, J = 9.6 Hz, 2C), 115.6 (d, J = 21.1 Hz, 2C), 45.2, 41.1, 32.3, 31.7, 30.0, 26.8, 22.3, 13.9; **IR** (ATR): 2957, 2930, 2860, 2350, 1716, 1679, 1597, 1542, 1507, 1457, 1411, 1359, 1299, 1228, 1192, 1156, 1106, 1013, 982, 914, 848, 816, 756, 687, 609 cm^{-1}; **HRMS** (APCI) *m/z* : [M+H]$^+$ Calcd for $C_{16}H_{22}O_2F$ 265.15983, found 265.15939; $[\alpha]_D^{19}$ = −56.8 (*c* = 0.81, $CHCl_3$)

(*S*)-1-(4-methoxyphenyl)-2-pentylpentane-1,4-dione (3cb)

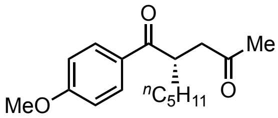

The product was isolated by silica gel column chromatography with hexane/EtOAc (90:10 to 70:30) as a colorless oil (36.3 mg, 0.13 mmol, 87% yield). The ee value (88% ee) was determined by HPLC analysis [CHIRALCEL® IC-3 column, 4.6 mm × 250 mm, Daicel Chemical Industries, hexane/2-propanol 90.0:10.0, 1.0 mL/min, 40 °C, 254 nm UV detector, retention time = 18.9 min for the *S* isomer and 15.2 min for the *R* isomer]. **^{1}H NMR** (400 MHz, $CDCl_3$): *δ* 7.98 (d, *J* = 8.9 Hz, 2H), 6.95 (d, *J* = 9.2 Hz, 2H), 3.92–3.85 (m, 4H), 3.14 (dd, *J* = 17.6, 9.2 Hz, 1H), 2.58 (dd, *J* = 17.9, 4.1 Hz, 1H), 2.16 (s, 3H), 1.71–1.62 (m, 1H), 1.48–1.39 (m, 1H), 1.33–1.24 (m, 6H), 0.84 (t, J = 7.1 Hz, 3H); **^{13}C NMR** (101 MHz, $CDCl_3$): *δ* 207.6, 201.8, 163.4, 130.7 (2C), 129.7 (2C), 113.8, 55.4, 45.3, 45.2, 40.8, 32.3, 30.2, 29.3, 22.7, 13.9; **IR** (ATR): 2931, 2859, 1715, 1670, 1599, 1575, 1510, 1457, 1420, 1397, 1358, 1309, 1242, 1163, 1112, 1028, 980, 916, 881, 840, 801, 757, 731, 699, 611 cm^{-1}; **HRMS** (APCI) *m/z* : [M+H]$^+$ Calcd for $C_{17}H_{25}O_3$ 277.17982, found 277.17935; $[\alpha]_D^{19}$ = −33.4 (*c* = 0.80, $CHCl_3$)

(*S*)-2-pentyl-1-(4-((1*s*,4*S*)-4-propylcyclohexyl)phenyl)pentane-1,4-dione (3db)

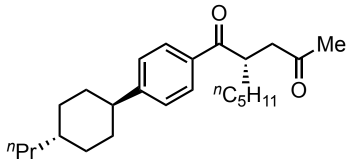

The product was isolated by silica gel column chromatography with hexane/EtOAc (90:10 to 70:30) as a colorless oil (42.7 mg, 0.12 mmol, 77% yield). The ee value (90% ee) was determined by HPLC analysis [CHIRALCEL® IC-3 column, 4.6 mm × 250 mm, Daicel Chemical Industries, hexane/2-propanol 90.0:10.0, 1.0 mL/min, 40 °C, 254 nm UV detector, retention time = 9.1 min for the *S* isomer and 11.3 min for the *R* isomer]. **^{1}H NMR** (400 MHz, $CDCl_3$): δ 7.91 (d, J = 8.7 Hz, 2H), 7.29 (d, J = 8.2 Hz, 2H), 3.94–3.88 (m, 1H), 3.14 (dd, J = 17.9, 9.2 Hz, 1H), 2.61–2.49 (m, 2H), 2.16 (s, 3H), 1.91–1.88 (m, 4H), 1.69–1.62 (m, 1H), 1.52–1.19 (m, 14H), 1.11–0.99 (m, 2H), 0.91 (t, J = 7.1 Hz, 3H), 0.83 (t, J = 6.6 Hz, 3H); **^{13}C NMR** (101 MHz, $CDCl_3$): δ 207.5, 202.8, 153.3, 134.4, 128.6 (2C), 127.1 (2C), 45.0, 44.7, 41.0, 39.6, 36.9, 33.9 (2C), 33.4 (2C), 32.3, 31.7, 30.1, 26.8, 22.4, 20.0, 14.4, 13.9; **IR** (ATR): 2955, 2921, 2853, 1717, 1676, 1606, 1568, 1542, 1448, 1416, 1398, 1358, 1240, 1181, 1165, 1112, 981, 846, 760, 734, 699, 660, 636 cm^{-1}; **HRMS** (APCI) *m/z* : [M+H]$^+$ Calcd for $C_{25}H_{39}O_2$ 371.19446, found 371.29358; $[\boldsymbol{\alpha}]_{\boldsymbol{D}}^{\mathbf{20}} = -37.3$ (*c* = 0.60, $CHCl_3$).

(*S*)-1-(3-fluoro-4-methoxyphenyl)-2-pentylpentane-1,4-dione (3eb)

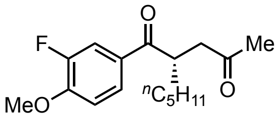

The product was isolated by silica gel column chromatography with hexane/EtOAc (90:10 to 70:30) as a colorless oil (41.1 mg, 0.14 mmol, 93% yield). The ee value (88% ee) was determined by HPLC analysis [CHIRALCEL® IC-3 column, 4.6 mm × 250 mm, Daicel Chemical Industries, hexane/2-propanol 90.0:10.0, 1.0 mL/min, 40 °C, 254 nm UV detector, retention time = 16.2 min for the *S* isomer and 17.2 min for the *R* isomer]. **^{1}H NMR** (400 MHz, $CDCl_3$): δ 7.81–7.72 (m, 2H), 7.01 (t, J = 8.5 Hz, 1H), 3.96 (s, 3H), 3.87–3.78 (m, 1H), 3.14 (dd, J = 18.1, 9.4 Hz, 1H), 2.60 (dd, J = 18.3, 4.1 Hz, 1H), 2.16 (s, 3H), 1.66–1.59 (m, 1H), 1.44–1.38 (m, 1H), 1.31–1.18 (m, 6H), 0.84 (t, J = 6.4 Hz, 3H); **^{13}C NMR** (101 MHz, $CDCl_3$): δ 207.4, 201.0, 152.0 (d, J = 251 Hz), 151.8 (d, J = 10.5 Hz), 129.9, 125.6, 116.0 (d, J = 7.7 Hz), 112.9, 111.7 (d, J = 7.7 Hz), 56.2, 40.8, 32.4, 31.7, 30.0, 26.8, 22.3, 13.9; **IR** (ATR): 2931, 2859, 1715, 1674, 1610, 1581, 1517, 1457, 1433, 1398, 1359, 1320, 1267, 1228, 1143, 1117, 1023, 907, 852, 816, 763, 731, 648, 626 cm^{-1}; **HRMS** (APCI) *m/z* : [M+H]$^+$ Calcd for $C_{17}H_{24}O_3F$ 295.17040, found 295.16983; $[\boldsymbol{\alpha}]_{\boldsymbol{D}}^{\mathbf{20}} = -57.2$ (*c* = 0.86, $CHCl_3$).

(*S*)-2-pentyl-1-(naphthalen-2-yl)pentane-1,4-dione (3fb)

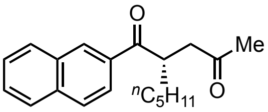

The product was isolated by silica gel column chromatography with hexane/EtOAc (90:10 to 70:30) as a colorless oil (38.4 mg, 0.13 mmol, 86% yield). The ee value (76% ee) was determined by HPLC analysis [CHIRALCEL® IC-3 column, 4.6 mm × 250 mm, Daicel Chemical Industries, hexane/2-propanol 90.0:10.0, 1.0 mL/min, 40 °C, 254 nm UV detector, retention time = 12.4 min for the *S* isomer and 13.2 min for the *R* isomer]. **^{1}H NMR** (400 MHz, $CDCl_3$): δ 8.54 (s, 1H), 8.05–7.98 (m, 2H), 7.89 (t, *J* = 9.2 Hz, 2H), 7.62–7.49 (m, 2H), 4.13–4.06 (m, 1H), 3.22 (dd, J = 18.1, 9.4 Hz, 1H), 2.66 (dd, *J* = 17.9, 4.1 Hz, 1H), 2.19 (s, 3H), 1.79–1.66 (m, 1H), 1.54–1.43 (m, 1H), 1.33–1.18 (m, 6H), 0.83 (t, *J* = 6.9 Hz, 3H); **^{13}C NMR** (101 MHz, $CDCl_3$): δ 207.5, 203.3, 135.5, 134.0, 132.6, 129.9, 129.6, 128.4, 128.3, 127.7, 126.6, 124.3, 45.2, 41.2, 32.4, 31.7, 30.1, 26.8, 22.3, 13.9; **IR** (ATR): 3059, 2955, 2929, 2858, 1715, 1673, 1626, 1596, 1542, 1508, 1466, 1436, 1358, 1276, 1259, 1223, 1164, 1122, 1021, 985, 942, 915, 864, 821, 777, 757, 700, 631 cm^{-1}; **HRMS** (APCI) *m/z* : $[M+H]^+$ Calcd for $C_{20}H_{25}O_2$ 297.18491, found 297.18427; $[\boldsymbol{\alpha}]_{\boldsymbol{D}}^{\mathbf{20}}$ = −35.4 (*c* = 0.58, $CHCl_3$).

(*S*)-3-benzoyloctanal (3ap)

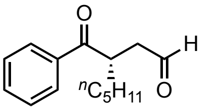

The product was isolated by silica gel column chromatography with hexane/EtOAc (90:10 to 70:30) as a colorless oil (29.6 mg, 0.13 mmol, 85% yield). The ee value (91% ee) was determined by HPLC analysis [CHIRALCEL® OZ-H column, 4.6 mm × 250 mm, Daicel Chemical Industries, hexane/2-propanol 90.0:10.0, 0.5 mL/min, 40 °C, 254 nm UV detector, retention time = 11.3 min for the *R* isomer and 11.8 min for the *S* isomer]. **^{1}H NMR** (400 MHz, $CDCl_3$): δ 9.80 (s, 1H), 7.99 (d, J = 6.9 Hz, 2H), 7.58 (t, J = 7.3 Hz, 1H), 7.49 (t, J = 7.6 Hz, 2H), 3.99–3.92 (m, 1H), 3.17 (dd, J = 18.3, 9.2 Hz, 1H), 2.66 (dd, J = 19.2, 4.1 Hz, 1H), 1.76–1.67 (m, 1H), 1.55–1.43 (m, 1H), 1.32–1.20 (m, 6H), 0.90–0.82 (m, 3H); **^{13}C NMR** (101 MHz, $CDCl_3$): δ 202.5, 200.7, 136.4, 133.1, 128.7 (2C), 128.4 (2C), 45.3, 40.0, 32.2, 31.7, 26.7, 22.3, 13.9; $[\boldsymbol{\alpha}]_{\boldsymbol{D}}^{\mathbf{25}}$ = −43.2 (*c* = 1.0, $CHCl_3$). Spectral data match those reported in the literature.[3]

(1*R*,2*S*)-2-pentyl-1-phenylbutane-1,4-diol (9)

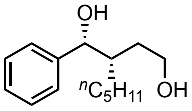

The product was isolated by silica gel column chromatography with hexane/EtOAc (85:15 to 50:50) as a colorless oil (19.4 mg, 0.12 mmol, 83% yield). The ee value (90% ee) was determined by HPLC analysis [CHIRALCEL® OD-H column, 4.6 mm × 210 mm, Daicel Chemical Industries, hexane/2-propanol 95.0:5.0, 1.0 mL/min, 40 °C, 254 nm UV detector, retention time = 14.7 min for the *S* isomer and 30.7 min for the *R* isomer]. **^{1}H NMR** (400 MHz, $CDCl_3$): δ 7.34 (d, J = 4.6 Hz, 4H), 7.29–7.24 (m, 1H), 4.79 (d, J = 4.6 Hz, 1H), 3.79–3.72 (m, 1H), 3.66–3.59 (m, 1H), 3.48 (q, J = 7.0 Hz, 1H), 1.92–1.85 (m, 1H), 1.74–1.66 (m, 1H), 1.57–1.49 (m, 1H), 1.40–1.19 (m, 7H), 0.87–0.83 (m, 3H); **^{13}C NMR** (101 MHz, $CDCl_3$): δ 143.0, 128.0 (2C), 127.1, 126.5 (2C), 76.3, 60.9, 43.1, 32.9, 32.0, 28.6, 26.8, 22.6, 14.0 **IR** (ATR): 3311, 2956, 2928, 2859, 1734, 1700, 1676, 1604, 1542, 1494, 1453, 1379, 1340, 1161, 1129, 1023, 951, 915, 817, 763, 738, 700 cm^{-1}; **HRMS** (ESI) *m/z* : $[M-H]^-$ Calcd for $C_{15}H_{23}O_2$ 235.17035, found 235.17053; $[\boldsymbol{\alpha}]_D^{23}$ = +27.9 (*c* = 0.20, $CHCl_3$).

References

(1) (a) Whittaker, M.; Floyd, C. D.; Brown, P.; Gearing, A. J. H. *Chem. Rev*. **1999**, *99*, 2735–2776. (b) Fujisawa, T.; Igeta, K.; Odake, S.; Morita, Y.; Yasuda, J.; Morikawa, T. *Bioorg. Med. Chem*. **2002**, *10*, 2569–2581. (c) DeMartino, M. P.; Chen, K.; Baran, P. S. *J. Am. Chem. Soc*. **2008**, *130*, 11546–11560. (d) Gavai, A. V.; Quesnelle, C.; Norris, D.; Han, W.-C.; Gill, P.; Shan, W.; Balog, A.; Chen, K.; Tebben, A.; Rampulla, R.; Wu, D.-R.; Zhang, Y.; Mathur, A.; White, R.; Rose, A.; Wang, H.; Yang, Z.; Ranasinghe, A.; D'Arienzo, C.; Guarino, V.; Xiao, L.; Su, C.; Everlof, G.; Arora, V.; Shen, D. R.; Cvijic, M. E.; Menard, K.; Wen, M.-L.; Meredith, J.; Trainor, G.; Lombardo, L. J.; Olson, R.; Baran, P. S.; Hunt, J. T.; Vite, G. D.; Fischer, B. S.; Westhouse, R. A.; Lee, F. Y. *ACS Med. Chem. Lett*. **2015**, *6*, 523–527.

(2) (a) Enders, D.; Han, J.; Henseler, A. *Chem. Commun*. **2008**, 3989−3991. (b) Enders, D.; Han, J. *Synthesis* **2008**, *2008*, 3864−3868. (c) Fang, X.; Chen, X.; Lv, H.; Chi, Y. R. *Angew. Chem., Int. Ed*. **2011**, *50*, 11782−11785.

(3) Goti, G.; Bieszczad, B.; Vega-Peñaloza, A.; Melchiorre, P. *Angew. Chem., Int. Ed*. **2019**, *58*, 1213−1217.

(4) (a) Kaldre, D.; Klose, I.; Maulide, N. *Science* **2018**, *361*, 664–667. (b) Zhao, J.-J.; Zhang, H.-H.; Shen, X.; Yu, S. *Org. Lett*. **2019**, *21*, 913–916. (c) Kuang, Y.; Wang, K.; Shi, X.; Huang, X.; Meggers, E.; Wu, J. *Angew. Chem., Int. Ed*. **2019**, *58*, 16859–16863. (d) Zhang, H.; Wang, Z.; Wang, Z.; Chu, Y.; Wang, S.; Hui, X.-P. *ACS Catal.* **2022**, *12*, 5510–5516. (e) Luo, Y.; Wei, Q.; Yang, L. K.; Zhou, Y. Q.; Cao, W. D.; Su, Z. S.; Liu, X. H.; Feng, X. M. *ACS Catal*. **2022**, *12*, 12984–12992.

(5) Blay, G.; Fernańdez, I.; Monje, B.; Muñoz, M. C.; Pedro, J. R.; Vila, C. *Tetrahedron* **2006**, *62*, 9174−9182.

(6) (a) Matsumoto, K.; Aoki, Y.; Oshima, K.; Utimoto, K.; Rahman, N. A. *Tetrahedron* **1993**, *49*, 8487–8502. (b) Liang, T.; Zhang, W.; Chen, T.-Y.; Nguyen, K. D.; Krische, M. J. *J. Am. Chem. Soc*. **2015**, *137*, 13066−13071.

(7) Pangborn, A. B.; Giardello, M. A.; Grubbs, R. H.; Rosen, R. K.; Timmers, F. J. *Organometallics* **1996**, *15*, 1518–1520.

(8) (a) Ito, K.; Tamashima, H.; Iwasawa, N.; Kusama, H. *J. Am. Chem. Soc*. **2011**, *133*, 3716–3719. (b) Ishida, K.; Tobita, F.; Kusama, H. *Chem. - Eur. J*. **2018**, *24*, 543–546. (c) Ye, J.-H.; Quach, L.; Paulisch, T.; Glorius, F. *J. Am. Chem. Soc*. **2019**, *141*, 16227−16231. (d) Ishida, K.; Yamazaki, H.; Hagiwara, C.; Abe, M.; Kusama, H. *Chem. - Eur. J*. **2020**, *26*, 1249–1253. (e) Lu, X.; Zhang, J.; Xu, L.; Shen, W.; Yu, F.; Ding, L.; Zhong, G. *Org. Lett.* **2020**, *22*, 5610–5616.

(9) (a) Lifchits, O.; Mahlau, M.; Reisinger, C. M.; Lee, A.; Fares, C.; Polyak, I.; Gopakumar, G.; Thiel, W.; List, B. *J. Am. Chem. Soc*. **2013**, *135*, 6677−6693. (b) Hoover, J.; Steves, J.; Stahl, S. *Nat Protoc*. **2012**, *7*, 1161–1166.

(10) (a) Harada, A.; Makida, Y.; Sato, T.; Ohmiya, H.; Sawamura, M. *J. Am. Chem. Soc*. **2014**, *136*, 13932–13939. (b) Ohmiya, H.; Zhang, H.; Shibata, S.; Harada, A.; Sawamura, M. *Angew. Chem., Int. Ed*. **2016**, *55*, 4777–4780. (c) Yasuda, Y.; Ohmiya, H.; Sawamura, M. *Angew. Chem., Int.*

Ed. **2016**, *55*, 10816−10820. (d) Hojoh, K.; Ohmiya, H.; Sawamura, M. *J. Am. Chem. Soc*. **2017**, *139*, 2184−2187. (e) Yasuda, Y.; Ohmiya, H.; Sawamura, M. *Synthesis* **2018**, *50*, 2235–2246.

(11) Esumi, N.; Suzuki, K.; Nishimoto, Y.; Yasuda, M. *Org. Lett.* **2016**, *18*, 5704−5707.

(12) Blay, G.; Fernández, I.; Monje, B.; Muñoz, M. C.; Pedro, J. R.; Vila, C. *Tetrahedron* **2006**, *62*, 9174–9182.

Publication List

1) Nickel-Catalyzed Amination of Aryl Fluorides with Primary Amines
Tomoya, Harada, Yusuke Ueda, Tomohiro Iwai, Masaya Sawamura
Chem. Commun. **2018**, *54*, 1718–1721.

2) Nickel-Copper-Catalyzed Hydroacylation of Vinylarenes with Acyl Fluorides and Hydrosilanes
Yusuke Ueda, Tomohiro Iwai, Masaya Sawamura
Chem. Eur. J. **2019**, *25*, 9410–9414.

3) Photoinduced Copper-Catalyzed Asymmetric Acylation of Allylic Phosphates with Acylsilanes.
Yusuke Ueda, Yusuke Masuda, Tomohiro Iwai, Keisuke Imaeda, Hiroki Takeuchi, Kosei Ueno, Min Gao, Jun-ya Hasegawa, Masaya Sawamura
J. Am. Chem. Soc. **2022**, *144*, 2218–2224.

Acknowledgment

The studies described in this thesis have been carried out under the direction of Professor Masaya Sawamura at Graduate School of Chemical Sciences and Engineering, Hokkaido University from April 2017 to March 2023.

The author wishes to express his grateful acknowledgment to Professor Masaya Sawamura for giving opportunities to study in his laboratory and for his kind guidance, constant encouragement, and valuable discussion. He is deeply grateful to Assistant Professor Yusuke Masuda for his practical guidance, helpful discussions and considerable suggestions. He also wishes to express his deepest appreciation to Associate Professor Yohei Shimizu for elaborated guidance and kind supports. He would like to express his appreciation to Lecture Tomohiro Iwai, Specially Appointed Assistant Professor Kousuke Higashida, and Assistant Professor Arteaga Arteaga Fernando for their kind discussions, advices, and supports.

The author is much grateful to Professor Aiichiro Nagaki, Professor Keiji Tanino and Professor Hajime Ito for their accurate advices and considerable suggestions on this thesis. He also thankful to Professor Jun-ya Hasegawa at Institute for Catalysis, Hokkaido University for significant assistance with computer calculations and Professor Kosei Ueno at Faculty of Science, Hokkaido University for cooperation in spectroscopic experiments.

Moreover, he would like to express his appreciation to all the members of Sawamura group's for the continuous encouragements and the helpful supports. Especially, he would like to express his appreciation to Dr. Yuto Yasuda for his kind discussions, advices, and encouragements. He is also thankful to Mr. Junpei Shimosato and Ms. Aiko Sueki for the excellent collaborations.

Financial support from JSPS, Research Fellowship of the Japan Society for the Promotion of Science for Young Scientists, was indispensable, and author deeply appreciates this support.

Finally, he would like to express his gratitude for his family, Mr. Kohji Ueda, Ms. Miyoko Ueda, and Ms. Yurina Ueda for warm encouragement and continuous assistance.

Yusuke Ueda
Graduate School of Chemical Sciences and Engineering
Hokkaido University
March, 2023